

# **OLIGONUCLEOTIDE BASED LIGANDS IN HOMOGENEOUS TRANSITION METAL CATALYSIS**

**Tanja Eichelsheim**

**A Thesis Submitted for the Degree of PhD  
at the  
University of St Andrews**



**2012**

**Full metadata for this item is available in  
St Andrews Research Repository  
at:**

**<http://research-repository.st-andrews.ac.uk/>**

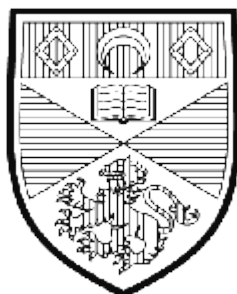
**Please use this identifier to cite or link to this item:**

**<http://hdl.handle.net/10023/3168>**

**This item is protected by original copyright**

**This item is licensed under a  
Creative Commons Licence**

# Oligonucleotide based ligands in homogeneous transition metal catalysis



University of  
St Andrews

*School of Chemistry*

*Fife, Scotland*

**Tanja Eichelsheim**

July 2012

*Thesis submitted to the University of St Andrews in application for the degree*

*Doctor in Philosophy*

**Supervisor: Professor Paul C.J. Kamer**



The following is an agreed request by candidate and supervisor regarding the electronic publication of this thesis: Embargo on both printed copy and electronic copy for the same fixed period of 2 years on the following ground: publication would preclude future publication.

Date

signature of candidate

signature of supervisor

Tanja Eichelsheim

Prof. Paul C.J. Kamer

# Abstract

Catalysis plays an important part in our society. Numerous transition metal catalysts have been developed which can convert many different substrates in a wide range of reactions. Catalysis also plays an important role in nature and therefore special catalysts, enzymes, have evolved over time. Enzymes are tremendously efficient giving high yields and selectivities both regio and chemical but have a limited substrate and reaction scope. It was speculated that by combining the two, an ideal catalyst can be obtained. We planned to achieve this by introducing a transition metal, the catalytic centre, into the chiral environment of a double helical oligonucleotide. The transition metals were introduced by coordinating them to a ligand which was located in the chiral environment of a double helix. The ligand was either covalently bound (Chapter 2) or non-covalently bound (Chapter 3) to the oligonucleotide (Figure 1).

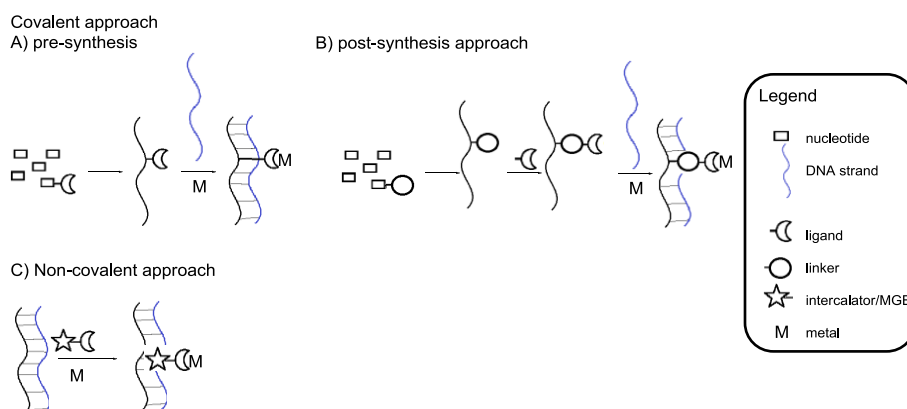


**Figure 1: A) covalent introduction of a transition metal into a nucleotide B) non-covalent introduction of a transition metal into a nucleotide**

For the covalent approach a phosphine ligand was chosen. A nucleoside was modified with an alkyne to which a phosphine moiety could be coupled *via* the copper catalysed 1,3-dipolar cycloaddition. The modified nucleoside was incorporated into an oligonucleotide before attempting to attach the phosphine moiety. The monomer was used as a ligand in allylic substitution and hydroformylation.

In the non-covalent approach polyamide minor groove binders were functionalised with an amine linker. Phosphine moieties were connected *via* amide bond formation. Although the coupling worked effortlessly the phosphines oxidised during purification therefore dienes were also investigated.

# Table of contents

## Chapter 1: Introduction

<b>1.1 Increased environmental awareness</b>	<b>1</b>
<b>1.2 Advantage of using catalysis</b>	<b>4</b>
<i>1.2.1 Enantioselective catalysis</i>	5
<b>1.3 Types of Catalysts</b>	<b>6</b>
<b>1.4 Organometallic catalysis</b>	<b>7</b>
<b>1.5 Enzymes</b>	<b>8</b>
<i>1.5.1 Natural enzymes</i>	8
<i>1.5.2 Artificial metalloproteins</i>	10
<b>1.6 Oligonucleotides as catalysts</b>	<b>12</b>
<i>1.6.1 Unmodified nucleic acids</i>	12
<i>1.6.2 Aptamers</i>	16
<i>1.6.3 Artificial metallo nucleic acids</i>	18
<b>1.7 Project Aim and thesis outline</b>	<b>24</b>
<b>1.8 References</b>	<b>26</b>

## Chapter 2: Covalent approach

<b>2.1 Introduction</b>	<b>29</b>
<i>2.1.1 CuAAC</i>	33
<i>2.1.2 RuAAC</i>	35
<i>2.1.3 Amide bond coupling</i>	36

<b>2.2 Results and discussion</b>	<b>38</b>
2.2.1 <i>Synthesis of a modified nucleotide</i>	38
2.2.2 <i>Synthesis of phosphine azides</i>	40
2.2.3 <i>Oligonucleotide synthesis</i>	41
2.2.4 <i>The 1,3-dipolar cycloaddition</i>	45
<b>2.3 Conclusion</b>	<b>46</b>
<b>2.4 Experimental</b>	<b>47</b>
<b>2.5 References</b>	<b>59</b>
<b>Chapter 3: Non-covalent approach</b>	
<b>3.1 Introduction</b>	<b>61</b>
<b>3.2 Results and discussion</b>	<b>66</b>
3.2.1 <i>Synthesis of minor groove binders</i>	66
3.2.2 <i>Ligand synthesis</i>	67
3.2.3 <i>Combining minor groove binders with ligands</i>	69
<b>3.3 Conclusion</b>	<b>72</b>
<b>3.4 Experimental</b>	<b>73</b>
<b>3.5 References</b>	<b>78</b>
<b>Chapter 4: Catalysis</b>	
<b>4.1 Introduction</b>	<b>79</b>
4.1.1 <i>Allylic substitution</i>	80
4.1.2 <i>1,4-Cycloaddition</i>	85
4.1.3 <i>Hydroformylation</i>	86

<b>4.2 Results and discussion</b>	<b>89</b>
4.2.1 <i>Allylic substitution</i>	90
4.2.2 <i>1,4-Cycloaddition</i>	96
4.2.3 <i>Hydroformylation</i>	96
<b>4.3 Conclusion</b>	<b>98</b>
<b>4.4 Experimental</b>	<b>101</b>
<b>4.5 References</b>	<b>105</b>
<b>List of abbreviations</b>	<b>107</b>
<b>Acknowledgments</b>	<b>110</b>

# Chapter 1: Introduction

## 1.1: Increased environmental awareness

At the moment Earth is the only planet we have found that supports complex life forms. In 2007 Bounama *et al.*<sup>1</sup> developed a model to predict the number of Earth-like planets in the Milky Way, in other words planets that can support life. From these predictions they concluded that the closest planet that can sustain primitive life (micro-organisms) is 30 light years (lyrs) away and for more complex life-forms we would need to look 130 to 200 lyrs away. So regardless if you believe climate change/global warming is caused by mankind,<sup>2</sup> that it is a natural occurrence<sup>3</sup> or that it is all blown out of proportion,<sup>4</sup> we have to take care of our world.

Over the last half a century environmental awareness has been growing, this has led to a demand for cleaner production methods. Although it is difficult to quantify the effect that production processes have on the environment a number of people have attempted to do so. Sheldon<sup>5</sup> proposed the term environmental factor, also known as the E-factor, as a tool for assessing the impact of a manufacturing process on the environment. The E-factor takes into account all the raw materials (excluding water) used during the manufacturing process of a product, including fuel, although this is often difficult to quantify. The E-factor is defined as the mass ratio of waste to product<sup>5</sup> (Equation 1).

### Equation 1

$$E = \frac{\text{kg raw material} - \text{kg product}}{\text{kg product}}$$

This means that the larger the E-factor the higher the environmental impact of a process is. In an ideal scenario all of the raw materials are converted into the product and therefore the E-factor should be 0. In 2007 Table 1 was published showing the E-factors associated with different sectors of the chemical industry.<sup>5</sup>

**Table 1: E-factors in different sectors of the chemical industry**

<b>Industrial sector</b>	<b>E-factor</b>	<b>Product tonnage</b>
<b>Bulk chemicals</b>	1 – 5	$10^4 - 10^6$
<b>Fine chemicals</b>	5 -50	$10^2 - 10^4$
<b>Pharmaceuticals</b>	25 -100	$10 - 10^3$

In 1991 Trost<sup>6</sup> introduced the term atom economy (Equation 2) after noticing that only a portion of the atoms of the starting materials were incorporated into the product in the methylation reaction utilising methyltriphenylphosphonium bromide (Figure 1).

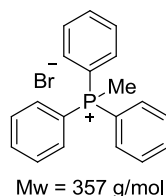


Figure 1: Methyltriphenylphosphonium bromide

In this model the molecular weight (Mw) of the product was compared to that of the reactants. Atom economy has been well received by the scientific community and has been incorporated into the 12 principles of green chemistry.<sup>7</sup>

Equation 2<sup>8</sup>      **Atom economy** =  $\frac{\text{Mw of desired product}}{\text{Mw of all of the reactants used}} \times 100\%$

Something that these and other proposals have in common is that they do not take into account the toxicity of the reagents used and waste produced. Hudlicky<sup>9</sup> attempted to take the toxicity of the utilised reagents into account when he proposed the effective mass yield. The effective mass yield is defined as the mass of the desired product divided by all the utilised non-benign reagents (Equation 3). In contrast to Sheldon's E-factor solvents and by-products, such as low concentration saline solutions, dilute ethanol and autoclaved whole cells with no known environmental impact, are not included in the equation.

Equation 3<sup>8</sup>      **Effective mass yield** =  $\frac{\text{mass of the products}}{\text{mass of non-benign reagents}} \times 100\%$

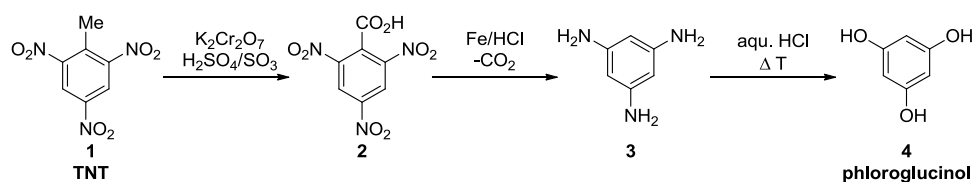
Sheldon also tried to take the toxicity of reagents into account by multiplying an environmental quotation(Q) with his E-factor giving an EQ-factor.<sup>5</sup> The Q in this equation is an arbitrary value and takes into account the amount of a particular substance, its toxicity and the ease of recycling.

It is very difficult to get an unambiguous value of environmental impact of a manufacturing process as among other things it is dependent on the process used, the ease of recycling and the amount of waste produced. Also there is limited information available on the environmental impact a substance has. However these equations (E(Q)-factor, atom economy and effective mass yield) as well as others give a good indication on the cleanness of a process.

All this focus on the environment led Anastas and Warner<sup>10</sup> to coin the term Green Chemistry and define 12 principles associated with it.<sup>7</sup> These principles can be summarised in four points.

- 1) Waste prevention by utilising real-time analysis, efficient catalysts and choosing reactions with a high atom economy and low energy requirements.
- 2) Minimise the effects of accidents such as release of toxic gas, explosions, fires and spillage by employing benign/less harmful chemicals.
- 3) Use of renewable feed stocks.
- 4) Design products that break down in benign degradation products that do not remain in the environment after they have fulfilled their purpose.

Before the early 1990's governments endeavoured to motivate companies to reduce waste by increasing the costs associated with waste disposal. This led to the closure of certain plants. The most famous of these was the phloroglucinol plant at OceaAndeno (part of the DSM concern) which closed its doors in the early 1980's.<sup>5</sup> The production process of phloroglucinol (**4**, Scheme 1) began with the oxidation of 2,4,6-trinitrotoluene (TNT, **1**) with potassium dichromate in sulphuric acid, this was followed by a reduction using iron and hydrochloric acid.<sup>5</sup> During this process a large amount of solid waste was produced e.g.  $\text{Cr}_2(\text{SO}_4)_3$ ,  $\text{NH}_4\text{Cl}$ ,  $\text{FeCl}_2$  and  $\text{KHSO}_4$  giving the plant an E-factor of about 40, which was high for a bulk chemical, and that combined with the increased costs of waste disposal made the process economically unfeasible.



**Scheme 1: Synthesis of phloroglucinol (4) from TNT (1)**

There are a number of possibilities that can be employed in order to reduce the amount of waste produced during a production process, these include changing the reactants and reagents and changing the reaction pathway. The last option can be achieved with the help of catalysts.

## 1.2 Advantage of using catalysis

Catalysts are responsible for increasing reaction rates and allowing reactions to take place under milder conditions. Consequently they play a key role in the production of bulk chemicals.<sup>11</sup> More than 90% of all products synthesised in the chemical industry have been obtained with at least one catalytic step and a prime example of this is the production of ammonia. By applying a high temperature and pressure to a vessel containing nitrogen and hydrogen nothing will happen despite the favourable chemical equilibrium.<sup>12</sup> However if iron is added to the mixture then ammonia is readily formed. In fact over 140 million tons of ammonia are generated like this each year.<sup>13</sup>

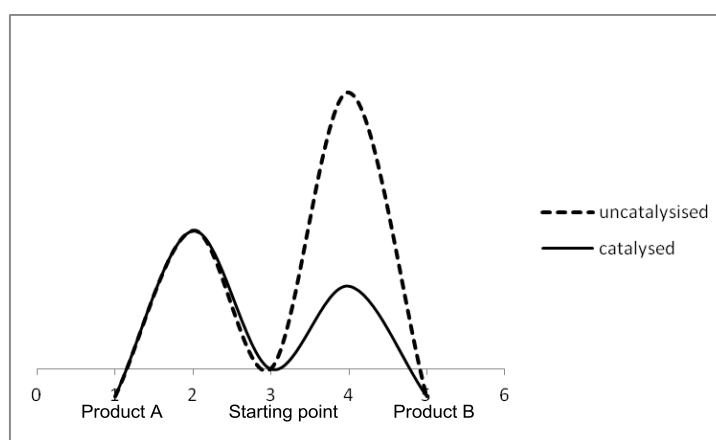


Figure 2: Catalysis energy diagram

Utilising catalysts has another benefit which the fine chemicals and pharmaceutical industries are keen to exploit.<sup>11</sup> Catalysts work by lowering the activation energy barrier of a specific route thus allowing the reaction pathway to change and thus changing product distribution (Figure 2). As a consequence selectivity can be tailored by choosing the right catalyst. For example in Figure 2 when no catalyst was used product A was the favoured product, however when a catalyst was used product B was the more favourable option.

In chemical reactions different types of selectivity can be distinguished. The four types are listed below.<sup>11</sup>

- 1) Chemoselectivity => Selective targeting of one functional group in the presence of multiple functional groups
- 2) Regioselectivity => Selective targeting of one functional group when it appears several times in the molecule
- 3) Enantioselectivity => Selective formation of one enantiomer
- 4) Diastereoselectivity => Selective formation of one diastereomer

### 1.2.1 Enantioselective catalysis

Organic compounds with one chiral centre (enantiomers) or multiple chiral centres (diastereomers) usually have at least two non-superimposable structures. In a chiral environment these structures interact differently so that the observed outcome differs. Most biologically active compounds are chiral; therefore enantiomers and diastereomers are of special interest to the pharmaceutical industry. The difference in activity can be innocent such as producing a different taste, as in the case of asparagine, or devastating, as in the case of penicillamine where one enantiomer is anti-arthritic and the other is toxic<sup>14</sup> (Figure 3). The differences are not necessarily this extreme and could simply be a difference in potency. Despite the importance of enantiomeric purity in the year 2000 only 40% of all drug sales were of enantiopure compounds.<sup>15</sup>

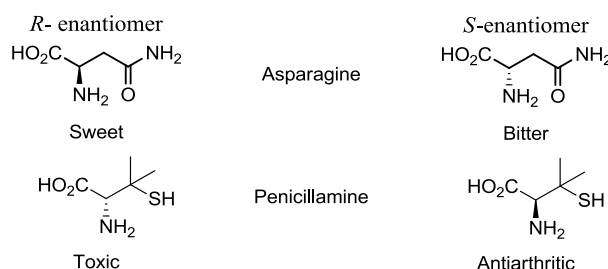
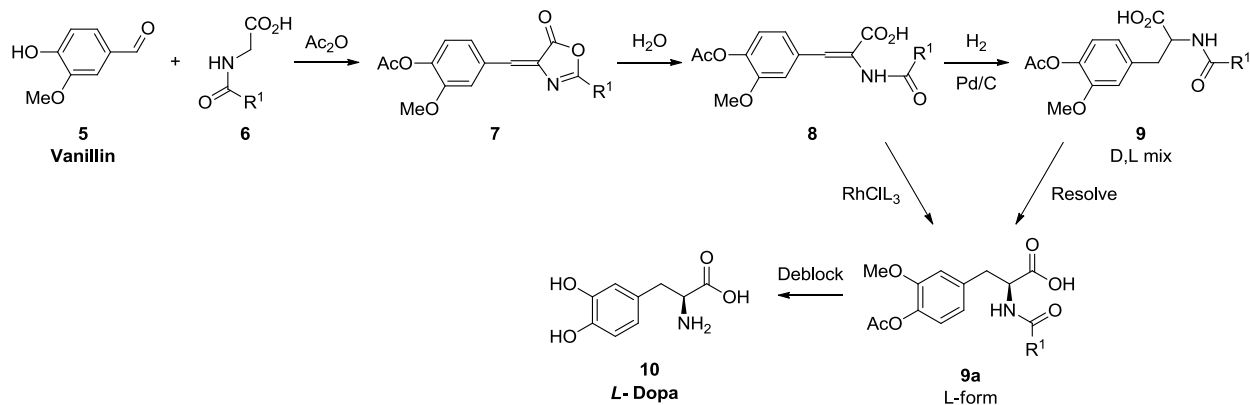


Figure 3: Effect of different enantiomers

In the past, industry often depended on a biochemical route when enantiopure products were required even though the reaction mixtures obtained were often dilute and required cumbersome separations. Efficient chemical routes were also available but these yielded the racemic mixture and thus needed to be resolved.<sup>16</sup> One way to circumvent this problem was to synthesise the product with the aid of an asymmetric catalyst. Knowles was one of the first people to pioneer this approach and his ground breaking discoveries contributed to him receiving the Nobel Prize in 2001.<sup>17</sup>

In the mid-twentieth century it was discovered that *L*-3,4-dihydroxyphenylalanine (*L*-Dopa) functioned as a potent anti-Parkinson's disease drug. The required doses were high and this created a large demand for the rare amino acid.<sup>18</sup> Monsanto was one of the companies to take advantage of this and started synthesising the drug starting from vanillin (**5**) (Scheme 2). The method involved utilising the Erlenmeyer-Plöchl azlactone synthesis before Hoffman-LaRoche resolved and deprotected the product.<sup>16-18</sup>



A breakthrough came when Knowles used a phosphine based ligand (Figure 4, **11**) to facilitate the rhodium catalysed asymmetric hydrogenation of intermediate **8** (Scheme 2). The product (**9a**, Scheme 2) was obtained with a modest enantiomeric excess (*ee*) of around the 30%.<sup>16</sup> Although the value was not high enough to be used industrially it showed that asymmetric catalytic hydrogenations employing a metal-ligand system were possible. After only a few optimisation attempts CAMP (cyclohexyl (2-methoxyphenyl)(methyl)phosphine, **12**) was developed and within 6 months of optimising incorporated into a 50 gallon production process. By employing an asymmetric catalyst the process was shortened and the amount of waste was reduced.<sup>16, 18</sup>

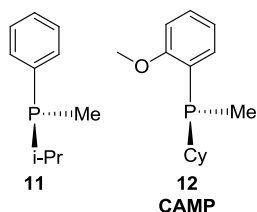


Figure 4: Development of ligands used in the hydrogenation of L-Dopa

Since this discovery the field of asymmetric catalysis has expanded exponentially leading to a multitude of types of catalysts.

### 1.3 Types of Catalysts

The term catalysis was first coined by Berzelius in 1836<sup>11, 13</sup> but mankind has been using catalysis longer than that. Initially catalysis was subdivided into two subgroups dependent on the phase in which the catalyst resided compared to the substrate, heterogeneous or homogeneous. In the case of heterogeneous catalysis the catalyst was in a different phase than the reaction mixture. For example the reactants can be present in a solution or as a gas which is then passed over the solid catalyst. This had the advantage that the reaction mixture was easily separated from the catalyst. In the case of homogeneous catalysis the catalyst and

the substrate both reside in the same phase, typically but not exclusively in solution. A classic example of homogeneous catalysis was the catalysed hydrolysis of starch by acids which Kirchhoff first noticed in 1814.<sup>13</sup>

This subdivision has become outdated with the invention and expansion of different types of catalysis. Currently there are four main types of catalysis namely heterogeneous, organometallic catalysis also known as homogeneous catalysis, organocatalysis and biocatalysis. The rest of this chapter will focus on homogeneous catalysis and biocatalysis. Man-made catalysts and natural catalysts each have their own advantages and disadvantages and therefore a new field has emerged combining these two,<sup>19</sup> this will also be highlighted.

Ideally a catalyst transforms one functional group in the presence of several, sometimes more reactive groups. The reaction must also be highly atom efficient and take place under mild conditions as dictated by green chemistry.<sup>10</sup> In the case of asymmetric catalysis the catalyst is responsible for subtle effects that enable the formation of one enantio/diastereomer over the other. The difference between the formation of enantiomers is very small as energy calculations revealed that there is only a 3 kcal (12.6 kJ) difference in transition states required to form the different enantiomers.<sup>18</sup> Although the differences are small specific enantiomers can be targeted, enzymes are especially accomplished in this.

## 1.4 Organometallic catalysis

The first organometallic catalysts used in industry were used for high volume production of chemical intermediates and polymers. Nowadays organometallic catalysts are also used for more complex compounds such as pharmaceuticals, flavours, fragrances and agrochemicals. They are especially good in carbonylation reactions, C-C coupling and enantioselective catalysis.<sup>20</sup>

Although homogeneous catalysts existed before Wilkinson discovered that chlorotris(triphenylphosphane) rhodium ( $[\text{RhCl}(\text{PPh}_3)_3]$ ) was an effective catalyst in hydrogenation reactions with unhindered olefins, this was the first time that the reaction rates rivalled those of heterogeneous catalysis.<sup>18</sup>

Metal complexes containing chiral ligands are currently the most used asymmetric catalysts. The chiral ligands were needed to direct the reactivity and selectivity of the metal centre. A lot of work has been done to further understand the mechanism of catalytic reactions giving a better understanding of the requirements of a ligand. In other words a ligand can potentially

be designed rationally. Unfortunately due to the complexity of these reactions the development is still largely dependent on trial and error.<sup>21</sup>

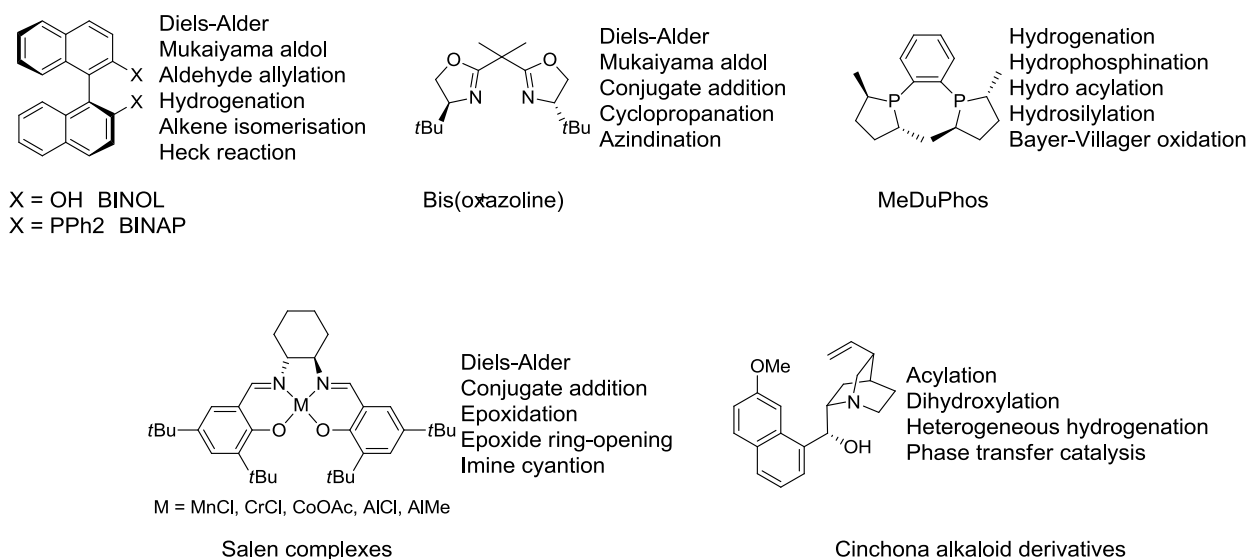


Figure 5: Examples of privileged ligands.<sup>22</sup>

In most cases the chiral moieties (the ligands) were covalently attached to the active site (the metal centre) to facilitate the transfer of chiral information.<sup>23</sup> In organometallic catalysis these enantiopure ligands were very diverse. This diversity was not limited to the ligand structure and metal centre but also to the type of reaction which is catalysed. Some of these catalysts can achieve high *ee*'s over a range of reactions and are denoted as “privileged ligands” (Figure 5).<sup>22</sup>

## 1.5 Enzymes

### 1.5.1 Natural enzymes

Enzymes are proteins, often containing a reactive cofactor, which can catalyse chemical reactions.<sup>24</sup> Enzymes have evolved over millennia and therefore, it is not surprising that they are highly efficient and selective catalysts.

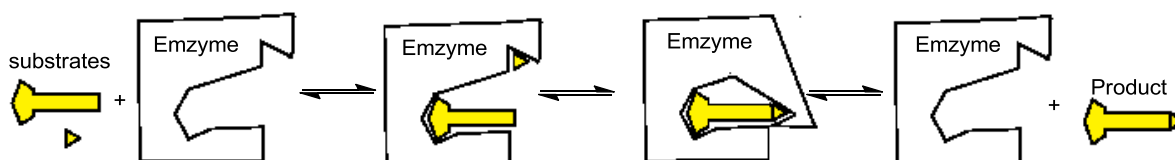


Figure 6: Schematic representation of the action of an enzyme

The active site is often buried deep inside the enzyme surrounded by the side chains of the amino acids that are in the vicinity. It is believed that the substrate is extracted from the

aqueous media and forms a complex with the enzyme (ES) in the active site. Once the reaction is complete the product is released freeing the active site for another cycle.<sup>25</sup> It is believed that the substrate is held in place *via* various noncovalent interactions such as hydrogen bonding, Van de Waals interactions, sulfur bridges and hydrophobic interactions.<sup>24</sup>

Proteins consist of amino acids which are connected to each other *via* stable amide bonds. These bonds have a partial double bond character (Figure 7) which reduces the flexibility and together with hydrogen bonding, disulfide bonds and hydrophobic effects help form the 3-dimensional structures that are required for biological activity. Proteins however are not rigid and can change their shape to bind substrates. This ability to change shape is caused by the free rotation around the C-C<sub>carboxyl</sub> bond which are single bonds (Figure 7).<sup>26</sup>

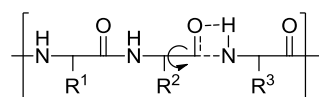


Figure 7: Coupled amino acids

Among the theories that exist to explain the mechanism of how an enzyme works the following two are most widely accepted. The first dates back to 1894 when Emil Fischer developed the “lock and key” model to explain how an enzyme works. Fischer speculated that the substrate (key) had to fit into the enzyme (lock). This would explain both the excellent enantioselectivity and substrate specificity.<sup>25</sup> However in Fischer’s model the enzyme was rigid and we now know that this is not the case.<sup>14</sup>

More recently (late 1960’s) Koshland revised this mechanism, giving rise to the induced fit theory (Figure 6). This theory assumes that a substrate binds to an active site and once bound the enzyme can wrap itself around the substrate thus changing the properties of the active site. However not all the substrates, which bind to the active site, induce a reaction. The most likely reason for this is that the active site is unable to rearrange itself into the required form.

Proteins are remarkable catalysts having many attractive features like providing high chemo-, regio- and stereoselectivities in reactions containing substrates with multiple functional groups and achieving this with exceptional turnover frequencies (TOF). This selectivity means that by employing enzymes lengthy procedures with protecting and deprotecting sequences of functional groups can potentially be avoided.

The benefits of using enzymes to catalyse chemical reactions has not been lost on chemists as they have been employing enzymes in organic chemistry for over one hundred years including several industrial applications.<sup>27</sup>

### 1.5.2 Artificial metalloproteins

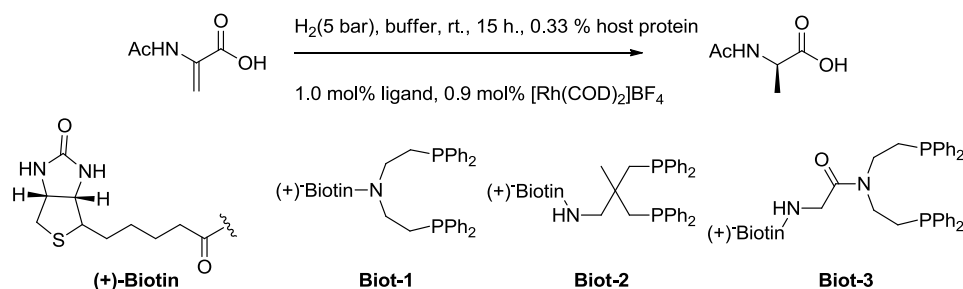
A great deal of effort has been applied to the manufacture of artificial metalloproteins for the purpose of catalysis and biomedicines as well as O<sub>2</sub> storage (Table 2).<sup>28</sup> As mentioned earlier enzymes are very efficient catalysts but unfortunately cannot assist in all the conversions that are beneficial in today's society. To enable enzymes to catalyse these reactions a substantial amount of work has been put into enzyme modification and transition metals have been introduced into the chiral environment of proteins. This is relatively new approach because in the past it was difficult and expensive to synthesise the desired protein. This field has seen an exponential growth due to developments made in protein manufacturing such as the development of cloning techniques, site-directed mutagenesis, protein expression and polymerase chain reactions (PCR).<sup>19</sup>

Table 2: Overview of proteins and metal complexes for the preparation of artificial metalloproteins and their functions

Protein	Metal complex	Function
<b>Myoglobin</b>	Heme derivatives	O <sub>2</sub> storage/Electron transfer
	Cr and Mn Schiff base complexes	Catalyst
<b>(Strept)avidin</b>	Biotinated Rh and Ru complexes	Catalyst <sup>29</sup>
<b>Albumin</b>	Hume, Cu and Rh complexes	Catalyst/O <sub>2</sub> + storage
<b>Lysozyme</b>	Ru and Cu complexes	Metal drug
<b>Kinase</b>	Ru complex	Inhibitor
<b>Virus</b>	Au, CoPt and FePt clusters	Material

One of the first studies on artificial metalloenzymes was done in the late 1970s. By embedding an achiral homogeneous catalyst within a protein, Whitesides and Wilson<sup>30</sup> pioneered the concept of artificial metalloenzymes and created a hybrid catalyst. Avidin was chosen as the protein because of its characterised structure and ability to bind tightly to biotin. Biotin was functionalised with a bidentate phosphine moiety (**Biot-1**, Scheme 3) and the tight binding ensures that the catalytic site does not migrate. When avidin-**Biot-1** complex was coordinated to a rhodium species and used in the hydrogenation of  $\alpha$ -acetamidoacrylic

acid, a modest *ee* of 44% was achieved. The observed *ee* was attributed to avidin as no noticeable *ee* was observed when only the **Biot-1** rhodium complex was used.



Scheme 3: Biotin modified with a bidentate phosphine

The modest *ee* that Whitesides obtained with avidin led Ward *et al.*<sup>29</sup> to question the affinity that the **Biot-1** rhodium complex had for avidin. They reasoned that at neutral pH avidin would have a cationic character (Isoelectric point (pI) = 10.4) and therefore the cationic rhodium complex would be forced away by coulomb repulsion. Therefore they opted to use streptavidin which like avidin readily binds to biotin ( $K_a$  ca.  $10^{14} M^{-1}$ ) but has a pI of 6.2. The deeper binding pocket of streptavidin, compared to avidin, could also have a beneficial effect.

Table 3: Results from Ward *et al.* on hydrogenation of  $\alpha$ -acetamidoacrylic acid using a metalloenzyme

Entry	Ligand	Host protein	Buffer	<i>ee</i> (%)
1	Biot-1	Avidin	Phosphate	37 ( <i>S</i> )
2	Biot-2	Avidin	MOPS <sup>a</sup>	0
3	Biot-1	Streptavidin	Acetate	92 ( <i>R</i> )
4	Biot-2	Streptavidin	Acetate	20 ( <i>S</i> )
5	Biot-3	Avidin	MOPS	60 ( <i>S</i> )
6	Biot-3	Streptavidin	Acetate	24 ( <i>S</i> )

<sup>a</sup>4-Morpholinepropanesulfonic acid

Their results are depicted in Table 3. When avidin was used as the host protein in combination with biotinylated amino-diphosphine ligands **Biot-1** and **Biot-2** low enantiomeric excesses were obtained (entries 1 and 2). By changing the protein to streptavidin higher enantiomeric excesses were attained (compare entries 1 with 3 and 2 with 4). Both the active site of the protein and the phosphine ligand can be modified to improve the *ee*, providing the association constant remains high.<sup>29</sup>

## 1.6 Oligonucleotides as catalysts

### 1.6.1 Unmodified nucleic acids

Enzymes are not the only catalysts that nature employs. It is believed that before enzymes evolved, ribonucleic acids (RNAs) were the catalyst of choice. This led to the development of the “RNA world” theory. This hypothesis started taking shape back in 1968 by Crick<sup>31</sup> and Orgel<sup>32</sup> but the term was not introduced until 1986 when Gilbert<sup>33</sup> used it for the first time. This theory was further strengthened when RNA molecules with catalytic properties were discovered. One example of the catalytic activity of RNA is ribosomal RNA (rRNA) which catalyses and regulates protein synthesis.<sup>34</sup>

It is truly remarkable that with just 4 different chemical subunits RNA has a multitude of functional structures. This potential of forming different structures can be very beneficial for catalysis.<sup>35</sup> It is conceivable that RNA achieves its selectivity by using the induced fit mechanism.<sup>36</sup> Mono-valent metal-ions such as sodium ( $\text{Na}^+$ ) and potassium ( $\text{K}^+$ ) primarily affect the secondary structure while divalent ions like magnesium ( $\text{Mg}^{2+}$ ) and calcium ( $\text{Ca}^{2+}$ ) have a profound effect on the tertiary structure of RNA. With the help of these ions RNA can adopt structures akin to those of a protein (Figure 8).<sup>34</sup> Besides helping the folding of RNA metal ions help to stabilise the molecule.<sup>37</sup>

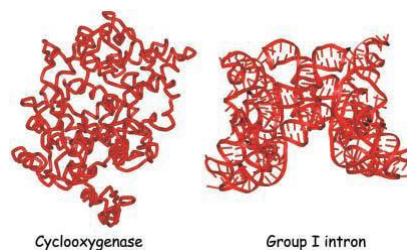


Figure 8: Structure of a protein (left) and RNA molecule (right) of similar size<sup>34</sup>

Over time nature made the transition from a purely “RNA world” to a “RNA-DNA-protein world”. It is assumed that nature evolved from using RNA to store genetic data to DNA (deoxyribonucleic acid), because of the chemical stability of the DNA backbone.<sup>38</sup> RNA and DNA are both nucleic acids which use nucleotides as building blocks. These nucleotides consist of a furanose sugar moiety and one of five bases. These subunits are held together *via* phosphodiester bridges to form a strand (Figure 9).<sup>24</sup>

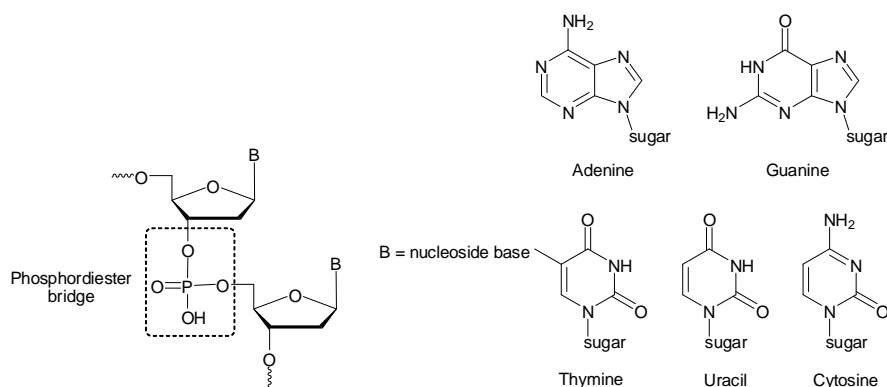


Figure 9: Nucleotides found in RNA and DNA.

The bases are derivatives of either pyrimidine or purine. The most common of these are cytosine (C), thymine (T), uracil (U), adenine (A) and guanine (G) (Figure 9). Cytosine, adenine and guanine can be found in both DNA and RNA. However thymine is primarily found in DNA while uracil is found in RNA. To distinguish between DNA and RNA strands a lowercase letter “d” which denotes deoxy, precedes the abbreviation of the base in DNA.<sup>26</sup>

The most substantial difference between RNA and DNA can be attributed to the furanose sugar moiety. In RNA the sugar moiety has three hydroxyl groups and is known as a ribose group while DNA has only two hence the name deoxyribose (Figure 10).<sup>26</sup> The extra hydroxyl group in RNA is also a reason why RNA is less stable than DNA. This 2'-hydroxyl group makes the phosphodiester linkage more prone to nucleophilic cleavage.

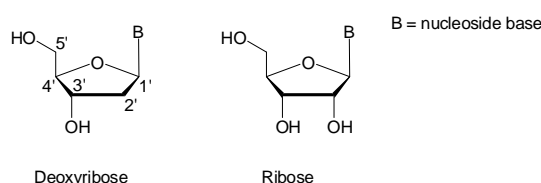


Figure 10: The sugar moieties found in DNA and RNA

In the late 1940's Chargaff discovered that the bases found in RNA and DNA form unique pairs. Cytosine and guanine bind to each other *via* three hydrogen bonds and adenine and thymine/uracil form the other pair and are held together *via* two hydrogen bonds (Figure 11). This is known as Chargaff's rules and more commonly as Watson and Crick base pairs.<sup>26</sup>

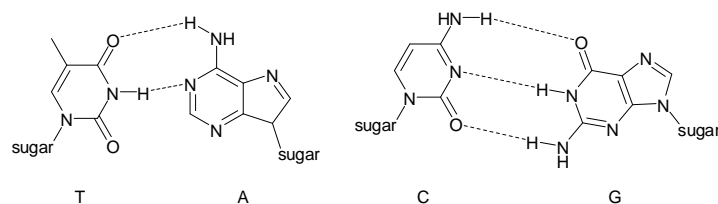


Figure 11: H-bonding between base pairs

Watson and Crick took advantage of Chargaff's findings and in 1953 concluded that DNA was a complementary double helix.<sup>26</sup> Two polynucleotide strands run in opposite direction and coil upwards from left to right to form a right handed helix. In the helix the polar sugar phosphate backbone is on the outside and the hydrophobic bases are stacked on the inside (Figure 12). Generally base pairing is perpendicular to the helix central axis. The helix is further stabilised *via*  $\pi$ - $\pi$  stacking of the bases on the same strand. The helix also forms two observable grooves namely a major and a minor.<sup>24,26</sup> A complete rotation of the double helix requires 10-10.5 bases and has a diameter of about 20 Å. The stacked bases are separated by 3.4 Å.<sup>39</sup> The DNA double helix described above is known as the B-DNA and is the most common double helix found in nature. DNA is very dynamic and other helices are also obtainable, the most renowned of these are known as A- and Z-DNA (Figure 12).

A-DNA is known as the dehydrated form and is found when the humidity is below 75 % so less water binds to the phosphate backbone. Like B-DNA it is a right handed double helix and contains a major and a minor groove, however it is shorter and wider and the bases are tilted about 19° out of plane. This structure is not confined to DNA, as RNA hairpins and RNA-DNA hybrids also adopt this form.<sup>26</sup>

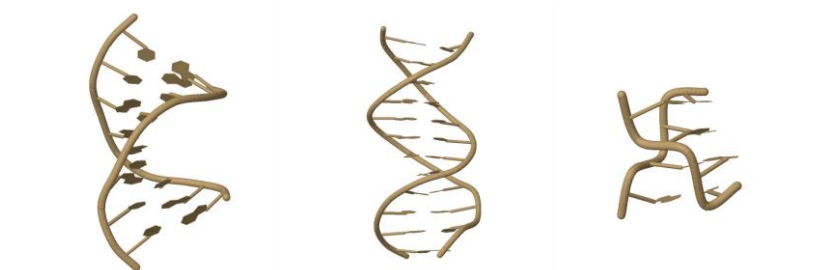


Figure 12: Three crystal structures of DNA from left to right A (5'-d(CCGGCC)-3'<sup>40</sup>, B (5'-d(CGC GAA TTC GCG)-3'<sup>41</sup> and Z (5'-d(CGC G)-3'<sup>42</sup>

Z-DNA was first resolved by Rich *et al.*<sup>43</sup> in 1979 and has different properties than both A- and B-DNA. Most noticeable is that the double helix is left handed. Unlike the other two forms only one deep helical groove. Z-DNA consists of short strands composed primarily of C and G bases.<sup>26</sup>

Double stranded DNA is the most abundant form of DNA although triple stranded DNA also exists. Early results showed that triple stranded DNA can form wherever there is a continuous sequence of purine bases in the DNA strand. Triple stranded DNA can obtain the A-form and consists of 11 to 12 bases per turn.<sup>44</sup> When there is a high concentration of G bases quadruplexes can form which are known as G4 structures. These structures are planar assemblies of four guanines bound together *via* Hoogsteen base pairing (Figure 13). The guanine bases can be located on one strand or multiple strands.<sup>45</sup>

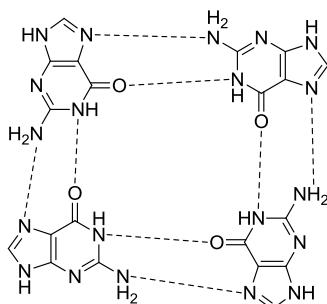


Figure 13: G-quadruplex structure held together *via* Hoogsteen hydrogen bonding.

Understanding how DNA helices are formed has facilitated the synthesis of 2- and 3-dimensional structures. DNA makes an ideal scaffold to build supra-molecular structures.<sup>46</sup> The formation of base pairs is energetically favourable and therefore DNA helices are formed so that the maximum number of bases are paired.

DNA nanotechnology generally utilises branched DNA structures containing junctions. One of simplest branched structures that can be envisioned is a four-arm junction which can be formed using four separate single strands of DNA. These strands are partially complementary to each other and contain single stranded end parts known as sticky ends (Figure 14).

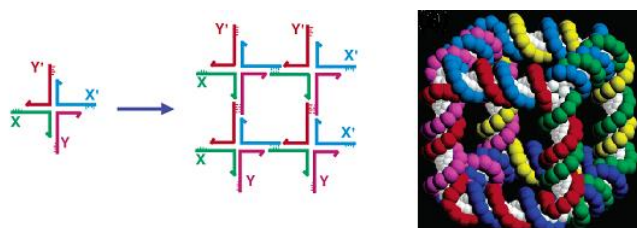


Figure 14: DNA superstructures containing sticky ends<sup>47</sup>

These junctions can be used as the backbone for constructing polygonal and polyhedral stick figure devices. The “sticks” or lines signify the double helix DNA, while the branches are the junctions where the helices come together.<sup>48</sup> For 30 years the sticky-ended cohesion has been used in genetic engineering for directing the assembly of DNA molecules.<sup>47a</sup>

Rothemund<sup>49</sup> has made 2-dimensional structures of DNA (see Figure 15). The scaffold is held in place by over 200 short oligonucleotides the so-called “staple strands”. These short double helices are placed parallel to each other within the scaffold and are held in place by a periodic collection of crossovers. This is then filled with a long single DNA strand of about 900 nucleotides which is folded back and forth. The resulting structure has a spatial resolution of 6 nm and is roughly 100 nm in diameter. Complex patterns have been synthesised using this method.

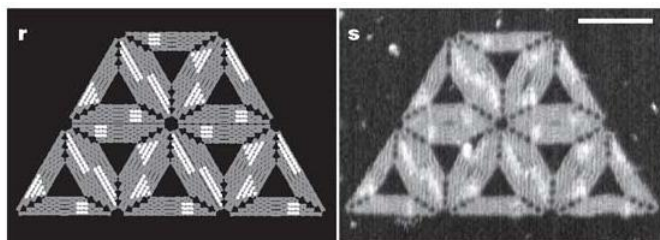


Figure 15: Left the model, right the experimental result using Rothemund’s method<sup>50</sup>

#### 1.6.1.1 The effect of metals on DNA helices

Like with RNA molecules metal ions have a profound effect on the stability and binding properties of DNA. Riggs *et al.*<sup>51</sup> demonstrated this back in the early 1970’s by comparing the binding constant of DNA with a *lac* repressor protein in 0.01 M MgCl<sub>2</sub> and either 0.01 M or 0.18 M of KCl. The binding constant decreased by two orders of magnitude when the concentration of the KCl solution was increased from 0.01 M to 0.18 M. The binding constant was further decreased by excluding MgCl<sub>2</sub>.<sup>52</sup> Lyons and Kotin,<sup>53</sup> Bauer<sup>54</sup> and Ott *et al.*<sup>55</sup> observed that low concentrations of magnesium had a stabilising effect on the helices, but high concentration tended to lower the helix coil melting temperatures. High concentrations of transition metals also have a destabilising effect on the DNA helix causing base pair dissociation at lower temperatures than with mono-valent alkali metal ions or divalent alkaline earth ions.<sup>56</sup>

#### 1.6.2 Aptamers

Oligonucleotides which bind effectively to a wide range of molecules are called aptamers.<sup>57</sup> Aptamer comes from the Latin word *aptus* meaning to fit and it is used for DNA and RNA molecules that specifically bind to target molecules from proteins to small organic and inorganic molecules. Aptamers are generally short oligonucleotides consisting of about 30 to a few hundred nucleotides. Smaller aptamers do exist as Anderson and Mecozzi<sup>58</sup> showed with their 13 nucleotide aptamer that binds theophylline but they are rare.

Since the advent of Systematic Evolution of Ligands by EXponential enrichment (SELEX) by Tuerk *et al.*<sup>59</sup> and Ellington *et al.*,<sup>46</sup> in the 1990s it has been used to identify aptamers. A benefit of using oligonucleotide aptamers is that they can be rapidly synthesised using a DNA synthesiser.<sup>60</sup> The great advantage of the SELEX method is that nucleotides that bind selectively to target molecules can be identified from large populations of random oligomers<sup>57</sup> (Figure 16). SELEX is typically performed utilising oligomers that are longer than 20 bases in length<sup>61</sup> and are flanked by defined 5' and 3' primer sequences that are generally 18-24 bases in length.<sup>60</sup>

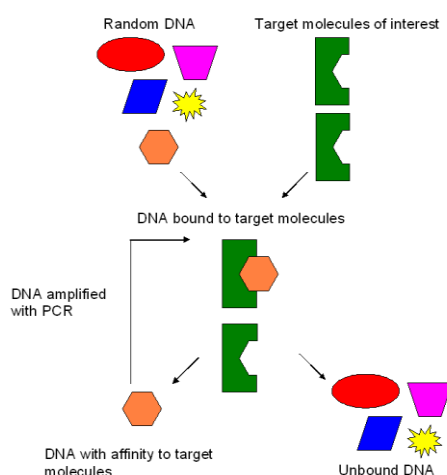


**Figure 16: A schematic representation of SELEX**

In Figure 16 a schematic representation of SELEX is given. First a library of random single stranded oligonucleotides<sup>57</sup> is synthesised *via* a DNA synthesiser using a mixture of nucleosides. This is then amplified using PCR. The affinity of DNA/RNA molecules for the substrate is investigated by loading the nucleic acids onto a column packed with immobilised target molecules. After washing away all the molecules that show no affinity to the targets, the bound DNA is removed by eluting the column with a solution containing target molecules. Using PCR the eluted strands are amplified again and the process is repeated. This is done several times until the percentage of nucleic acids that are washed away is small leaving behind only the DNA/RNA molecules that shows a high affinity for a target compound.<sup>60</sup>

## 1.6.3 Artificial metallo nucleic acids

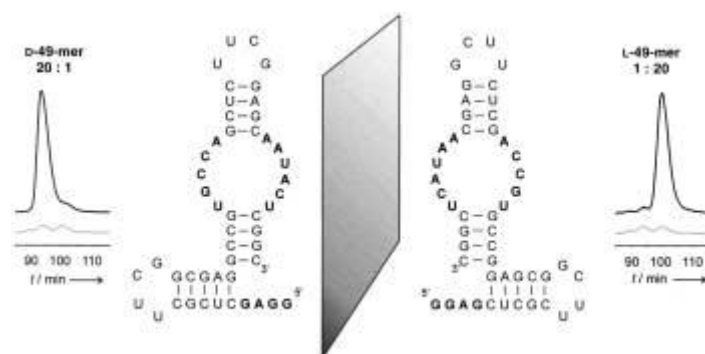
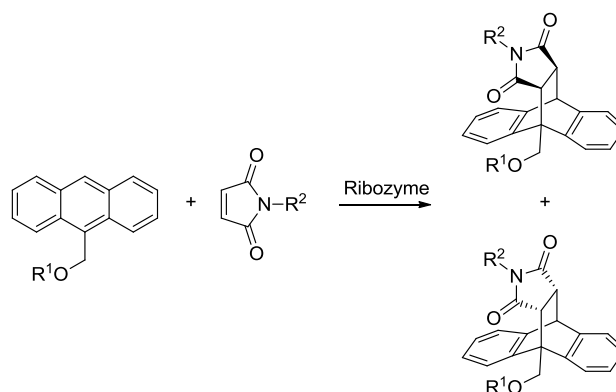


Figure 17: Left: the HPLC trace of the Diels-Alder reaction catalysed by D-RNA and a representation of D-RNA, Right: the HPLC trace of the Diels-Alder reaction catalysed by L-RNA and a representation of L-RNA. The light gray trace in the chromatogram corresponds to the uncatalysed background reaction.<sup>62</sup>

In 2000 Jäschke *et al.*<sup>63</sup> reported that a 49-mer D-RNA enzyme, a ribozyme composed of D-nucleotides (Figure 17), accelerated the bimolecular C-C bond formation between anthracene derivatives and small maleimides through a Diels-Alder reaction (Scheme 4). In the uncatalysed reaction the expected racemate was obtained however when the D-RNA enzyme was employed 90 % *ee* was obtained. This good enantioselectivity can be attributed to the fact that the RNA molecule is a homochiral molecule. When the mirror image (a synthetic 49-mer composed of nucleotides with the L-configuration (L-RNA), Figure 17) was employed a similar reaction rate was observed and the opposite enantiomer was formed.<sup>63</sup>



Scheme 4: Diels-Alder reaction catalysed by a RNA enzyme reported by Jäschke

The increasing popularity of replacing organic solvents with water and the discovery of RNAzymes has fuelled the interest in using nucleic acids as catalysts. Two approaches can be envisioned for the introduction of transition metal complexes into the chiral environment of a DNA molecule. Firstly a metal-ligand complex can be introduced *via* a non-covalent approach with the help of intercalators or groove binders and secondly it can be covalently attached to the nucleotide (Figure 18).

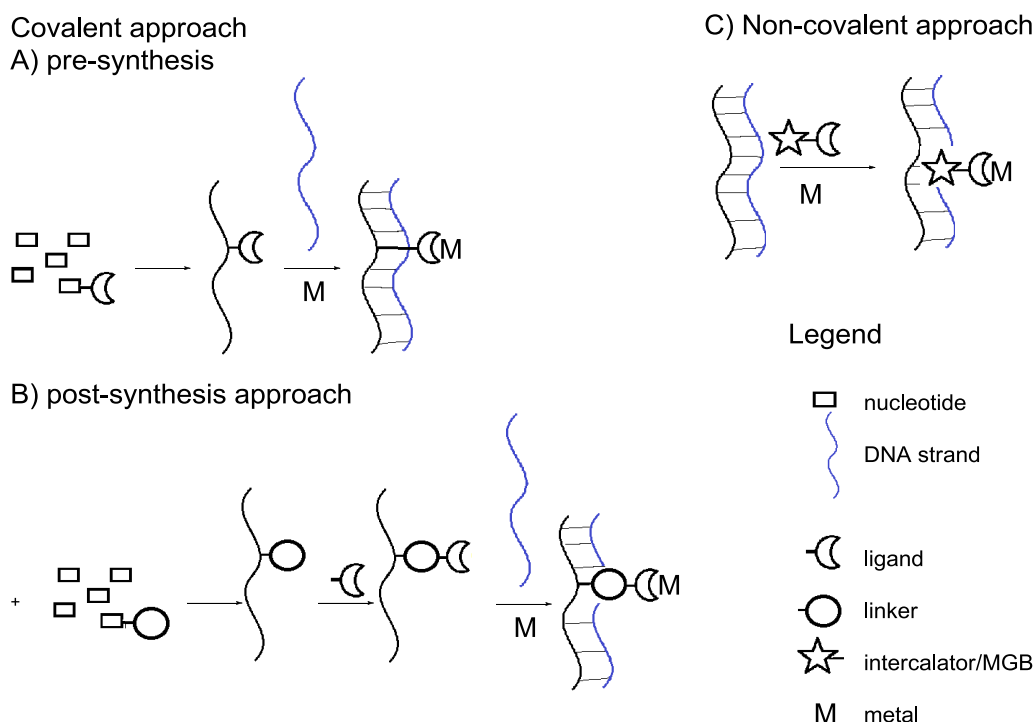


Figure 18: Schematic representation of DNA-based asymmetric catalysis using the supramolecular (A) covalent (B) non-covalent

The difference between groove binders and intercalators is where they bind. In Figure 19 a schematic representation is shown depicting a groove binder (thick vertical line, A) in a double helix and an intercalator (horizontal thick line) binding to a double helix (B). In principle groove binding substances fit into the minor or major groove without causing major changes to the helix. An intercalator on the other hand by definition stacks itself between successive base pairs,<sup>64</sup> which does affect the double helix.

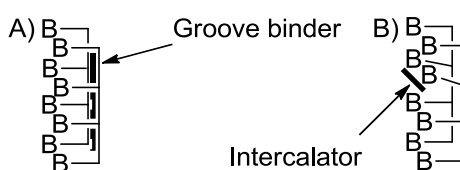
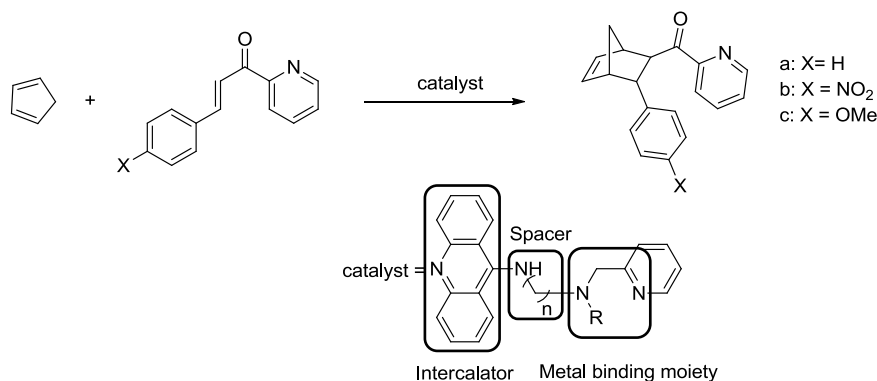


Figure 19: A) Schematic representation of a groove binder (fat vertical line), B) Schematic representation of an intercalator (fat horizontal line)

In 2005 Roelfes and Feringa<sup>65</sup> reported an asymmetric Diels-Alder reaction catalysed by a DNA-based metal catalyst. Salmon testes DNA were used for this study. The catalyst complex was formed *in situ* by reacting Cu(II) with a ligand which consists of a DNA intercalator such as 9-aminoacridine, a spacer and a metal binding group (Scheme 5).

A series of control experiments were carried out whereby one of the three elements of the catalyst was excluded in each reaction. The results indicated that DNA, a ligand and Cu(II) were needed to obtain *ee*. The ligand and the spacer length played a crucial role in obtaining

good *enantiomeric excesses*. With  $n = 1$  (Scheme 5) an *ee* of 49% was obtained however when the chain length was increased to 5 carbons the *ee* was negligible.



**Scheme 5: DNA catalysed asymmetric Diels-Alder**

Roelfes *et al.*<sup>66</sup> have since optimised this approach by removing the need for a spacer entirely (Figure 20). This was achieved by utilising achiral copper complexes based on bidentate ligands known to intercalate with DNA. As a result the reactive Cu(II) centre was brought in closer vicinity to the DNA double helix and as a result the *ee* increased dramatically from 49% *ee* to 96 %.<sup>66</sup>

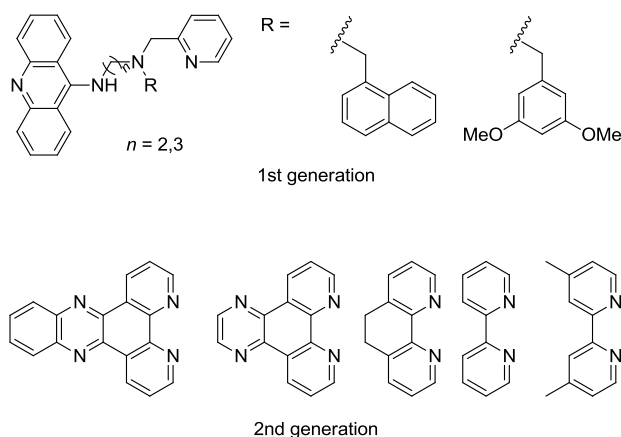
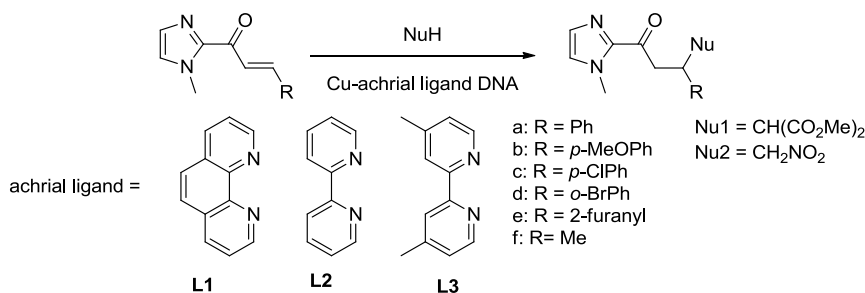


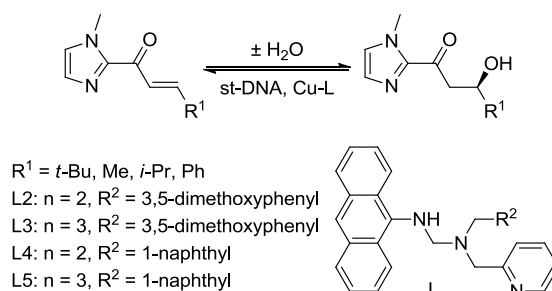
**Figure 20: First and second generation intercalators for DNA based catalysis**

In 2007 Roelfes *et al.*<sup>67</sup> used their approach to catalyse Michael additions in water. Using Salmon testes DNA and a copper catalyst coordinated to **L3** high enantiomeric excesses of up to 99% could be obtained (Scheme 6). These reactions could be performed on a preparative scale with the possibility of recycling the catalyst. Friedel-Crafts alkylations were also carried out using this method generating enantiomeric excesses of up to 93 %.<sup>68</sup>



Scheme 6: The Michael addition using an artificial DNAzyme

Originally their focus was on reactions that have successively been catalysed by organometallic complexes. In 2010 they reported a method for asymmetric conjugate addition of water to  $\alpha,\beta$ -unsaturated ketones.<sup>69</sup> Synthesising chiral  $\beta$ -hydroxy ketones, a structural building block for the synthesis of natural products, *via* the asymmetric conjugate addition of water to  $\alpha,\beta$ -unsaturated ketones is problematic when using transition metal catalysts especially when the reactions take place in water. Hydratase enzymes can catalyse such transformation with high enantiomeric excesses however the substrate scope is limited. Similar to their other endeavours Roelfes *et al.*<sup>69-70</sup> have employed salmon testes DNA along with a catalytically active Cu<sup>2+</sup> complex (Cu-L). Their model reaction was the hydration of 2-acyl imidazole to form  $\beta$ -hydroxy ketone (Scheme 7).

Scheme 7: The hydration of 2-acyl imidazole to form  $\beta$ -hydroxy ketone

The minimum catalyst loading required was 3 mol% which corresponds to a ratio of Cu-complex to DNA base pair of 1:6. Utilising the lower catalyst loading had an effect on both the conversion and the *ee* (Table 4).

Although this research shows that metallo-DNA catalysis is possible there is a major problem with their approach. The ligands bind randomly to the double helix in multiple locations. Therefore, there are several different catalytic sites and it is difficult to determine which site is responsible for the observed selectivity and hence it cannot be easily optimised to improve its performance.

Table 4: Hydration of 2-acyl imidazoles to form  $\beta$ -hydroxy ketones

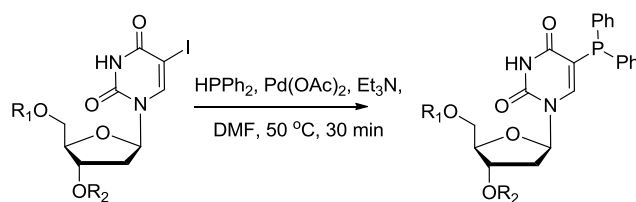
Entry	R <sup>1</sup>	Reaction time (h)	Ligand	Conversion (%)	ee (%)
1	<i>t</i> -Bu	24	L2	55	72 ( <i>R</i> )
2	Me	7	L2	100	72 ( <i>R</i> )
3	<i>i</i> -Pr	7	L2	71	60 ( <i>R</i> )
4	Ph	24	L2	0	--
5	<i>t</i> -Bu	24	Cu(NO <sub>3</sub> ) <sub>2</sub>	20	42 ( <i>S</i> )

The results of Roelfes and Feringa were impressive nevertheless some groups have opted to use the covalent approach. The greatest advantage of this approach is that it enables a certain amount of control in adapting the chiral environment of the transition metal. In this approach the nucleotide is modified to allow coordination of a transition metal.

In 2010 Jäschke *et al.*<sup>71</sup> modified a nucleotide with a diene functionality. This was subsequently coordinated to iridium and tested in allylic amination. Although the *enantiomeric excesses* were low (around 20 %) they did notice that the complementary strand had an effect on the observed *ee*. When single stranded DNA was used an *ee* of up to 24% was found on the other hand when double stranded DNA was used the *ee* was negligible. When RNA was used as the complementary strand the other enantiomer was obtained.

Phosphines are more versatile ligands than dienes so ideally we would like to employ this functional group. Phosphine chemistry has been employed in other branches of DNA chemistry. Triphenylphosphine has been introduced into one DNA strand while the other strand holds a fluorescein-labelled probe containing an  $\alpha$ -azido ether linker connected to a fluorescence quencher. When the two strands are mixed together the phosphine reacts with the azide and cleaves the linker thus liberating the fluorescence quencher and allowing fluorescence to be detected.<sup>72</sup> The phosphine modified DNA strand was purified by HPLC. Mass spectrometry showed the presence of phosphine oxide which they presumed happened during purification;<sup>73</sup> however this could also have happened during sample preparation for mass spectrography.

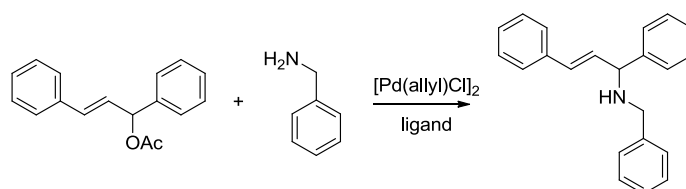
In the method employed by our group<sup>74</sup> we incorporate a modified nucleotide into a DNA strand which was subsequently coupled to a ligand containing a phosphine (Scheme 8). This nucleotide was then coordinated to a transition metal.



$R^1=R^2=H$  (dppdU);  $R^1=R^2=Ac$  (AcddppdU);  $R^1=$  deoxyadenosine-3-phosphate,  $R^2=$  deoxythymidine-5-phosphate dinucleotide dAdppdUdT)

**Scheme 8: Synthesis of 5-diphenylphosphine-2'-deoxyuridine**

When the monodentate ligand dppdU, where dpp is diphenylphosphine, was used in palladium catalysed asymmetric allylic amination (Scheme 9) an *ee* of up to 82% was obtained. Like in previously mentioned reactions the solvent influenced the *ee*, when THF is used the absolute configuration was *S* while in DCM it was *R*. Unfortunately when trinucleotides dAdppdUdT and dCdppdUdG were used the *ee* dropped.<sup>74</sup>



**Scheme 9: Asymmetric allylic amination: addition of benzylamine to 1,3-diphenyl-2-propenyl acetate**

Recently we have managed to introduce a phosphine moiety onto a long DNA strand (15 nucleotides) and coordinate  $[PdCl(\eta^3\text{-allyl})]$  to it.<sup>75</sup> Caution had to be taken to avoid oxidation of the phosphine moiety although Jäschke *et al.*<sup>76</sup> reported that their phosphine modified DNA was stable under HPLC conditions and two of the strands were sufficiently stable on storage in solution. This illustrates the importance of choosing the sequence of the nucleotides.

The examples above show that both DNA and RNA are well-suited scaffolds for the development of hybrid transition-metal catalyst. There are however a number of reasons to focus on the use of DNA over RNA. Firstly DNA nucleotides cost considerably less than RNA nucleotides.<sup>77</sup> This can be attributed to the protection of the 2'-OH of RNA during oligonucleotides synthesis. Secondly DNA is both chemically and biochemically more stable; furthermore DNA synthesis gives slightly better yields than RNA synthesis.

## 1.7 Project Aim and thesis outline

As mentioned earlier waste production is a major concern in chemical industry and in particular in the fine chemical industry. In order to combat this waste production, effective catalysts need to be developed. These catalysts have to provide exceptional chemo-, regio- and enantioselectivities rivalling those found in nature, enzymes. Nature's catalysts unfortunately cannot perform all the types of catalysis that play an important part in industry today. Mankind has therefore turned to transition metals to catalyse these reactions. Unfortunately, only a few existing transition-metal catalysts, rival the performance of enzymes.

In recent years a new field has emerged whereby large bio-molecules are used in combination with transition metals. This field aims to combine the powerful molecular recognition properties of biomolecules with the catalytic power of transition metal catalysis, to create artificial metalloenzymes. The selected bio-molecule for this thesis was DNA. DNA is a homochiral molecule which can easily be modified and this is an enormous advantage when designing a catalyst. Furthermore ligands can be used to orientate the substrate in a favourable way, which enhances selectivity. Hydrogen bonding has been used as a tool to accomplish this.<sup>78</sup> The nucleotide is in fact one large ligand which has the potential to form multiple hydrogen bonds and thus orientates the substrate. The DNA ligand can be optimised by altering the 3-dimensional structure of DNA. This can be done by varying the backbone length and composition of the base sequence. By carefully choosing the base sequence hairpins and loops can be generated thus changing the environment of the metal and thus influence the catalytic site (Figure 21).

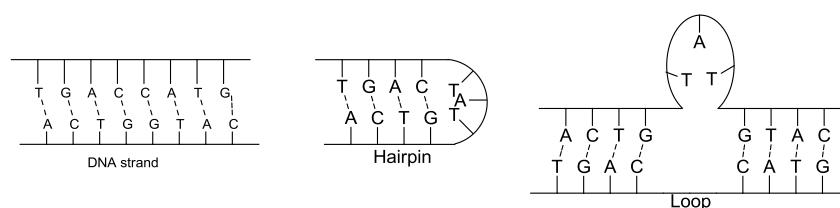


Figure 21: Hairpins and loops in DNA

Two approaches can be envisioned to introduce a transition metal into the double helix. The metal moiety can either be covalently attached to a DNA strand or it can be non-covalently bound. Chapter 2 will focus on the first approach and Chapter 3 on the second. The choice of the ligand coordinating to the metal is vital. Phosphine moieties were selected because they are known to be effective ligands in homogeneous catalysis, especially in combination with

late transition metals for reactions such as hydrogenation and allylic substitution. Phosphines have an additional advantage that they coordinate more strongly to the late transition metals used in these reactions than nitrogen which is abundant in DNA, thus reducing the chances of creating multiple catalytic sites during catalysis. In Chapter 4 the following catalytic reactions with phosphine nucleotides as catalysts will be discussed: allylic substitution, 1,4-dipolar cycloaddition and hydroformylation.

## 1.8 References

1. Bounama, C.; von, B. W.; Franck, S., *Astrobiology* **2007**, *7* (5), 745-756.
2. Thomas R. Karl, J. M. M., Thomas C. Peterson, (eds), *Global Climate Change Impacts in the United States*. Cambridge University Press: United States of America, 2009.
3. Khilyuk, L.; Chilingar, G., *Environmental Geology* **2006**, *50* (6), 899-910.
4. Michaels, P. J., Science behind the times? *The Washington Times* 2003.
5. Sheldon, R. A., *Green Chem.* **2007**, *9* (12), 1273-1283.
6. (a) Trost, B. M., *Angew. Chem. Int. Ed.* **1995**, *34* (3), 259-281;(b) Trost, B. M., *Science* **1991**, *254* (5037), 1471-1477.
7. Tabone, M. D.; Cregg, J. J.; Beckman, E. J.; Landis, A. E., *Environ. Sci. Technol.* **2010**, *44* (21), 8264-8269.
8. Constable, D. J. C.; Curzons, A. D.; Cunningham, V. L., *Green Chem.* **2002**, *4* (6), 521-527.
9. Hudlicky, T.; Frey, D. A.; Koroniak, L.; Claeboe, C. D.; Brammer, L. E., Jr., *Green Chem.* **1999**, *1* (2), 57-59.
10. EPA *Twelve principles of green chemistry* Science Matters newsletter. **June 2011**  
<http://www.epa.gov/sciencematters/june2011/principles.htm>.
11. Leeuwen, P. W. N. M., *Homogeneous Catalysis understanding the Art*. Kluwer Academic Publishers: Dordrecht, 2004.
12. Gates, B. C., *Catalytic Chemistry*. John Wiley & sons inc.: 1992.
13. Thomas, J. M.; Thomas, W. J., *Principles and practice of heterogeneous catalysis*. Wiley VCH: 1997; p. 669.
14. Faber, K., *Biotransformations in Organic Chemistry*. 4th ed.; Springer: Berlin, 2000.
15. Thomas, C. M.; Ward, T. R., *Chem. Soc. Rev.* **2005**, *34* (4), 337-346.
16. Knowles, W. S., *J. Chem. Educ.* **1986**, *63* (3), 222-225.
17. Yun, O., *PNAS* **2005**, *102* (47), 16913-16915.
18. Knowles, W. S., Asymmetric Hydrogenations-The Monsanto *L*-Dopa Process. In *Asymmetric catalysis on industrial scale: challenges, approaches and solutions*, H.U., B., Ed. Wiley-VCH: 2004; pp 23-28.
19. Lu, Y., *Angew. Chem. Int. Ed.* **2006**, *45* (34), 5588-5601.
20. Blaser, H.-U.; Adriano, I.; Anita, S., *Curr. Sci.* **2000**, *78* (11), 1336-1344.
21. Pfaltz, A.; Drury, W. J., III, *Proc. Natl. Acad. Sci. U. S. A.* **2004**, *101*, 5723-5726.
22. (a) Yoon, T. P.; Jacobsen, E. N., *Science* **2003**, *299*, 1691-1693;(b) Wei, Y.; Shi, M., *Chin. Sci. Bull.* **2010**, *55*, 1699-1711.
23. Hamilton, G. L.; Kang, E. J.; Mba, M.; Toste, F. D., *Science* **2007**, *317*, 496-499.
24. Stryer, L., *Biochemistry*. 4th ed.; WH Freeman and company: New York, 1995.
25. Stein, R., *Foundations of Chemistry* **2006**, *8* (1), 3-29.
26. Garret, R. H.; Grisham, C. M., *Biochemistry*. 2 ed.; Saunders College Publishing: 1999.
27. Reetz, M. T.; Krebs, G. P. L., *C. R. Chim.* **2011**, *14* (9), 811-818.
28. Abe, S.; Ueno, T.; Wantanabe, Y., *Artificial Metalloproteins Exploiting Vacant Space: Preparation, Structures, and Functions*. Springer Berlin / Heidelberg: 2008; pp 1-19.

29. Collot, J.; Gradinaru, J.; Humbert, N.; Skander, M.; Zocchi, A.; Ward, T. R., *J. Am. Chem. Soc.* **2003**, *125* (30), 9030-9031.
30. Wilson, M. E.; Whitesides, G. M., *J. Am. Chem. Soc.* **1978**, *100*, 306-7.
31. Crick, F. H. C., *J. Mol. Biol.* **1968**, *38* (3), 367-379.
32. Orgel, L. E., *J. Mol. Biol.* **1968**, *38* (3), 381-393.
33. Gilbert, W., *Nature* **1986**, *319* (6055), 618-618.
34. Pyle, A., *J. Biol. Inorg. Chem.* **2002**, *7* (7), 679-690.
35. Talini, G.; Branciamore, S.; Gallori, E., *Biochimie* **2011**, *93* (11), 1998-2005.
36. Xiao, H.; Murakami, H.; Suga, H.; Ferre-D'Amare, A. R., *Nature* **2008**, *454* (7202), 358-361.
37. Cate, J. H.; Doudna, J. A., *Structure* **1996**, *4* (10), 1221-1229.
38. Leu, K.; Obermayer, B.; Rajamani, S.; Gerland, U.; Chen, I. A., *Nucleic Acids Res.* **2011**, *39*, 8135-8147.
39. Seeman, N., *Mol. Biotechnol.* **2007**, *37* (3), 246-257.
40. Wang, A. H.; Fujii, S.; van Boom, J. H.; Rich, A., *Proc. Natl. Acad. Sci.* **1982**, *79* (13), 3968-3972 (PDB ID: 1VTC).
41. Drew, H. R.; Wing, R. M.; Takano, T.; Broka, C.; Tanaka, S.; Itakura, K.; Dickerson, R. E., *Proc. Natl. Acad. Sci.* **1981**, *78* (4), 2179-2183 (PDB ID: 1BNA).
42. Drew, H. R.; Dickerson, R. E., *J. Mol. Biol.* **1981**, *152* (4), 723-736 (PDB ID: 1ZNA).
43. Wang, A. H. J.; Quigley, G. J.; Kolpak, F. J.; Crawford, J. L.; van Boom, J. H.; van der Marel, G.; Rich, A., *Nature* **1979**, *282* (5740), 680-686.
44. Raae, A. J.; Kleppe, K., *Biochemistry* **1978**, *17* (14), 2939-42.
45. Johnson, J. E.; Smith, J. S.; Kozak, M. L.; Johnson, F. B., *Biochimie* **2008**, *90* (8), 1250-1263.
46. Ellington, A. D.; Szostak, J. W., *Nature* **1990**, *346* (6287), 818-822.
47. (a) Seeman, N. C., *Biochemistry* **2003**, *42* (24), 7259-7269;(b) Seeman, N. C., *Biochemistry* **2003**, Reprinted (adapted) with permission from Copyright 2003 American Chemical Society." I;(c) Seeman, N., *Biochemistry* **2003**, *42* (24), 7259-7269, Reprinted (adapted) with permission from Copyright 2003 American Chemical Society.
48. Chen, J. H.; Kallenbach, N. R.; Seeman, N. C., *J. Am. Chem. Soc.* **1989**, *111*, 6402-7.
49. Rothemund, P. W. K., *Nature* **2006**, *440* (7082), 297-302.
50. Rothemund, P. W. K., *Nature* **2006**, *440* (7082), 297-302, Printed with permission from Copyright 2006 Nature.
51. (a) Riggs, A. D.; Suzuki, H.; Bourgeois, S., *J. Mol. Biol.* **1970**, *48* (1), 67-83;(b) Riggs, A. D.; Bourgeois, S.; Cohn, M., *J. Mol. Biol.* **1970**, *53* (3), 401-417.
52. Record Jr, M. T.; Lohman, T. M.; Haseeth, P. d., *J. Mol. Biol.* **1976**, *107* (2), 145-158.
53. Lyons, J. W.; Kotin, L., *J. Am. Chem. Soc.* **1965**, *87*, 1781-5.
54. Bauer, W. R., *Biochemistry* **1972**, *11*, 2915-20.
55. Ott, G. S.; Ziegler, R.; Bauer, W. R., *Biochemistry* **1975**, *14*, 3431-8.
56. Duguid, J. G.; Bloomfield, V. A., *Biophys. J.* **1996**, *70* (6), 2838-2846.
57. Tombelli, S.; Minunni, M.; Mascini, M., *Biosens. Bioelectron.* **2005**, *20* (12), 2424-2434.
58. Anderson, P. C.; Mecozzi, S., *J. Am. Chem. Soc.* **2005**, *127* (15), 5290-5291.

- 
59. Tuerk, C.; Gold, L., *Science* **1990**, *249* (4968), 505-510.
  60. Ito, Y.; Kawazoe, N.; Imanishi, Y., *Methods* **2000**, *22* (1), 107-114.
  61. Bruno, J. G.; Kiel, J. L., *Biosensors & Bioelectronics* **1999**, *14* (14), 457-464.
  62. Seelig, B.; Keiper, S.; Stuhlmann, F.; Jäschke, A., *Angew. Chem. Int. Ed. Engl.* **2000**, *39* (24), 4576-4579, Printed with permission from Copyright 2000 Wiley-VCH Verlag GmbH.
  63. Seelig, B.; Keiper, S.; Stuhlmann, F.; Jäschke, A., *Angew. Chem. Int. Ed.* **2000**, *39*, 4576-4579.
  64. Trieb, M.; Rauch, C.; Wibowo, F. R.; Wellenzohn, B.; Liedl, K. R., *Nucleic Acids Res.* **2004**, *32* (15), 4696-4703.
  65. Roelfes, G.; Feringa, B. L., *Angew. Chem. Int. Ed.* **2005**, *44*, 3230-3232.
  66. Roelfes, G.; Boersma, A.; Feringa, B. L., *Chem. Comm.* **2006**, 635-637.
  67. Deuss, P. J.; den Heeten, R.; Laan, W.; Kamer, P. C. J., *Chem.-Eur. J.* **2011**, *17* (17), 4680-4698.
  68. Boersma, A. J.; Feringa, B. L.; Roelfes, G., *Angew. Chem. Int. Ed.* **2009**, *48* (18), 3346-3348.
  69. Boersma, A. J.; Megens, R. P.; Feringa, B. L.; Roelfes, G., *Chem. Soc. Rev.* **2010**, *39*, 2083-2092.
  70. (a) Roelfes, G.; Boersma, A. J.; Feringa, B. L., *Chem. Commun.* **2006**, (6), 635-637; (b) Roelfes, G.; Feringa, B. L., *Angew. Chem. Int. Ed.* **2005**, *44* (21), 3230-3232.
  71. Hu, Y.-Z.; Tsukiji, S.; Shinkai, S.; Oishi, S.; Hamachi, I., *J. Am. Chem. Soc.* **1999**, *122* (2), 241-253.
  72. Li, H.; Franzini, R. M.; Bruner, C.; Kool, E. T., *ChemBioChem* **2010**, *11* (15), 2132-2137.
  73. Abe, H.; Wang, J.; Furukawa, K.; Oki, K.; Uda, M.; Tsuneda, S.; Ito, Y., *Bioconjugate Chem.* **2008**, *19* (6), 1219-1226.
  74. Ropartz, L.; Meeuwenoord, N. J.; Van der Marel, G. A.; Van Leeuwen, P. W. N. M.; Slawin, A. M. Z.; Kamer, P. C. J., *Chem. Comm.* **2007**, 1556-1558.
  75. Nuzzolo, M.; Grabulosa, A.; Slawin, A. M. Z.; Meeuwenoord, N. J.; van der Marel, G. A.; Kamer, P. C. J., *Eur. J. Org. Chem.* **2010**, *2010* (17), 3229-3236.
  76. Caprioara, M.; Fiammengo, R.; Engeser, M.; Jäschke, A., *Chem.-Eur. J.* **2007**, *13* (7), 2089-2095.
  77. Glen Research, 2006 Catalog. <http://www.glenres.com>: 2006.
  78. Breuil, P.-A. R.; Patureau, F. W.; Reek, J. N. H., *Angew. Chem. Int. Ed.* **2009**, *48* (12), 2162-2165.

## Chapter 2: Covalent approach

### 2.1 Introduction

As mentioned in Chapter 1, ligands coordinating to a transition metal can be introduced into the nucleic acid either non-covalently<sup>1</sup> (Chapter 3) or covalently.<sup>2</sup> This chapter will focus on the covalent approach. Using this approach the ligand can be introduced either *via* a pre-synthesis (oligonucleotide is synthesised) or a post-synthesis (oligonucleotide is modified) protocol<sup>3</sup> (Figure 1). Either way a non-natural oligonucleotide is formed containing a moiety with the desired functionality. In the pre-synthesis protocol a nucleotide is modified with a ligand and subsequently incorporated into an oligonucleotide either by enzymatic means or by chemical DNA synthesis. In post-modification a moiety is introduced to which a ligand can be attached after the oligonucleotide has been synthesised.

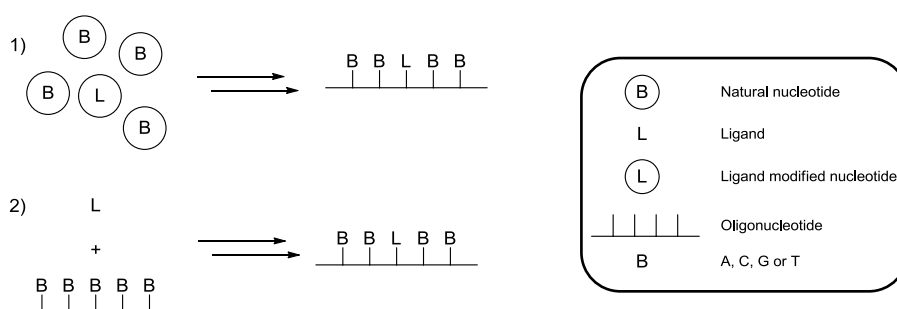


Figure 1: 1) pre-synthetic incorporation of a ligand, 2) post-synthetic incorporation of a ligand

Chemical synthesis of oligonucleotides can take place manually or using automated methods (employing a DNA synthesiser). The automated synthesis takes place on a solid support, often with the first base of the sequence already attached *via* the 3'hydroxyl group. A clear advantage of solid support synthesis is that large excesses of reactants can be used to increase the yield and subsequently washed away. The use of large excesses of reactants ensures that high conversions can be obtained, often approaching 100 %.

In 1964 it was shown that a dipeptide could be synthesised on a styrene-divinylbenzene copolymer and subsequently removed. Letsinger and Mahadevan<sup>4</sup> adopted this approach to synthesise oligonucleotides on a solid support. The phosphorylation was achieved by reacting a  $\beta$ -cyanoethyl phosphate with the nucleoside on the styrene polymer. Short strands of oligonucleotides could effectively be synthesised on a large scale using this approach. This was later improved<sup>5</sup> by using phosphites instead of phosphates to introduce the phosphate into the backbone. Beaucage and Caruthers<sup>6</sup> further optimised the coupling by changing from

phosphorochloridites ( $\text{ROPCl}_2$  or  $\text{ROP}(\text{OR}')\text{Cl}$ ) to phosphoramidites. This simple change revolutionised DNA synthesis and is now widely used in (automated) DNA synthesis.

The sugar moiety of a deoxy nucleoside contains two hydroxyl groups therefore one needs to be protected to avoid double phosphorylation when introducing the phosphoramidite. Fortunately the two hydroxyl groups have different reactivities. The 5' hydroxyl group is a primary functionality and therefore more reactive. This group is first protected with a DMT-group (4,4'-dimethoxytrityl). After this the 3' hydroxyl group can be phosphorylated (Figure 2). The advantage of using DMT as protecting-group is that upon removal a red DMT-cation is formed. This cation is used to quantitate the efficiency of the coupling either *via* UV spectroscopy or more regularly in automated synthesis by measuring the conductivity of the trityl cation in the waste mixture.

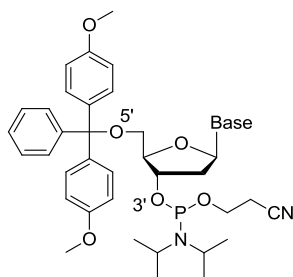
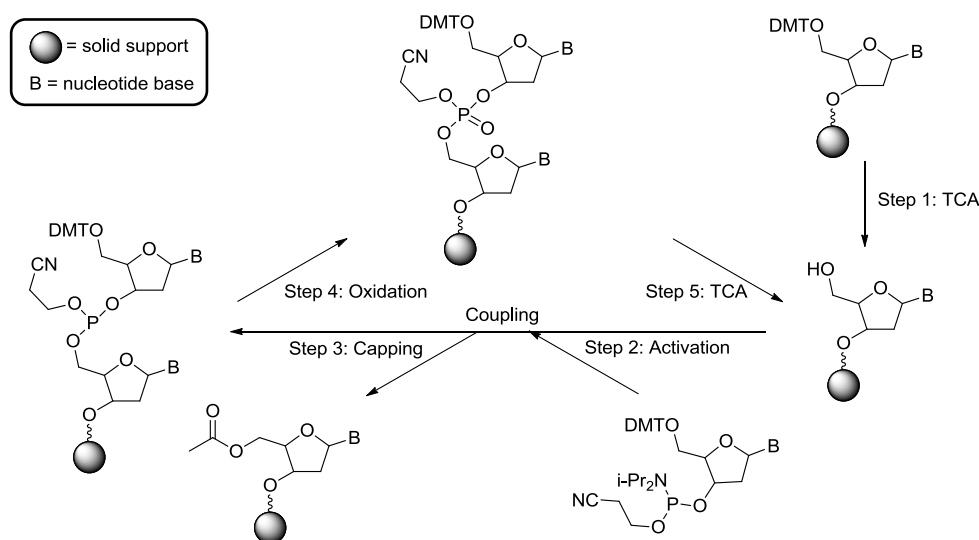


Figure 2: Nucleoside functionalised for DNA synthesis

The automated synthesis (Scheme 1) proceeds from 3' to 5' with the initial 3' hydroxyl group attached to the solid support, and the 5' hydroxyl group of the growing strand is protected with a DMT- group. This protecting group is removed by the addition of an acid (often TCA (trichloroacetic acid)). An activated phosphoramidite is added which subsequently reacts with the liberated hydroxyl group. Ideally the yield of this coupling is 100% but this is not always the case, especially in the past, therefore a capping agent, generally a mixture containing acetic anhydride, is added to cap the 5' hydroxyl group. The capping prevents unreacted smaller chains from growing and thus simplifies purification. The final step in the synthesis is the oxidation of the phosphite group forming a phosphate. The oligonucleotide can then be removed from the solid support by heating it in the presence of a base, generally ammonia. This has the added advantage that the protecting groups are removed at the same time. The protecting groups which are used will be explained later on.



**Scheme 1: Schematic representation of automated solid supported DNA synthesis**

The activation of the phosphoramidite usually takes place by reacting it with 1*H*-tetrazole, a weak acid. Once activated it becomes reactive and can react with other functionalities, such as the 5' hydroxyl group on the previous nucleotide. To avoid unwanted side-reactions during the synthesis all reactive functionalities present on the nucleoside need to be protected. Apart from the hydroxyl group there are other reactive groups present in the nucleosides i.e. exocyclic amine groups. This amine group also has the potential to react with the activated phosphoramidite. Thymidine and uridine are the only natural occurring nucleotides that do not have a reactive functional group and thus do not require protecting groups on the base. Figure 3 shows some of the commercially available protected “natural nucleotides”.<sup>7</sup>

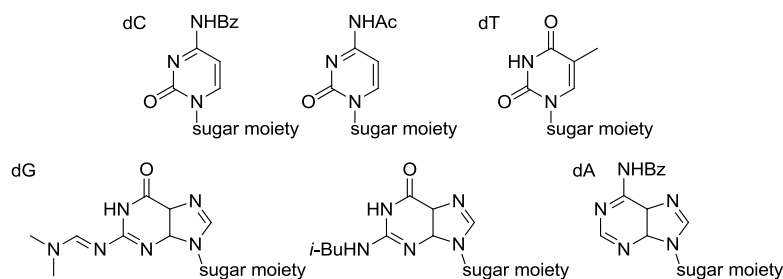


**Figure 3: Commercially available nucleotides with their protecting groups**

The protecting groups on the amines are simultaneously removed with cleaving the oligonucleotide from the solid support.

The objectives for functionalising nucleosides are diverse and include but are not limited to the development of new binding motifs applied in nanotechnology,<sup>8</sup> nucleic acid detection for clinical and research diagnostics,<sup>9</sup> inhibiting the transfer of genetic information<sup>10</sup> and as catalysts.<sup>2</sup>

There are multiple places in DNA which can be modified.<sup>10-11</sup> Firstly the base part of the nucleotide can be altered. This can be done by introducing a moiety onto one of the 4 naturally occurring bases<sup>12</sup> or changing the base completely.<sup>13</sup> The sugar moiety can also be modified<sup>10, 14</sup> as well as the phosphate bridges<sup>15</sup> (Figure 4). These functionalisations should not significantly compromise the formation of the double helix.<sup>16</sup>

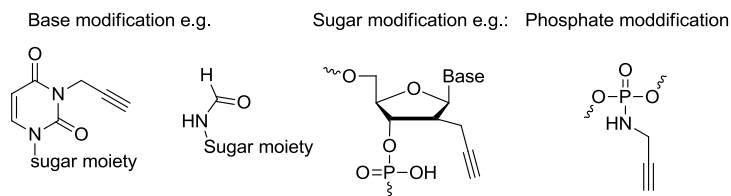


Figure 4: Possible positions for covalent functionalization of a DNA strand

By synthesising the oligonucleotide we aim to have some control of the catalytic environment where the reaction takes place. This can be done by using a variety of different base sequences, by changing the length of the strand and the position in the strand where the ligand is situated. The complementary strand can also be adjusted to add to the unique surroundings. By having mismatches or making the complementary strand longer or shorter than the modified strand, bulges and loops can be created (Figure 5).

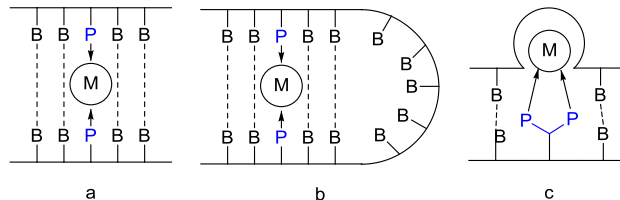


Figure 5: Some of the possible motifs that can be created with DNA

It was theorised that for the transfer of chiral information on to the substrate the transition metal should be located within the chiral environment created by the double helix. It was suspected that if the modification was to occur on a phosphate bridge or a sugar moiety that the transition metal would be situated on the edge of the double helix and therefore will not feel the full effect of the chiral environment therefore base modification was selected.

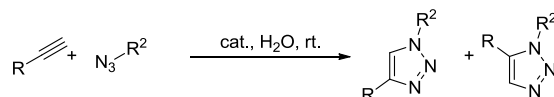
Phosphine ligands are of interest because they form stable catalytically active complexes with a variety of metals. This makes them versatile ligands in catalysis. Moreover phosphines coordinate stronger to late transition metals such as Rh and Pd than nitrogen does. As there are numerous nitrogens present in nucleic acids this is definitely an advantage and increases the probability that only one active site gets formed. Phosphines are not compatible with the DNA synthesis as oxidation will occur during the oxidation step required for the formation of

the phosphate bridge in the backbone, thus the post-synthesis approach was applied. A linker was introduced to attach the phosphine moiety to the oligonucleotide. Ideally the coupling method and reagents used as well as the linkage formed during the coupling of the phosphine moiety to the linker need to be water compatible. Furthermore it was essential that the utilised coupling method was very efficient and chemoselective.<sup>17</sup>

### 2.1.1 CuAAC

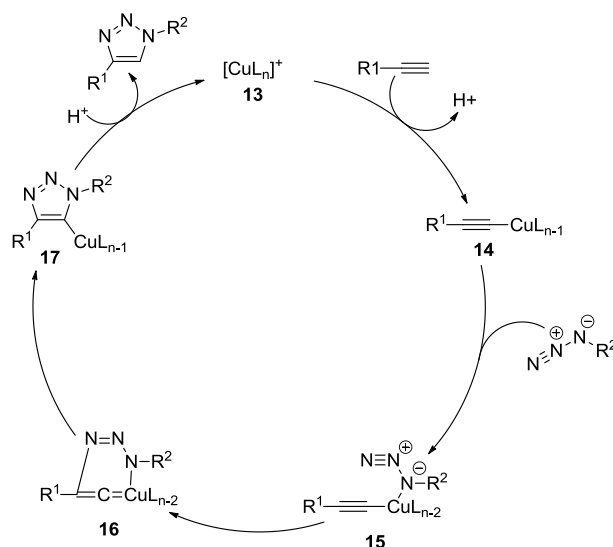
In the early 2000's Sharpless *et al.*<sup>18</sup> introduced the term click chemistry to describe reactions which are modular, highly efficient, wide in scope, stereoselective and which generate only environmentally benign by-products. Furthermore these reactions are also required to be insensitive to oxygen and water. Reactions which fall into this category include 1,3-dipolar cycloadditions, Diels-Alder reactions, ring opening reactions of strained heterocyclic electrophiles by nucleophilic substitution and additions to carbon-carbon multiple bonds such as in the Michael addition.

A multitude of reactions have been employed to modify oligonucleotides such as peptide bond formation, Diels-Alder reactions, Staudinger ligations and copper catalysed 1,3-dipolar cycloadditions also referred to as the click reaction. The latter is one of the most convenient, chemoselective and compatible methods to help functionalise oligonucleotides.<sup>15b</sup> This reaction belongs to the Huisgen's [2 + 3] cycloaddition family. The uncatalysed reaction has been known since 1893<sup>19</sup> and involves reacting an azide with an alkyne to form a triazole (Scheme 2) whereby a mixture of 1,4- and 1,5-regioisomers is formed. The reaction can be denoted as an AAC (azide alkyne cycloaddition) reaction. The reaction is exothermic but the high activation barrier means that the uncatalysed reaction is slow even at elevated temperatures.<sup>20</sup>



**Scheme 2: Representation of a 1,3 dipolar cycloaddition**

Although the formation of triazoles *via* 1,3-cycloadditions is arguably the most useful of the Huisgen's reactions, safety concerns with regard to the azide meant that this reaction did not receive the attention it deserved. The reaction has increased in popularity after Sharpless *et al.*<sup>21</sup> published a regioselective version of this reaction using a copper catalyst (CuAAC) which exclusively generates the 1,4-regioisomer. The catalyst is best prepared by reducing copper(II) sulfate with ascorbate.<sup>22</sup>

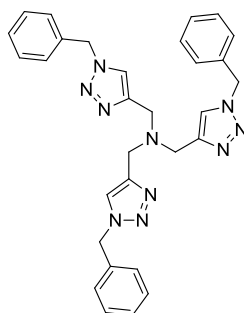


**Scheme 3: Proposed mechanism for the copper catalyzed 1,3-dipolar cycloaddition**

The bridging coordination chemistry found with copper-acetylides means that each step in the proposed catalytic cycle (Scheme 3) could involve multinuclear copper species.<sup>23</sup> The cycle begins with the coordination of the alkyne to the copper (I) species displacing a ligand (**14**). This step is exothermic (11.7 kcal/mol, 49.0 kJ/mol) when the reaction is carried out in water while if it is performed in acetonitrile the reaction was calculated<sup>22</sup> to be endothermic (0.6 kcal/mol, 2.5 kJ/mol). The azide then replaces one of the ligands on the copper species and binds to the copper *via* the nitrogen proximal to the carbon (**15**). The terminal nitrogen can then attack the C-2 carbon in the acetylide to form a Cu<sup>III</sup> vinylidene metallacycle (**16**).<sup>19, 22</sup> This step is endothermic with a calculated barrier of 18.7 kcal/mol (78.3 kJ/mol) in water which is considerably lower than the uncatalysed reaction (barrier 26.0 kcal/mol, 108.9 kJ/mol). An increase of the barrier of 1.4 kcal/mol (5.9 kJ/mol) corresponds to a decrease in reaction rate of 1 order of magnitude. The barrier to form the triazolyl-copper intermediate is very low. The subsequent proteolysis releases the product and regenerates the catalyst.<sup>22</sup>

A Cu<sup>II</sup> species is often used as a catalyst precursor in the CuAAC reaction but the active complex is a Cu<sup>I</sup> species. It is known that some Cu<sup>II</sup>-species can cleave DNA molecules<sup>24</sup> therefore Carell *et al.*<sup>25</sup> used a Cu<sup>I</sup>-species in their initial test reactions. Unfortunately this resulted in multiple products which corresponded to strand breaks. This is not too surprising since Cu<sup>I</sup> is thermodynamically instable and is easily oxidised to Cu<sup>II</sup>. Therefore inert atmospheres and anhydrous solvents are normally employed when utilising Cu<sup>I</sup> complexes.<sup>26</sup> Sodium ascorbate is used as a reducing agent in the CuAAC reaction to continuously convert Cu<sup>II</sup> into Cu<sup>I</sup>. To keep the Cu<sup>I</sup>-complex active without introducing a reducing agent Fokin *et*

*al.*<sup>26a</sup> developed, *tris*-(benzyltriazolylmethyl)amine (TBTA), (Figure 6). When Carell *et al.*<sup>25</sup> used TBTA they DNA cleaving was dramatically reduced.

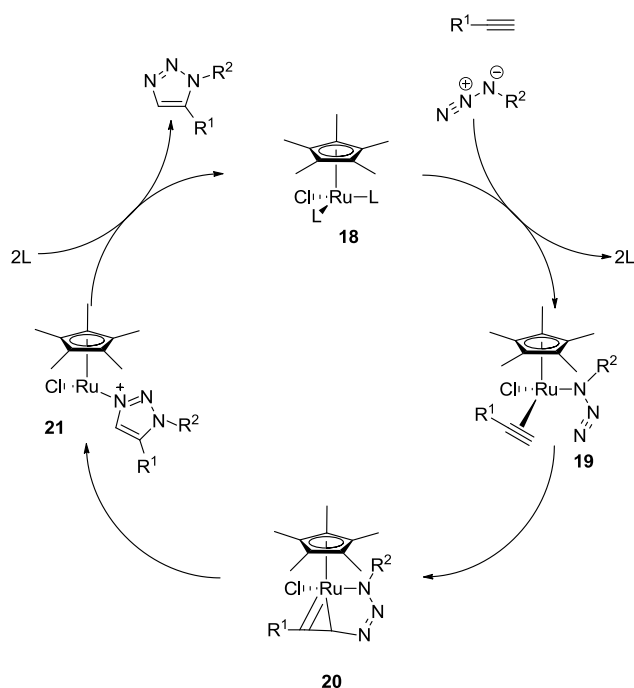


TBTA

Figure 6: *tris*-(benzyltriazolylmethyl)amine

### 2.1.2 RuAAC

While the CuAAC reactions provided an efficient method to synthesise 1,4-substituted 1,2,3-triazoles a method to obtain 1,5-substituted 1,2,3-triazoles was lacking until Fokin *et al.*<sup>20</sup> reported a ruthenium catalysed version of the CuAAC. Unlike with the copper-catalysed reaction internal alkynes are also accessible in this reaction. Depending on the ruthenium complex used either 1,4- or 1,5-substituted regioisomers could be formed. In most cases the yield was extremely low. Pentamethylcyclopentadienyl ruthenium chloride complexes ( $\text{Cp}^* \text{RuClL}_n$ ) formed an exception.<sup>20</sup> These complexes were generally very active and formed solely the 1,5-substituted adduct.



Scheme 4: Proposed reaction mechanism for the Ruthenium catalyzed 1,3-dipolar cycloaddition

Since different types of ruthenium complexes (e.g.  $\text{Cp}^*\text{RuCl}(\text{PPh}_3)_2$ ,  $\text{Cp}^*\text{RuCl}(\text{COD})$ ,  $\text{Cp}^*\text{RuCl}(\text{nbd})$ , and  $[\text{Cp}^*\text{RuCl}]_4$ ) showed catalytic activity it was presumed that the neutral  $[\text{Cp}^*\text{RuCl}]$  intermediate was the catalytically active species (Scheme 4). The alkyne and azide replace the spectator ligands forming active species **19**. There are 4 possible ruthenium-alkyne-azide complexes (Figure 7). **RuAA1** and **RuAA3** generate the 1,5-substituted product while **RuAA2** and **RuAA4** would result in the 1,4-regioisomer.<sup>20</sup> Looking at the activation energies it is clear that **RuAA1** is the favoured intermediate and the 1,5-substituted triazole the favoured product.

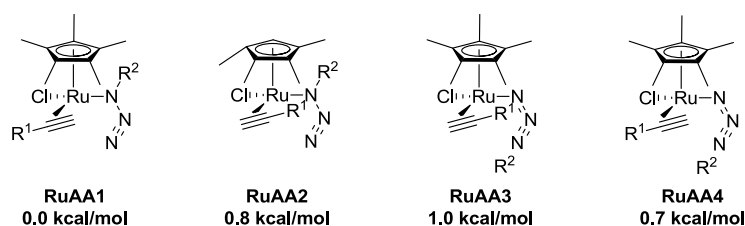


Figure 7: Possible ruthenium-alkyne-azide complexes with their activation barriers

The subsequent step, oxidative coupling of the azide and alkyne, is the step that controls the regioselectivity. A C-N bond is formed between the more electronegative and less sterically hindered carbon of the alkyne and the terminal nitrogen of the azide. Reductive elimination of the metallacycle releases the product and completes the cycle (Scheme 4).<sup>20</sup>

Initial experiments indicated that protic solvents should be avoided although reagents did not need to be dried.<sup>20</sup> Later it was discovered that under certain circumstances the reaction proceeded in systems containing water.<sup>27</sup>

### 2.1.3 Amide bond coupling

One of the most important bond types in biological systems is the amide bond. These bonds are formed by reacting amines with carboxylic acids. This union does not occur spontaneously at ambient temperatures. Therefore either elevated temperatures are used and/or an activated carboxylic acid. This activation usually takes place by exchanging the OH of the acid for a better leaving group (Figure 8).<sup>28</sup>

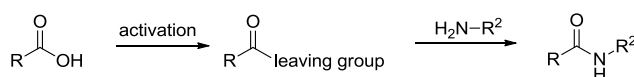


Figure 8: Amide bond formation

This is done with the help of so-called coupling reagents. There are numerous coupling reagents available (Figure 11) such as:

- 1) Carbodiimides e.g. dicyclohexylcarbodiimide (DCC)
- 2) 1*H*-benzotriazole salts e.g. Benzotriazol-1-yloxy)tripyrrolidin phosphonium hexafluorophosphate (PyBOP)
- 3) Other coupling reagents

Carbodiimides are notorious for causing epimerisation. Koenig and Geiger minimised the formation of these by-products by adding the additive, 1-hydroxy-1*H*-benzotriazole (HOBt). HOBt is believed to work by reacting with the carboxylic acid (Figure 9) to form an active OBt ester. This stabilises the approach of the amine *via* hydrogen bonds and thus enhances the reactivity. Carbodiimides include dicyclohexylcarbodiimide (DCC), 1,3-diisopropylcarbodiimide (DIC) and ethyl-(*N,N'*-dimethylamino)propyl carbodiimide hydrochloride (EDC).<sup>28</sup>

DCC Activated carboxylic acid    OBt Activated carboxylic acid

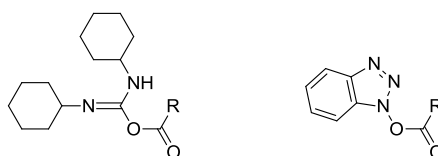


**Figure 9: Activated carboxylic acids**

1*H*-benzotriazole salts which activate carboxylic acids include uronium/aminium and phosphonium salts. These salts form the more reactive OBt ester without the aid of adding an additive. When uronium/aminium salts are used the order of addition is crucial as they can react with the amine to form a guanidinium by-product (Figure 10). Uronium/aminium salts include *O*-(Benzotriazol-1-yl)-*N,N',N'*-tetramethyluronium hexafluorophosphate (HBTU), *O*-(Benzotriazol-1-yl)-*N,N',N'*-tetramethyluronium tetrafluoroborate (TBTU). Utilising phosphonium salts circumvents this problem. (Benzotriazol-1-yloxy) tris(dimethylamino) phosphonium hexafluorophosphate (BOP) was the first phosphonium salt used but because of its carcinogenicity the implementation was limited. A less hazardous version was developed by replacing the methyl group with pyrrole rings and is known as PyBOP (Benzotriazol-1-yloxy)tripyrrolidin phosphonium hexafluorophosphate) (Figure 11).<sup>28</sup>

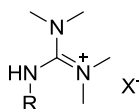


Figure 10: Guanidinium by-product

Other couplings reagents include carbonyldiimidazole (CDI). This reagent is commonly used in peptide synthesis. With this reagent Sharma showed that it could be used to couple unprotected amino acids to amines with moderate yields.<sup>28</sup>

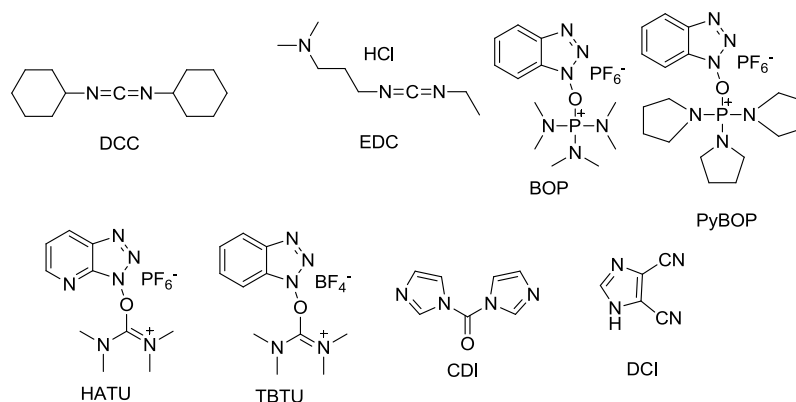


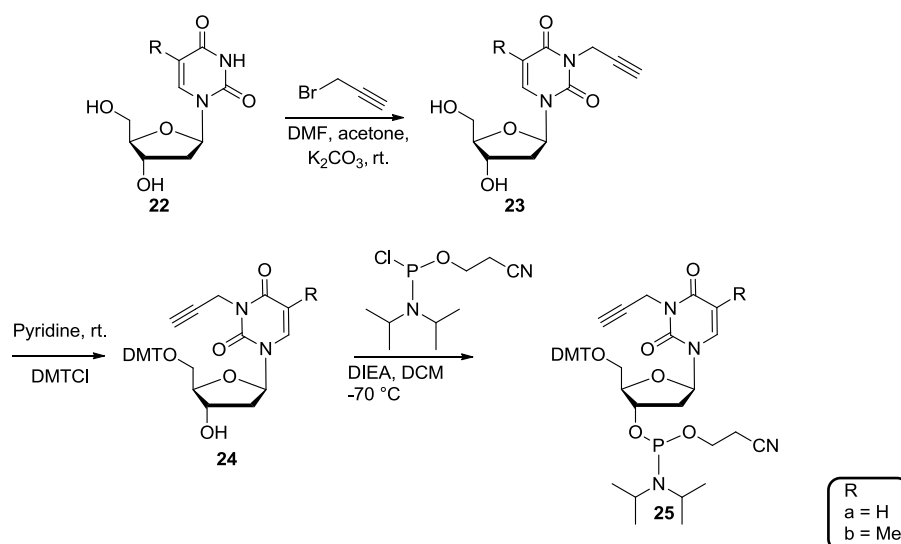
Figure 11: Coupling reagents

Amide formation has been successfully employed to modify nucleotides.<sup>29</sup> This method has also been used to introduce phosphorus containing moieties into oligonucleotides.<sup>2b, 30</sup> The coupling reagent used for these couplings was EDC.<sup>2b, 30</sup> In these examples the amine functionality is located on the nucleotide. Others in our group were working on this approach therefore it was decided to have the carboxylic acid on the nucleotide.

## 2.2 Results and discussion

### 2.2.1 Synthesis of a modified nucleotide

In order to see if minor changes in the ligand structure would have an effect on the catalytic reaction both a thymidine and uridine alkyne were synthesised. Propargyl bromide was used to introduce a terminal alkyne to deoxyuridine (Scheme 5). During this reaction DMF (dimethylformamide) was used as a solvent which proved cumbersome to remove. Most of the DMF was removed under reduced pressure to give a sticky viscous oil. Attempts to remove the residual DMF, by washing the reaction mixture with water, proved unsuccessful because the product was highly soluble in water. This ensured that most of the product ended up in the aqueous (aq.) layer along with the DMF. Further purification by flash chromatography also failed to remove the DMF. The presence of DMF did not interfere with the next step therefore we continued without further purification.

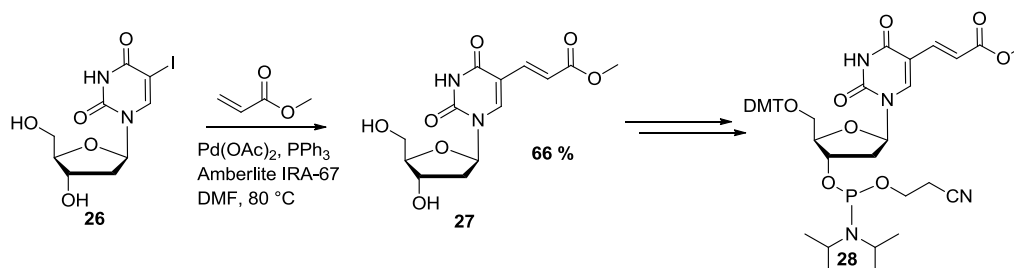


**Scheme 5: Synthesis of nucleoside 2 followed by preparation for DNA synthesis**

After coupling the alkyne to a nucleoside (**23**) the modified nucleoside could then be prepared for DNA synthesis (Scheme 5). The 5'-hydroxyl group was first protected with DMT before the 3'-hydroxyl group was phosphorylated using 2-cyanoethyl *N,N*-diisopropylchlorophosphoramidite. Two diastereomers are formed in a ratio of about 1 to 1. For incorporation into a DNA strand there is no need to separate the diastereomeric mixture, but if separation is required this can easily be achieved by chromatographic methods.

Our attention was then directed to synthesising a nucleoside with a protected carboxylic acid. Methyl acrylate was chosen as the protected carboxylic acid. The methoxy group was not a good leaving group but the convenience of it being commercially available outweighed the benefits of using a potentially better leaving group.

The commercially available 2-iodo-5'-deoxyuridine (**26**) was converted into nucleoside **27** via a Heck reaction (Scheme 6). The yield of this reaction was moderate to good. Once the nucleoside was obtained it was converted into nucleotide **28** using the same methods as described for the synthesis of alkyne nucleotide **25**.



**Scheme 6: Heck coupling with methylacrylate**

### 2.2.2 Synthesis of phosphine azides

Apart from an alkyne, which we placed on the nucleoside, an azide is also required for the cycloaddition. This azide was attached to the ligand moiety. In the presence of azides phosphines undergo the Staudinger reaction (Figure 12) and therefore the phosphine needs to be protected with e.g. a BH<sub>3</sub>-group.

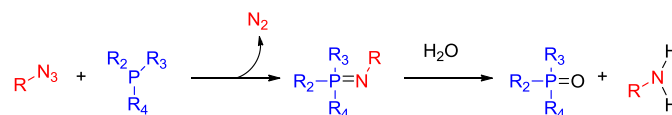
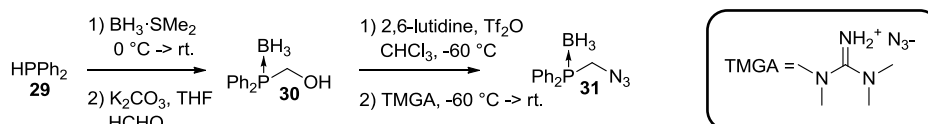


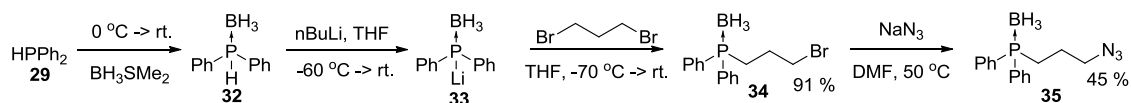
Figure 12: The Staudinger reaction

A phosphine moiety containing an azide was reported by Van Maarseveen *et al.*<sup>31</sup> Azide **18** was synthesised (Scheme 7) using this method. First alcohol **30** was synthesised *via* a 2 step procedure reported by He *et al.*<sup>32</sup> After protecting diphenylphosphine with BH<sub>3</sub>, the excess BH<sub>3</sub>•SMe<sub>2</sub> was removed under reduced pressure and the product was used without further purification. The conversion to the alcohol with formaldehyde in presence of a base proceeded smoothly and a yield of 98 % was achieved. Alcohol **30** was activated with triflic anhydride before reacting with TMGA (*N,N,N',N'*-tetramethylguanidinium azide) to afford azide **31** as an oil. Unfortunately this azide was not a very stable compound and decomposed over time even in the freezer, but it was reasonably stable when stored in benzene at -20 °C.



Scheme 7: Azide synthesis

In order to obtain a more stable compound the chain length between the phosphine and the azide was increased (Scheme 8). Like in the synthesis of phosphine azide **31** the first step in this reaction was the protection of diphenylphosphine with BH<sub>3</sub>. This was then lithiated to quantitatively give **33**, according to <sup>31</sup>P-NMR, and subsequently reacted with a large excess of 1,3-dibromopropane to afford **34** in 91 % yield. Using sodium azide the bromo substituent was converted to azide **35**.



Scheme 8: Second phosphine azide synthesised

Although phosphine azide **35** was more stable than **31** it is still advisable to make a stock solution in dioxane and store it in the freezer at -20 °C.

### 2.2.3 Oligonucleotide synthesis

For the synthesis of the oligonucleotides it is important that the coupling proceeds with a high efficiency. Table 1 shows the overall yield of oligonucleotides of different lengths with different coupling efficiencies. For a 15 mer with a coupling efficiency of 99 % the overall yield is still respectable with 86%. If only 90% coupling efficiency is obtained the yield drops to 21%. In our case the DNA synthesiser did not work optimally and coupling yields as low as 85% were often obtained.

**Table 1: Overall yield with different coupling efficiencies**

<b>X-mer</b> (Length of the oligonucleotide strand)	<b>Coupling efficiency</b>		
	<b>99%</b>	<b>98%</b>	<b>90%</b>
2	99	98	90
5	95	90	59
10	90	82	35
15	86	74	21

A complete turn of the double helix in B-DNA requires a minimum of 10 base pairs. To ensure that the double helix remains intact once the modified nucleotide has been introduced several bases were added on either side giving a total of 15 nucleotides. A 15 mer was synthesised using a DNA synthesiser on a controlled pore glass (CPG) support with a succinyl linker. The modified nucleotide was introduced into a 15 mer with a coupling efficiency similar to that of natural bases. The coupling efficiency of the subsequent coupling was also in line with the efficiency of those preceding it, indicating that the modification did not influence coupling efficiency. The final step in the synthesis was the removal of the remaining DMT protecting group. In the past the DMT was left on to facilitate the purification of the strand and subsequently removed. Purification techniques have improved making this extra step obsolete.

Modified nucleotide **28** was incorporated into 15mer **36** (Figure 13). The coupling efficiency of the modified nucleotide fell into the same range as the “natural nucleotides” so this modification did not have any negative effects on the coupling.

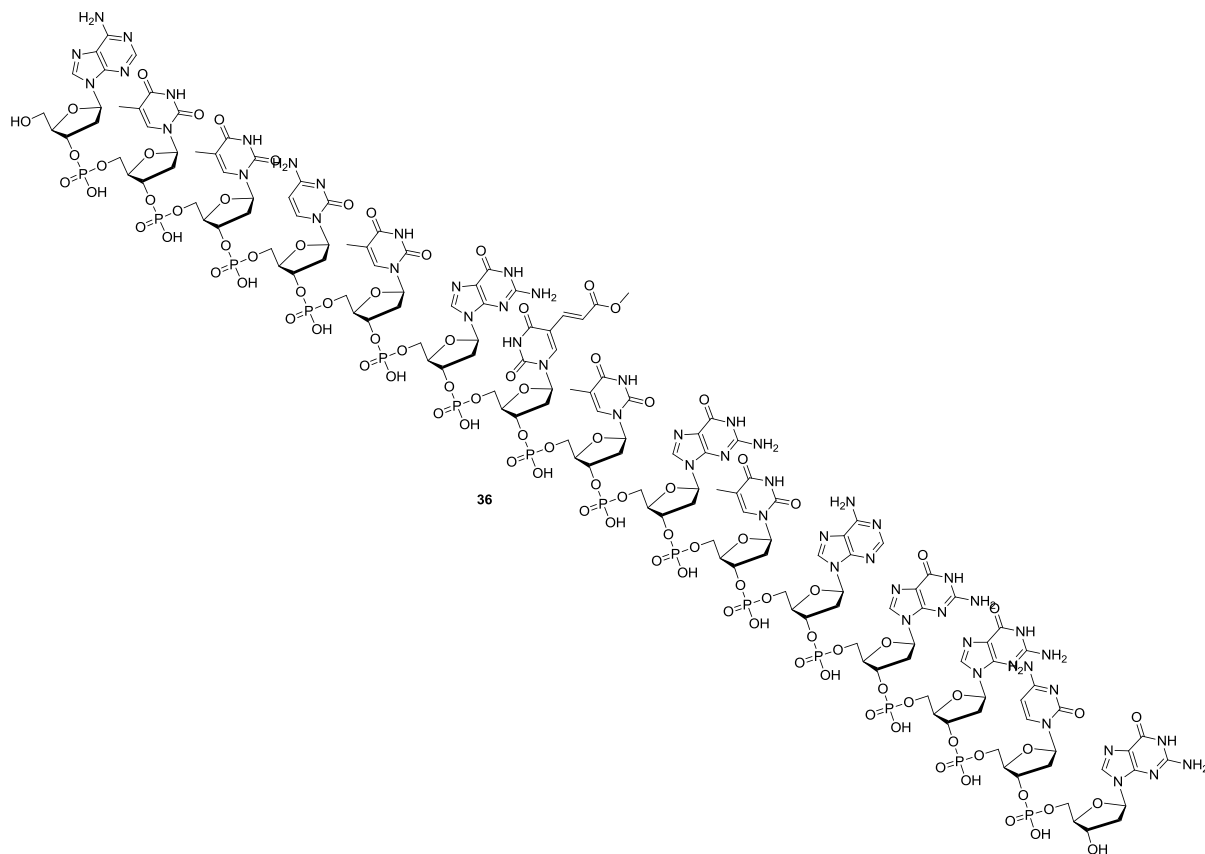


Figure 13: Oligonucleotide **36**, a 15 mer with nucleotide **28** in the middle

The normal procedure for cleaving DNA strands from the solid support is heating for several hours in aqueous ammonium hydroxide. This method was not compatible with strand **36** because ammonolysis can potentially take place generating an amide and thus prevent further functionalisation.

A 0.5 M solution of sodium hydroxide in a methanol/water mixture was used instead. After removing the solid support, *via* filtration, the reaction mixture was neutralised with HCl before purifying *via* preparative HPLC using a reverse phase column.

A MALDI (Matrix-Assisted Laser Desorption Ionisation) spectrum (Figure 14) was taken of this strand and a mass of 4670 was observed which corresponded to the protonated expected mass ( $M_w = 4669$ ).

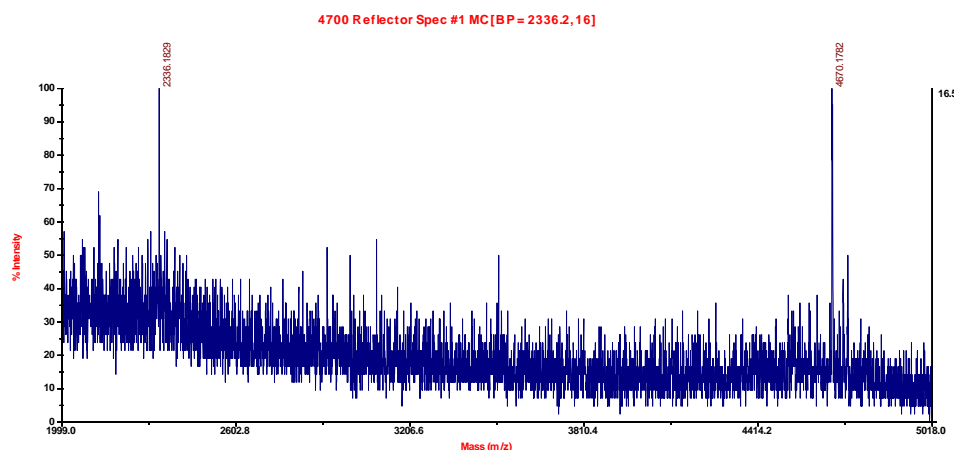


Figure 14:: MALDI spectrum of oligonucleotide 36

Another mass was also detected at 2336 Dalton (D). It is unclear what the mass indicates as it does not correspond to a shorter strand nor is it doubly charged.

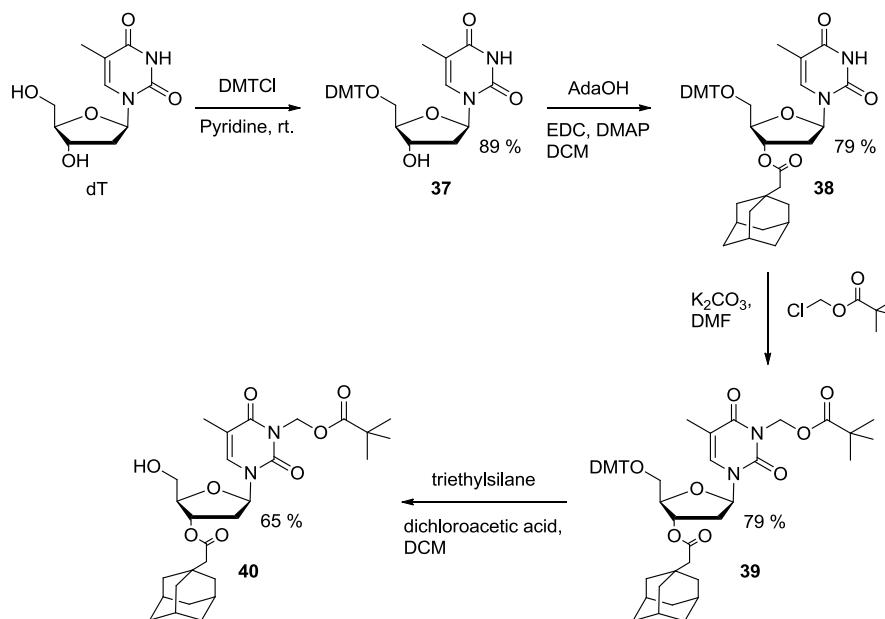
An attempt was made to remove the methoxy protecting group which resulted in only partial deprotection. Different deprotection methods still need to be attempted if this remains unsuccessful the leaving group should be altered.

A trimer was also synthesised. Because there were only two coupling steps involved it could easily be synthesised manually. This had the added advantage that larger amounts can be synthesised. An efficient method to synthesise oligonucleotides manually in solution was reported in 2006 by Vander Marel and co-workers.<sup>33</sup> Using this method they synthesised a 6-mer. Therefore we decided to use this method to synthesise a trimer with a non-natural nucleotide containing an alkyne at the central position (Scheme 10).

This synthesis takes place in solution and consequently the 3' hydroxyl group of the first monomer was not protected by a solid support. To prevent unwanted side-reactions taking place this group was protected by an adamantylacetyl-group (Ada-group). This group, like all the protecting groups on the bases, not only protects the reactive moiety but also enhances the solubility of the growing strand in the organic solvents. This was of paramount importance as the work up between coupling steps involves washing with an aqueous solution.

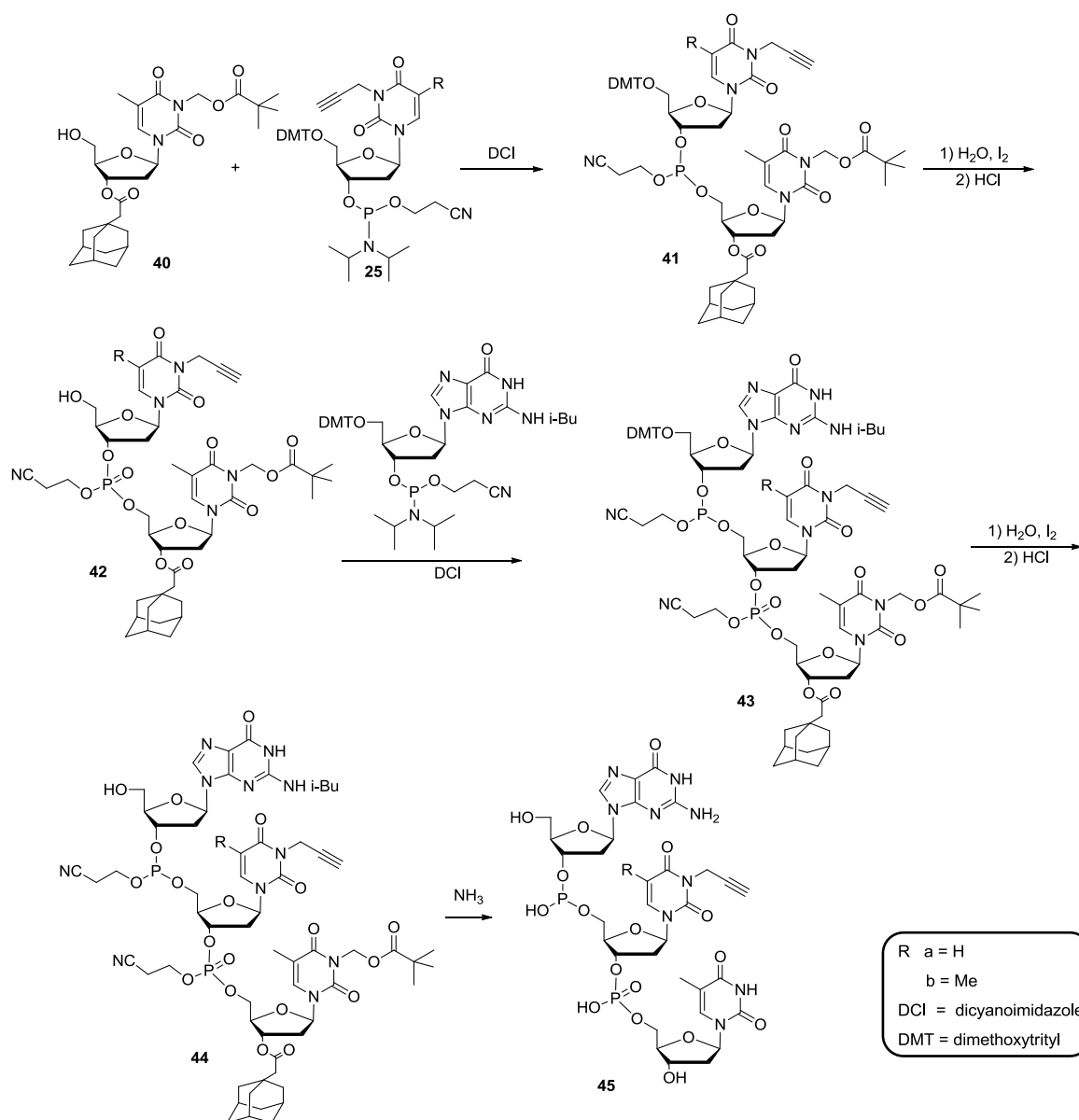
Thymidine was chosen as the first nucleotide. As in the case of preparation of the nucleotide for DNA synthesis on solid support the 5' hydroxyl was protected first with a DMT group generating **37** in 89% yield. Once the DMT group was in place the 3' hydroxyl group could be protected using AdaOH affording compound **38** in 79 % yield. To increase the solubility in organic solvents further a chloromethylpivalate (POM) group was attached to the amino

functionality present on the thymidine base. The DMT group was subsequently removed to allow for coupling to a subsequent nucleotide (Scheme 9).



**Scheme 9: Synthesis of the first nucleotide for the solution phase synthesis of oligonucleotides**

The first step in synthesising trimer **45** involved coupling nucleotides **40** and **25** together with the help of DCI as activator (Scheme 10). After complete conversion, the phosphoramidite was oxidised using iodine in THF/pyridine. The excess of **25** was washed away before the DMT group was removed. Dimer **42** was washed before adding dG-phosphoramidite and repeating the steps. Once the DMT group was removed from the trimer the protecting groups were removed by heating at 55°C in ammonium hydroxide for 3 days. The ammonium hydroxide was removed under reduce pressure. The majority of the protecting groups were subsequently removed by adding water and allowing them to precipitate out of solution before purifying by chromatography over reverse phase silica gel.

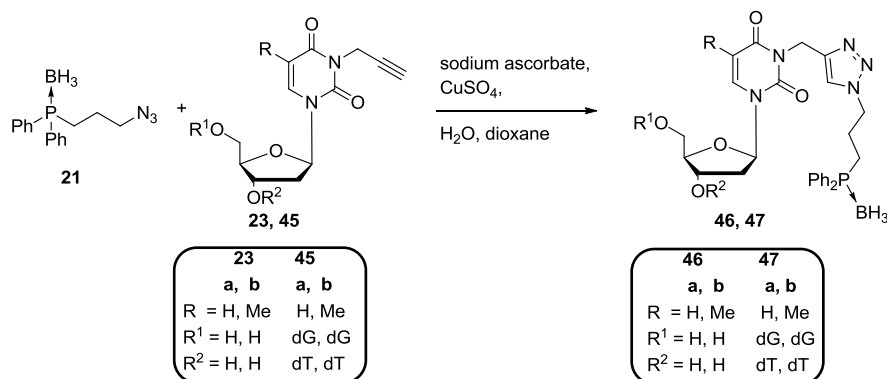


Scheme 10: Synthesis of a trimer in solution

### 2.2.4 The 1,3 dipolar cycloaddition

The 1,3-dipolar cycloaddition was carried out with monomer **23**, trimer **45** and a 15 mer. Monomer **23** and trimer **45** were synthesised *via* the 1,3 dipolar cycloaddition by making the copper catalyst *in situ* (Scheme 11). The next stage involved removing the  $\text{BH}_3$  group. Monomer **23b** and trimer **45b** were selected for testing deprotection conditions. The  $\text{BH}_3$  on the monomer could easily be removed with DABCO (1,4-diazabicyclo[2.2.2]octane), a strongly basic diamine, in organic solvents but when the solvent was changed to water no deprotection occurred. TCEP (*tris*(2-carboxyethyl)phosphine) in an aqueous buffer (pH = 12) was subsequently tried. This also removed the  $\text{BH}_3$  group on the monomer but when this was

tried with the trimer the  $\text{BH}_3$  group remained. Refluxing in methanol overnight however, resulted in the removal of the  $\text{BH}_3$  group in both the monomer and trimer.



Scheme 11: 1,3 cycloaddition with a monomer and trimer

With the 15 mer the copper catalyst was pre-formed by reacting  $\text{CuSO}_4$  with ascorbate in the presence of TBTA, as stabilising agent, before adding it to the alkyne/azide mixture. Unfortunately no product formation could be detected with MALDI TOF.

## 2.3 Conclusion

By lengthening the carbon chain of the phosphine azide **31** to form compound **35** a more stable azide could be synthesised. Although **35** is more stable it is recommended to store it in solution, under argon at  $-20\text{ }^\circ\text{C}$ . The compound remained stable in a solution of dioxane for several years under these conditions.

Nucleosides and small oligonucleotides containing an alkyne functionality could be synthesised and after which reacted with compound **35** to afford the 1,3-cycloaddition products **46** and **47**. Normal procedures for the removal of the  $\text{BH}_3$ -group involve heating in the presence of amines. This worked for the monomer but when the solvent was changed to water the amines were insufficiently nucleophilic to remove the  $\text{BH}_3$ . Methanol proved to be successful in the removal of the  $\text{BH}_3$  group present on the trimer.

The 1,3-dipolar cycloaddition did not work on the 15-mer when  $\text{CuSO}_4$  was used as copper source. Using a different copper source could potentially remedy this problem.

Methyl groups are ideal carboxylic acid protecting groups however initial attempts to remove this functionality resulted in only partial deprotection. Increasing reaction times or changing the deprotection conditions might solve the problem otherwise a different protecting group should be considered.

## 2.4 Experimental

### General Procedures

All air- and water-sensitive reactions were carried out under argon utilising standard Schlenk techniques. Chemicals were purchased from Sigma Aldrich, Acros, Link Technologies, Fisher Scientific, Strem and Glen Research and used as is unless otherwise stated. Pyridine, dichloromethane, acetonitrile and diisopropylethylamine were distilled from CaH<sub>2</sub>. CDCl<sub>3</sub> was distilled from CaCl<sub>2</sub> and stored under argon over K<sub>2</sub>CO<sub>3</sub>. Acetone was distilled from K<sub>2</sub>CO<sub>3</sub>. Methanol and ethanol were distilled over Mg/I<sub>2</sub>, Dioxane was distilled over sodium, THF and diethyl ether were distilled over sodium/benzophenone. All the distilled solvents were stored under argon or nitrogen. Dry DMF was purchased and transferred into a youngs ample. Organic solvents were degassed by three freeze/thaw cycles. Aqueous solutions were degassed by bubbling argon or nitrogen through for several hours.

Thin Layer Chromatography (TLC) was performed using silica plates (plates (polygram 0.3 mm silica gel with fluorescent indicator UV<sub>254</sub> on aluminium plates) purchased from Merck. Compounds on TLC were visualised by UV-detection unless otherwise stated. Flash chromatography or purification *via* a chromatotron<sup>TM</sup> were performed using the indicated eluent. The silica used for flash chromatography was silica gel 60 mesh 70-230 and was purchased from Fluka.

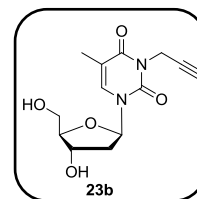
NMR spectra were recorded at room temperature on a Bruker Avance NMR spectrometer (300,400 or 500 MHz). Chemical shifts ( $\delta$ ) are given in ppm. Shifts are relative to a TMS reference (<sup>1</sup>H or <sup>13</sup>C) or an 85% H<sub>3</sub>PO<sub>4</sub> reference (<sup>31</sup>P). <sup>13</sup>C and <sup>31</sup>P spectra were measured with <sup>1</sup>H decoupling unless otherwise stated.

Oligonucleotides were synthesised on an Applied Biosystems 392 DNA/RNA synthesizer using protocols obtained from Applied Biosystems. WHATMAN 0.2  $\mu$ m PTFE syringe filters were used to separate the oligonucleotides from the solid support and the released water-insoluble protecting groups. HPLC purification was performed on a Waters machine equipped with a waters 2700 sample manager, Waters 600 controller and waters 2487 dual absorption detector. The column used was a Phenomenex Clarity C18 5 $\mu$  oligo-RP column (250 x 21.20 mm) monitoring wavelength 260 nm.

FPLC purification was carried out on a FPLC Akta Basic 100 (P-901). The column used was a HiLoad 16/10 Q Sepharose HP column. Monitoring was done *via* a UV-900 at 260 nm.

**3-(2-Propyn-1-yl)thymidine (23b)**

An 80% solution of propargyl bromide in THF (0.75 ml, 8.4 mmol) was added to a solution of thymidine (1.22 g, 5.05 mmol) and potassium carbonate (1.9 g, 13.75 mmol) in DMF/acetone (25 ml, 1:1). The reaction mixture was stirred at 50 °C for 3 days. The reaction mixture was filtered and evaporated to remove most of the solvents. The product was purified by column chromatography (eluent: DCM/acetone 1:1 volume/volume (v/v)). DMF was still present. The product was obtained as a yellowish oil. Yield 61 % (0.85 g, 3.03mmol).



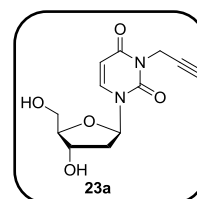
Characterisation agreed with the literature.<sup>34</sup>

<sup>1</sup>H NMR (300 MHz, D<sub>2</sub>O):  $\delta_{\text{H}} = 1.80$  (3H, s, CH<sub>3</sub>), 2.10 (1H, s, CH $\equiv$ ), 2.23-2.32 (2H, m, H-2'), 3.60-3.76 (2H, m, H-5'), 3.88-3.97 (1H, m, H-3'), 4.29-4.38 (1H, m, H-4'), 4.56 (2H, s, NCH<sub>2</sub>), 6.20 (1H, t, <sup>3</sup>J = 6.6 Hz, H-1'), 7.56 (1H, s, H-6)

<sup>13</sup>C NMR (75 MHz, D<sub>2</sub>O):  $\delta_{\text{C}} = 12.16, 30.67, 38.79, 61.07, 70.36, 71.79, 77.92, 85.95, 86.56, 110.56, 135.82, 150.88, 164.41$ ;

**3-(2-Propyn-1-yl)uridine (23a)**

Compound **23a** was synthesised using the same procedure describe above. The product was obtained as a yellowish oil. Yield 87% (4.96 g, 18 mmol).



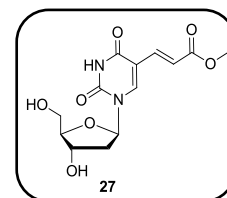
Characterisation agreed with the literature.<sup>12</sup>

<sup>1</sup>H NMR (300 MHz, MeOD):  $\delta_{\text{H}} 2.19$ -2.44 (2H, m, H-2'), 2.58 (1H, t, <sup>3</sup>J = 2.3 Hz, CH $\equiv$ ), 3.72-3.84 (2H, m, H-5'), 3.95-4.00 (1H, m, H-3'), 4.40-4.45 (1H, m, H-4'), 4.46 (2H, d, J = 2.3 Hz, NCH<sub>2</sub>), 5.84 (1H, d, J = 8.1 Hz, H-5) 6.28 (1H, t, <sup>3</sup>J = 6.6 Hz, H-1'), 8.01 (1H, d, 8.1 Hz, H-6)

<sup>13</sup>C NMR (75 MHz, CDCl<sub>3</sub>):  $\delta_{\text{C}} = 31.3, 41.5, 62.9, 72.2, 72.4, 79.4, 87.7, 89.0, 102.2, 141.2, 151.7, 164.0$

**5-(2-carbomethoxyvinyl)-2'-deoxyuridine (27)**

Methyl acrylate (1.7 ml, 17.8 mmol) was added to a stirred solution of 5-iodo-2'-deoxyuridine (2.05 g, 5.78 mmol), PPh<sub>3</sub> (213.46 mg, 0.81 mmol), Pd(OAc)<sub>2</sub> (91.06 mg, 0.41 mmol) and Amberlite IRA-67 (5.02 mg) in dry, degassed DMF (50 ml) at 60 °C. The yellow reaction mixture was heated at 80 °C overnight resulting in a dark brown or green suspension. The solution was allowed to cool to rt. before filtering over a silica plug topped with celite, eluting with methanol-DCM (1:3 v/v). The filtrate was concentrated *in vacuo* to afford an orange/brown oil and purified by flash

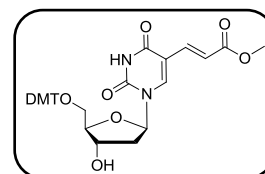


chromatography (MeOH:DCM 1:9 v/v,  $R_f = 0.28$ ). Compound **27** was obtained as a white solid in 66 % yield (1.134 g, 3.6 mmol).

Characterisation agreed with the literature.<sup>35</sup>

<sup>1</sup>H NMR (300 MHz, CD<sub>3</sub>OD):  $\delta_H = 2.13$ -2.27 (2H, m, H-2'), 3.39 (3H, s, CH<sub>3</sub>), 3.77 (2H, m, H-5'), 3.85 (1H, m, H-4'), 4.32 (1H, dt,  $3J = 3.5$  Hz,  $3J = 6.1$  Hz, H-3'), 6.16 (1H, t,  $3J = 6.4$  Hz, H-1'), 6.80 (1H, d,  $3J = 15.9$  Hz, CHCHCO<sub>2</sub>Me), 7.30 (1H, d,  $3J = 15.9$  Hz, CHCHCO<sub>2</sub>Me), 8.40 (1H, s, H-6).

### 5-(2-carbomethoxyvinyl)-5'-(O-4,4'-dimethoxytrityl)-2'-deoxyuridine

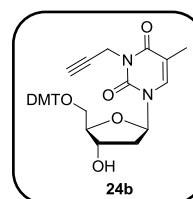


5-(2-carbomethoxyvinyl)-2'-deoxyuridine (**27**) (1.01 g, 3.2 mmol) was azeotropically dried with pyridine (3x 4 ml) and then dissolved in pyridine (16 ml). To this stirred solution 4,4'-dimethoxytrityl chloride (1.19 g, 3.51 mmol) was added. The resulting mixture was stirred at rt. until the reaction was complete. Methanol (3.2 ml) was added to the reaction mixture and stirring continued for a further 30 min. The reaction mixture was then concentrated to dryness *in vacuo* and the residue was dissolved in ethyl acetate (170 ml) and washed with 5 % weight/weight (w/w) aq. NaHCO<sub>3</sub> (2x 40 ml). The organic layer was dried over Na<sub>2</sub>SO<sub>4</sub>, filtered and concentrated *in vacuo*. The compound was purified by flash chromatography whereby the silica was treated with a mixture of hexane:ethyl acetate:triethyl amine (2:3:0.05) before the compound was brought onto the column (eluent: hexane:ethyl acetate 2:3). The product was afforded as a white foam in 75 % yield (1.49 g, 2.4 mmol,  $R_f = 0.24$ ).

Characterisation agreed with the literature.<sup>35</sup>

<sup>1</sup>H NMR (400 MHz, CDCl<sub>3</sub>):  $\delta_H = 2.20$  -2.25 (1H, m, H-2'), 2.44-2.50 (1H, m, H-2'), 3.35-3.36 (2H, m, H-5'), 3.60 (3H, s, CO<sub>2</sub>CH<sub>3</sub>), 3.71 (6H, s, Ar-OCH<sub>3</sub>), 4.05 (1H, m, H-4'), 4.45 (1H, m, H-3'), 6.20 (1H, t,  $^3J = 6.5$  Hz, H-1'), 6.77-6.93 (6H, m, Ar-H and CHCHCO<sub>2</sub>Me), 7.21-7.45 (9H, m, Ar-H and CHCHCO<sub>2</sub>Me), 7.77 (1H, s, H-6) and 8.59 (1H, s, NH).

### 3-(2-Propyn-1-yl)-5'-(O-4,4'-dimethoxytrityl)-thymidine (24b)



3-(2-propyn-1-yl)thymidine (**23b**) (0.62 g, 2.23 mmol) was azeotropically dried with pyridine (3x 1 ml) and then dissolved in pyridine (10 ml). 4,4'-Dimethoxytrityl chloride (0.83 g, 2.45 mmol) was added to this stirred solution. The resulting mixture was stirred at rt. until the reaction was complete. Methanol (2.8 ml) was added to the reaction mixture and stirred for a further 30 min. The reaction

mixture was then concentrated to dryness *in vacuo* and the residue was dissolved in ethyl acetate (120 ml) and washed with 5 % w/w aq. NaHCO<sub>3</sub> (2x 30 ml) followed by brine (30 ml). The organic layer was dried over Na<sub>2</sub>SO<sub>4</sub>, filtered and concentrated under reduced pressure. The compound was purified by flash chromatography whereby the silica was treated with a mixture of acetone:DCM:triethyl amine (1:4:0.05) before the compound was brought onto the column. Eluent acetone:DCM 1:4.

The product was obtained as a white foam. Yield 66% (0.86 g, 1.48 mmol).

Characterisation agreed with the literature<sup>36</sup>

<sup>1</sup>H NMR (400 MHz, C<sub>6</sub>D<sub>6</sub>): δ<sub>H</sub> = 1.66 (3H, s, NCH<sub>3</sub>), 1.76-1.77 (1H, m, CH≡), 1.90-1.96 (2H, m, H-2'), 3.18-3.22 (1H, m, H-5'), 3.28 (6H, s, Ar-OCH<sub>3</sub>), 3.39-3.43 (1H, m, H-5'), 3.79-3.80 (1H, m, H-4'), 4.05-4.07 (1H, m, H-3'), 4.60 (2H, dq, J = 2.5 Hz, J = 4.5 Hz, NCH<sub>2</sub>), 6.50 (1H, m, H-1'), 6.74-6.77 (4H, m, Ar-H), 7.03-7.20 (3H, m, Ar-H), 7.34-7.38 (5H, m, H-6' and Ar-H), 7.50-7.53 (2H, m, Ar-H)

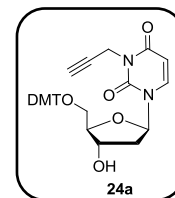
<sup>13</sup>C NMR (100 MHz, C<sub>6</sub>D<sub>6</sub>): δ<sub>C</sub> = 11.5, 29.4, 40.2, 54.2, 62.4, 69.5, 70.9, 84.5, 85.2, 85.9, 109.3, 112.2, 126.1, 127.0, 127.1, 129.1, 133.1, 134.3, 135.1, 143.3, 148.4, 149.2, 157.7, 161.5

### 3-(2-Propyn-1-yl)-5'-(O-4,4'-dimethoxytrityl)-uridine (24a)<sup>35</sup>

Compound **24a** was synthesised using the same procedure describe above.

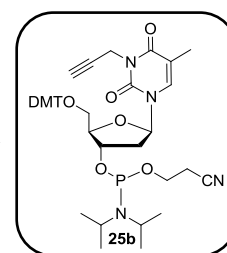
The product was obtained as a white foam. Yield 82% (6.72 g, 11.89 mmol)

Characterisation agreed with the literature.<sup>12</sup>



### 3-(2-Propyn-1-yl)-5'-(O-4,4'-dimethoxytrityl)-thymidine-3'-(O-2-cyanoethyl-N,N-diisopropylamino)phosphoramidite (25b)

A 1 M solution of 2-cyanoethyl diisopropylchlorophosphoramidite in acetonitrile (1.2 ml, 1.16 mmol) was added drop wise to a stirred solution of compound **24b** (0.52 g, 0.89 mmol) and diisopropylethylamine (290 μl,



1.78 mmol) in DCM (10 ml) at 0 °C. The cooling was removed and the reaction mixture was left to stir at rt. for 2 h. Ethyl acetate (30 ml), pre-washed with 5% aq. NaHCO<sub>3</sub>, was added to the reaction mixture and washed with 5% aq. NaHCO<sub>3</sub> (2x 25 ml) followed by brine (2x 25 ml). The organic phase was dried over Na<sub>2</sub>SO<sub>4</sub>, filtered and concentrated under reduced pressure to afford the crude product as a white foam. The compound was purified by chromatotron<sup>TM</sup>. The plate was first treated with diethyl ether:hexane:triethyl amine 4:1:0.5

before bringing the compound onto the plate. Eluent diethyl ether:hexane 4:1. The product was obtained as a white foam in 37 % yield (0.27 g, 0.33 mmol).

Characterisation agreed with the literature<sup>36</sup>

<sup>1</sup>H NMR (300 MHz, CDCl<sub>3</sub>) diastereomer A:  $\delta_{\text{H}} = 0.82\text{-}0.90$  (2H, m, *i*-Pr-CH), 1.07 (3H, s, *i*-Pr-CH<sub>3</sub>), 1.17 (9H, s, *i*-Pr-CH<sub>3</sub>), 1.46 (3H, s, NCH<sub>3</sub>), 2.17 (1H, t, <sup>4</sup>*J* = 3 Hz, CH≡), 2.28-2.59 (2H, m, H-2'), 3.25-3.35 (1H, m, H-5'), 3.44-3.67 (5H, m, H-5' and CH<sub>2</sub>CH<sub>2</sub>CN), 3.79 (3H, s, 2x Ar-OCH<sub>3</sub>), 4.17-4.20 (1H, m, H-4'), 4.61-4.68 (1H, m, H-3'), 4.72 (2H, d, <sup>4</sup>*J* = 3 Hz, NCH<sub>2</sub>), 6.45 (1H, t, <sup>3</sup>*J* = 6 Hz, H-1'), 6.84-6.85 (4H, m, Ar-H), 7.24-7.32 (4H, m, Ar-H), 7.37-7.39 (2H, m, Ar-H), 7.67 (1H, d, <sup>3</sup>*J* = 1.1 Hz, H-6).

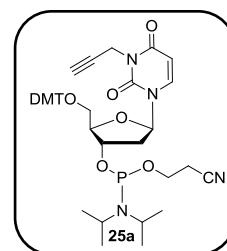
<sup>1</sup>H NMR (300 MHz, CDCl<sub>3</sub>) diastereomer B:  $\delta_{\text{H}} = 0.82\text{-}0.90$  (2H, m, *i*-Pr-CH), 1.05 (3H, s, *i*-Pr-CH<sub>3</sub>), 1.15 (9H, s, *i*-Pr-CH<sub>3</sub>), 1.46 (3H, s, NCH<sub>3</sub>), 2.17 (1H, t, <sup>4</sup>*J* = 3 Hz, CH≡), 2.28-2.59 (2H, m, H-2'), 3.25-3.35 (1H, m, H-5'), 3.44-3.67 (5H, m, H-5' and CH<sub>2</sub>CH<sub>2</sub>CN), 3.79 (3H, s, 2x Ar-OCH<sub>3</sub>), 4.13-4.16 (1H, m, H-4'), 4.61-4.68 (1H, m, H-3'), 4.72 (2H, d, <sup>4</sup>*J* = 3 Hz, NCH<sub>2</sub>), 6.47 (1H, t, <sup>3</sup>*J* = 6 Hz, H-1'), 6.80-6.82 (4H, m, Ar-H), 7.24-7.32 (4H, m, Ar-H), 7.40-7.42 (2H, m, Ar-H), 7.62 (1H, d, <sup>3</sup>*J* = 1.1 Hz, H-6).

<sup>31</sup>P (121 MHz, CDCl<sub>3</sub>):  $\delta_{\text{P}} = 149.6$  (s), 150.2 (s).

**3-(2-Propyn-1-yl)-5'-(*O*-4,4'-dimethoxytrityl)-thymidine-3'-(*O*-2-cyanoethyl-*N,N*-diisopropylamino)phosphoramidite (**25a**)**

Compound **25a** was synthesised using the same procedure describe above.

Product was obtained as a white foam. Yield 87% % (4.96 g, 18.6 mmol) .



Characterisation agreed with the literature.<sup>12</sup>

<sup>1</sup>H NMR (300 MHz, CDCl<sub>3</sub>) diastereomer A:  $\delta_{\text{H}} = 1.11$  (12 H, d, 6.8 Hz), 2.11 (1H, t, *J* = 2.4 Hz), 2.17-2.25 (1H, m), 2.38-2.49 (3H, m), 3.28-3.39 (2H, m), 3.49-3.67 (4H, m), 3.71 (6H, s), 4.09 (1H, m), 4.55 (2H, d, *J* = 2.4 Hz), 4.57-4.64 (1H, m), 5.35 (1H, d, *J* = 8.2 Hz), 6.22 (1H, t, *J* = 6.3 Hz), 6.75-6.78 (4H, m), 7.14-7.35 (9H, m), 7.69 (1H, d, *J* = 8.2 Hz)

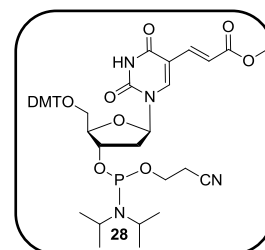
<sup>13</sup>C NMR (75 MHz, CDCl<sub>3</sub>) diastereomer A:  $\delta_{\text{C}} = 24.7, 24.8, 30.2, 43.6, 43.8, 55.6, 63.0, 86.2, 113.6, 127.4, 128.3, 128.5, 130.5, 135.6, 135.8, 159.2$

<sup>31</sup>P NMR (121 MHz CDCl<sub>3</sub>) diastereomer A:  $\delta_{\text{P}} = 149.0$

<sup>1</sup>H NMR (300 MHz, CDCl<sub>3</sub>) diastereomer B:  $\delta_{\text{H}} = 1.05$  (12 H, dd, 6.8, 23 Hz), 2.11 (1H, t, *J* = 2.4 Hz), 2.14-2.26 (1H, m), 2.46-2.57 (3H, m), 3.26-3.33 (2H, m), 3.44-3.79 (4H, m), 3.70

(6H, s), 4.01-4.06 (1H, m), 4.54 (2H, d,  $J = 2.4$  Hz), 4.55-4.62 (1H, m), 5.34 (1H, d,  $J = 8.2$  Hz), 6.22 (1H, t,  $J = 6.4$  Hz), 6.72-6.78 (4H, m), 7.13-7.34 (9H, m), 7.64 (1H, d,  $J = 8.2$  Hz)  
 $^{13}\text{C}$  NMR (75 MHz,  $\text{CDCl}_3$ ) diastereomer B:  $\delta_{\text{C}} = 21.1, 25.0, 25.1, 30.7, 41.1, 43.9, 44.1, 56.0, 58.9, 59.2, 63.6, 70.8, 73.7, 74.0, 79.2, 86.0, 86.5, 87.6, 114.0, 118.5, 127.8, 128.7, 128.8, 130.9, 136.0, 136.2, 139.2, 145.3, 151.0, 159.6, 162.2$   
 $^{31}\text{P}$  NMR (121 MHz  $\text{CDCl}_3$ ) diastereomer B:  $\delta_{\text{P}} = 148.7$

**5-(2-carbomethoxyvinyl)-5'-(*O*-4,4'-dimethoxytrityl)-2'-deoxyuridine-3'-(*O*-2-cyanoethyl-*N,N*-diisopropylamino)phosphoramidite (**28**)**

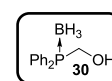


A 1 M solution of 2-cyanoethyl diisopropylchlorophosphoramidite in acetonitrile (1.2 ml, 1.2 mmol) was added drop wise to a stirred solution of 5-(2-carbomethoxyvinyl)-5'-(*O*-4,4'-dimethoxytrityl)-2'-deoxyuridine (462.34 mg, 0.75 mmol) and diisopropylethylamine (0.3 ml, 1.73 mmol) in DCM (15 ml) at  $-78$  °C. The cooling was removed and the reaction mixture was left to stir at rt. for 2 h. Ethyl acetate (15 ml), pre-washed with 5% aq.  $\text{NaHCO}_3$ , was added to the reaction mixture and washed with 5% aq.  $\text{NaHCO}_3$  (2x 15 ml) followed by brine (15 ml). The organic phase was dried over  $\text{Na}_2\text{SO}_4$ , filtered (eluting with DCM) and concentrated *in vacuo* to afford the crude product as a white foam. The compound was purified by chromatotron (eluent: hexane:ethyl acetate 1:4,  $R_f = 0.86$ ). The plate was first treated with hexane:ethyl acetate:triethyl amine 1:4:0.5 before bringing the compound onto the plate. The product was obtained as a white foam in 49 % yield (300 mg, 0.37 mmol).

$^1\text{H}$  NMR (400 MHz,  $\text{C}_6\text{D}_6$ ):  $\delta_{\text{H}} = 1.09$  (2H, m,  $\text{CH}(\text{CH}_3)_2$ ), 1.16-1.24 (12H, m, *i*-Pr- $\text{CH}_3$ ), 1.80-1.83 (1H, m,  $\text{CH}-\text{Me}_2$ ), 1.91-1.94 (1H, m,  $\text{CH}-\text{Me}_2$ ), 2.32-2.43 (1H, m, H-2'), 2.57-2.75 (1H, m, H-2'), 3.20-3.48 (2H, m, H-5'), 3.53 (9H, s, 2x  $\text{ArOCH}_3$  and  $\text{CO}_2\text{CH}_3$ ), 3.57-3.63 (4H, m,  $\text{CH}_2-\text{CH}_2-\text{CN}$ ), 4.39-4.44 (1H, m, H-4'), 4.83-4.86 (1H, m, H-3'), 6.32-6.37 (1H, m, H-1'), 6.99 (4H, d  $^3J = 8.8$  Hz, Ar-H), 7.21 (1H, m,  $\text{CHCO}_2$ ), 7.22-7.42 (3H, m, Ar-H), 7.58-7.78 (8H, m, 6H Ar-H and H-1' and  $\text{CH}=\text{C}$ ).

$^{31}\text{P}$  (162 MHz,  $\text{CD}_3\text{OD}$ ):  $\delta_{\text{P}} = 149.00$  (s), 148.66 (s).

**Diphenylphosphino(borane)methane alcohol (**30**)**



Diphenylphosphine (1.1 ml, 6.3 mmol) was added in one go to a cooled ( $-70$  °C) 2 M solution of borane dimethyl sulfide (4 ml, 8.0 mol) in THF. The reaction mixture was allowed to warm to room temperature. After 2 h the excess borane dimethyl sulphide

complex was removed under reduced pressure. The residue was dissolved in 8 ml of THF. Formaldehyde (4 ml, 37 %) and potassium hydroxide (0.58 g, 10.2 mmol) were added turning the solution cloudy. After a couple of minutes the solution cleared up. After 3 h the THF was removed under reduced pressure and subsequently extracted 3 times with ethyl acetate (10 ml). The combined organic layers were washed twice with brine (8 ml) and dried over  $\text{Na}_2\text{SO}_4$ . The compound was further purified by flash chromatography (eluent ethyl acetate:petroleum ether 2:5).

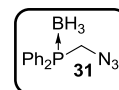
The product was obtained as a whitish oil. Yield 98 % (1.42 g, 6.17 mmol).

Characterisation agreed with the literature.<sup>31</sup>

$^1\text{H}$  NMR (400 MHz,  $\text{CDCl}_3$ ):  $\delta_{\text{H}} = 0.61\text{-}1.26$  (3H, m,  $\text{BH}_3$ ), 4.45 (2H, s,  $\text{CH}_2$ ), 7.45-7.56 (6H, m, Ar-H), 7.70-7.75 (4H, m, Ar-H).

$^{31}\text{P}$  NMR (162 MHz,  $\text{CDCl}_3$ ):  $\delta_{\text{P}} = 17.45$  (q,  $^2J = 55$  Hz).

### Azidomethyl(diphenyl)phosphine borane complex (31)



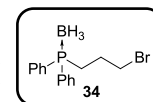
To a solution of **30** (0.44 g, 1.9 mmol) in chloroform (8 ml, filtrated over alumina) at  $-60$  °C  $\text{Tf}_2\text{O}$  (0.45 ml, 2.7 mmol) and 2,6-lutidine (0.4 ml, 3.4 mmol) were added. The solution was stirred for 3 hours before adding tetramethylguanidinium azide (TMGA, 1.0 g, 6.6 mmol). The mixture was stirred overnight and allowed to warm to rt. After 24 h saturated aqueous ammonium chloride (50 ml) was added and the mixture was extracted 3 times with DCM (25 ml). The combined organic layers were washed with water (2 x 25 ml) and once with brine (25 ml). The organic layer was dried over  $\text{Na}_2\text{SO}_4$  and concentrated under reduce pressure. The residue was purified by flash chromatography (diethyl ether:petroleum ether 1:7  $R_f = 0.28$ ). The product was obtained as a pale yellow oil in an 80% yield (387 mg, 1.52 mmol).

Characterisation agreed with the literature.<sup>31</sup>

!! BE AWARE POTENTIALLY EXPLOSIVE!!

$^1\text{H}$  NMR (300 MHz,  $\text{CDCl}_3$ ):  $\delta_{\text{H}} = 0.57\text{-}1.52$  (3H, m,  $\text{BH}_3$ ), 4.04 (d,  $J = 3.4$ , 2H,  $\text{CH}_2$ ), 7.46-7.60 (m, 6H, Ar-H), 7.71-7.78 (m, 4H, Ar-H)

$^{31}\text{P}$  NMR (121 MHz,  $\text{CDCl}_3$ ):  $\delta$  (ppm) = 19.8 (b).

**Borane (3-bromopropyl)diphenylphosphine (34)**

Diphenylphosphine (9.1 ml, 52.4 mmol) was added in one go to a cooled 2 M solution of borane dimethyl sulfide (55 ml, 110 mmol) in THF. The reaction mixture was allowed to warm to room temperature. After 2 h the excess borane dimethyl sulphide complex was removed under reduced pressure. The reaction mixture was subsequently dissolved in 200 ml of THF and cooled to -70 °C before dropwise adding a 2.5M solution of *n*-BuLi (22 ml, 55 mmol).

In a separate flask 1,3-dibromopropane (50 ml, 494 mmol) was dissolved in 100 ml of THF and cooled to -65 °C. The borane diphenylphosphine from the previous step was added to this solution *via* a cannula and the reaction mixture was allowed to warm to room temperature overnight. The reaction mixture was quenched with water (50 ml) before diluting with DCM (50 ml). The two layers were separated and the aqueous layer was extracted 3 times with DCM (3 x 50ml). The combined organic layers were washed with water (25 ml) and brine (25 ml) and dried over MgSO<sub>4</sub>. The solvent and excess 1,3-dibromopropane were removed under reduced pressure. The reaction mixture was dissolved in refluxing hexane before precipitating the product out by cooling in a dry ice bath.

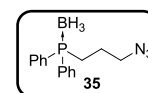
The product was obtained as a white solid. Yield 12.6 g (75%).

<sup>1</sup>H NMR (300 MHz, CDCl<sub>3</sub>): δ<sub>H</sub> 0.50-1.44 (3H, bm, BH<sub>3</sub>), 2.01-2.14 (2H, m, CH<sub>2</sub>), 2.34-2.44 (2H, m, CH<sub>2</sub>), 3.45 (2H, t, <sup>3</sup>J = 6.5 Hz, CH<sub>2</sub>-Br), 7.42-7.53 (6H, m, Ar-H), 7.66-7.72 (4H, m, Ar-H)

<sup>13</sup>C NMR (75 MHz, CDCl<sub>3</sub>): δ<sub>C</sub> 24.4, 26.1, 34.3, 128.6, 131.3, 132.1

<sup>31</sup>P NMR (121 MHz, CDCl<sub>3</sub>): δ<sub>P</sub> 15.7 (b)

HRMS cald. for C<sub>15</sub>H<sub>16</sub>BrP (M-BH<sub>3</sub>) 306.0168 found 306.0165

**Borane (3-azidopropyl)diphenylphosphine (35)**

Compound **34** (5.13 g, 16.7 mmol) was dissolved in degassed DMF (50 ml).

Sodium azide (2.03 g, 31.2 mmol) was dissolved in degassed water (20 ml) before adding to the solution of compound **34**. The reaction mixture was warmed to 50 °C for 24 hours. The product was extracted with diethyl ether (3 x 100 ml) and dried over MgSO<sub>4</sub>. The crude reaction mixture was purified by flash chromatography using silica gel. Eluent petroleum ether: diethyl ether 7:2. The product was obtained as a cloudy oil.

Yield 2.04 g (43 %).

**!! BE AWARE POTENTIONALLY EXPLOSIVE!!**

$^1\text{H}$  NMR (300 MHz,  $\text{CDCl}_3$ ):  $\delta_{\text{H}} = 0.51\text{-}1.44$  (3H, bm,  $\text{BH}_3$ ), 1.74-1.87 (2H, m,  $\text{CH}_2\text{CH}_2\text{CH}_2$ ), 2.25-2.34 (2H, m,  $\text{PCH}_2$ ), 3.36 (2H, t,  $^3J = 6.4$  Hz,  $\text{CH}_2\text{-N}_3$ ), 7.42-7.54 (6H, m, Ar-H), 7.65-7.73 (4H, m, Ar-H)

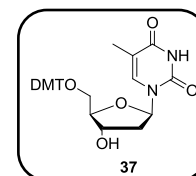
$^{13}\text{C}$  NMR (75 MHz,  $\text{CDCl}_3$ ):  $\delta_{\text{C}} = 22.5$  ( $\text{CH}_2\text{CH}_2\text{CH}_2$ ), 23.0 ( $\text{PCH}_2$ ), 51.9 ( $\text{CH}_2\text{-N}_3$ ), 128.9 (Ar), 131.4 (Ar), 132.0(Ar)

$^{31}\text{P}$  NMR (121 MHz,  $\text{CDCl}_3$ ):  $\delta_{\text{P}} = 15.9$  (b)

### 5'-O-dimethoxytrityl-deocytidine (37)

The compound was synthesised *via* the same procedure as compound **24**.

The product was obtained as a white foam. Yield 85% (13.8 g, 25.4 mmol).



Characterisation agreed with the literature.<sup>33</sup>

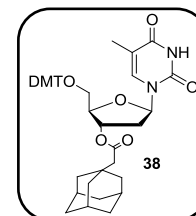
$^1\text{H}$  NMR (400 MHz,  $\text{CDCl}_3$ ):  $\delta_{\text{H}} = 1.33$  (3H, s, Me), 2.20-2.23 (1H, m, 3' or 4'), 2.34-2.38 (1H, m, 3' or 4'), 3.24-3.36 (2H, ddd  $^3J = 3.1$  Hz,  $^3J = 10.5$  Hz,  $^3J = 20.8$  Hz, 2'), 3.65 (6H, s, OMe), 4.00-4.02 (1H, m,) 4.5-4.53 (1H, m) 6.36 (1H, t  $^3J = 6.9$  Hz, 1'), 6.72 (4H, d  $^3J = 8.9$  Hz, Ar), 7.13-7.23 (7H, m, Ar), 7.31-7.33 (2H, m, Ar), 7.53 (1H, s, 6)

$^{13}\text{C}$  NMR (100.6 MHz,  $\text{CDCl}_3$ ):  $\delta_{\text{C}} = 10.8, 39.9, 44.7, 54.2, 62.7, 71.4, 83.8, 85.4, 85.8, 110.2, 112.2, 126.0, 126.9, 127.1, 129.1, 134.4, 134.9, 143.4, 149.8, 157.6, 163.3$

### 3'-O-adamantaneacetyl-5'-O-dimethoxytrityldeoxythymidine (38)

Compound **38** was synthesised according to the literature procedure.<sup>33</sup>

The compound was obtained as a white foam. Yield 79% (3.67 g, 5.1 mmol).



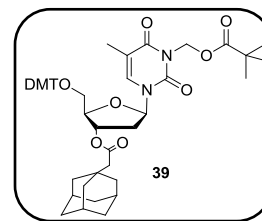
Characterisation agreed with the literature.<sup>33</sup>

$^1\text{H}$  NMR (400 MHz,  $\text{CDCl}_3$ ):  $\delta_{\text{H}} = 1.30$  (3H,s), 1.52-1.63 (12H, m), 1.88 (3H, bs), 2.20-2.01 (2H, bs), 2.34-2.40 (2H, m), 3.40 (1H- m), 3.70 (6H), 4.04-4.06 (1H, m,) 5.37-5.38 (1H, m) 6.37 (1H, t  $^3J = 7.1$  Hz, 1'), 6.75 (4H, d  $^3J = 8.7$  Hz), 7.13-7.23 (7H, m), 7.31-7.33 (2H, m), 7.53 (1H, s), 9.47 (1H, bs)

$^{13}\text{C}$  NMR (100.6 MHz,  $\text{CDCl}_3$ ):  $\delta_{\text{C}} = 10.6, 27.5, 32.0, 35.6, 37.0, 41.4, 47.6, 54.2, 62.7, 73.7, 83.2, 83.4, 86.1, 110.6, 112.3, 126.2, 127.0, 127.1, 129.1, 134.2, 134.7, 134.8, 143.2, 149.7, 157.7, 162.9, 170.2$

**3'-*O*-adamantaneacetyl-5'-*O*-dimethoxytrityl-*N*-pivaloyloxymethyl-deoxythymidine (39)**

Compound **39** was synthesised according to the literature procedure.<sup>33</sup> The compound was obtained as a white foam. Yield 79% (3.36 g, 4.0 mmol).



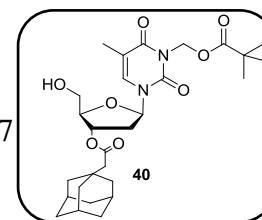
Characterisation agreed with the literature.<sup>33</sup>

<sup>1</sup>H NMR (400 MHz, CDCl<sub>3</sub>): δ<sub>H</sub> = 1.10 (9H, s), 1.33 (3H, s), 1.50-1.62 (12H, m), 1.87 (3H, bs), 1.99 (2H, s), 2.37-2.40 (2H, m), 3.40 (2H, m), 3.68 (6H, s), 4.05-4.07 (1H, m), 5.37-5.40 (1H, m), 5.84-5.89 (2H, m) 6.38 (1H, t <sup>3</sup>J = 7.1 Hz, 1'), 6.75 (4H, d <sup>3</sup>J = 8.9 Hz), 7.12-7.16 (1H, m) 7.19-7.22 (6H, m), 7.30-7.33 (2H, m), 7.56 (1H, s)

<sup>13</sup>C NMR (100.6 MHz, CDCl<sub>3</sub>): δ<sub>C</sub> = 10.5, 25.3, 26.7, 31.2, 34.9, 36.3, 37.0, 40.7, 46.8, 53.4, 61.8, 63.4, 72.8, 83.3, 85.4, 108.9, 111.5, 125.4, 126.4, 128.3, 132.7, 133.4, 133.5, 142.5, 148.6, 157.0, 160.7, 165.4, 175.7

**3'-*O*-adamantaneacetyl-*N*-pivaloyloxymethyl-deoxythymidine (40)**

Compound **40** was synthesised according to the literature procedure.<sup>33</sup> The compound was obtained as a white foam. Yield 65 % (1.44 g, 2.7 mmol).



Characterisation agreed with the literature.<sup>33</sup>

<sup>1</sup>H NMR (400 MHz, CDCl<sub>3</sub>): δ<sub>H</sub> = 1.11 (9H, s), 1.53-1.66 (12H, m), 1.90 (3H, bs), 2.03 (2H, s), 2.31-2.35 (2H, m), 3.87 (2H, m), 4.03-4.05 (1H, m), 5.26-5.30 (1H, m), 5.85-5.91 (2H, m) 6.25 (1H, t <sup>3</sup>J = 7.3 Hz), 7.61 (1H, s)

<sup>13</sup>C NMR (100.6 MHz, CDCl<sub>3</sub>): δ<sub>C</sub> = 13.2, 27.0, 28.5, 33.0, 36.6, 37.5, 38.8, 42.4, 48.6, 62.5, 65.1, 74.2, 85.3, 86.2, 110.5, 135.3, 150.4, 162.6, 171.6, 177.7

**General procedure for solution phase synthesis of trimers.<sup>33</sup>**

Compound **40** (237 mg, 0.45 mmol) and nucleotide **23** (523 mg, 0.67 mmol) were azeotropically dried 3 times by co-evaporating with acetonitrile before dissolving in 3.3 ml of acetonitrile. DCI (dicyano imidazole) (266 mg, 2.3 mmol) was subsequently added and the reaction mixture was left to stir until the reaction had gone to completion according to TLC. 200 µl of water was added and the reaction mixture was stirred for a minute longer before adding 7.2 ml of 0.2M I<sub>2</sub> in a mixture of THF/pyridine 4:1. After 5 minutes the reaction mixture was diluted with 25 ml of ethyl acetate and 5 ml of THF and washed with a saturated solution of Na<sub>2</sub>S<sub>2</sub>O<sub>4</sub>

**General procedure for oligonucleotide synthesis**

Oligonucleotides were synthesised using an Applied Biosystems 392 DNA/RNA synthesizer. A preprogrammed synthesis was used. The unmodified nucleotides were bought from Link technologies or Glen research. The reagents used for the synthesis were an activator (sublimed 1H-tetrazole in anhydrous acetonitrile), oxidizing solution (0.10 M I<sub>2</sub> in THF/pyridine/acetic anhydride), capping mix A (THF/pyridine/acetic anhydride), capping mix B (10% 1-methylimidazole in THF/pyridine) and deblocking mix (3% trichloro acetic acid in DCM). The coupling efficiency was determined by measuring the conductivity generated by the release of the DMT-cation. The nucleotide was released from solid support either by removing the solid support from the column reactor or leaving it in there and treating it with an ammonium hydroxide solution. In the first case (removing the nucleotide on solid support from the reactor) the beads were placed in a flask before adding ammonium hydroxide solution and heating at 55 °C for 16 hours. Before purification *via* HPLC (eluent methanol, 0.15 M TEAA pH =7) the freed nucleotide was filtered over a syringe filter.

In the latter case a 3.5 M solution of ammonia in methanol was added to the reactor. After a couple of hours the solution was removed before adding ammonia hydroxide and heating at 55 °C for 15 hours. After this time the solution was removed and the solid support in the reactor was wash with ethanol and water. The protecting groups were removed by FPLC (fast protein liquid chromatography), using water as the eluent.

Ion exchange resin (Dowex 50W) was used to improve mass spectroscopy results.

**General procedure for the copper catalysed 1,3-cycloaddition**

A 0.07 M solution of compound **35** (10 ml, 0.7 mmol) in dioxane was placed in a Schlenk. The alkyne containing compound (149 mg, 0.56 mmol) was dissolved in THF (10 ml) and added to compound **35**. Degassed water (6 ml) was added before adding sodium ascorbate (90.8 mg, 0.46 mmol) and copper sulphate hydrate (39.9 mg). The reaction mixture was stirred for 20 hours. The organic layer was removed under reduced pressure. The reaction mixture was extracted with diethyl ether (3 x 20 ml). The solvent was removed and the crude product was purified *via* flash chromatography over silica. Eluent DCM: acetone 1:1. The product was obtained as a white solid.

**Compound 46a**

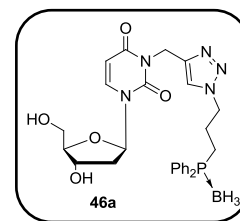
Yield 40% (0.22 mmol).

$^1\text{H}$  NMR (400 MHz,  $\text{CDCl}_3$ ):  $\delta_{\text{H}} = 1.11$  (9H, s), 1.53-1.66 (12H, m), 1.90 (3H, bs), 2.03 (2H, s), 2.31-2.35 (2H, m), 3.87 (2H, m), 4.03-4.05 (1H, m), 5.26-5.30 (1H, m), 5.85-5.91 (2H, m) 6.25 (1H, t  $^3J = 7.3$  Hz), 7.61 (1H, s)

$^{13}\text{C}$  NMR (100.6 MHz,  $\text{CDCl}_3$ ):  $\delta_{\text{C}} = 13.2, 27.0, 28.5, 33.0, 36.6, 37.5, 38.8, 42.4, 48.6, 62.5, 65.1, 74.2, 85.3, 86.2, 110.5, 135.3, 150.4, 162.6, 171.6, 177.7$

$^{31}\text{P}$  NMR (121 MHz,  $\text{CDCl}_3$ )  $\delta_{\text{P}} = 15.8$  (b)

HRMS (ESI) calcd for  $\text{C}_{27}\text{H}_{31}\text{O}_5\text{N}_5\text{P}$  ( $\text{M-BH}_3 + \text{H}$ ) $^+$  536.2057 found 536.2045



## 2.5 References

1. (a) Boersma, A. J.; Feringa, B. L.; Roelfes, G., *Angew. Chem. Int. Ed.* **2009**, *48* (18), 3346-3348;(b) Roelfes, G.; Boersma, A. J.; Feringa, B. L., *Chem. Commun.* **2006**, (6), 635-637.
2. (a) Fournier, P.; Fiammengo, R.; Jäschke, A., *Angew. Chem. Int. Ed.* **2009**, *48* (24), 4426-4429;(b) Nuzzolo, M.; Grabulosa, A.; Slawin, A. M. Z.; Meeuwenoord, N. J.; van der Marel, G. A.; Kamer, P. C. J., *Eur. J. Org. Chem.* **2010**, *2010* (17), 3229-3236.
3. Borsenberger, V.; Howorka, S., *Nucleic Acids Res.* **2009**, *37* (5), 1477-1485.
4. Letsinger, R. L.; Mahadevan, V., *J. Am. Chem. Soc.* **1965**, *87* (15), 3526-3527.
5. Letsinger, R. L.; Finnan, J. L.; Heavner, G. A.; Lunsford, W. B., *J. Am. Chem. Soc.* **1975**, *97* (11), 3278-3279.
6. Beaucage, S. L.; Caruthers, M. H., *Tetrahedron Lett.* **1981**, *22* (20), 1859-1862.
7. [http://www.linktech.co.uk/products/standard\\_dna\\_phosphoramidites/7\\_bz-da-ce-phosphoramidite](http://www.linktech.co.uk/products/standard_dna_phosphoramidites/7_bz-da-ce-phosphoramidite), accessed 01-2012.
8. Ehrenschwender, T.; Barth, A.; Puchta, H.; Wagenknecht, H.-A., *Org. Biomol. Chem.* **2012**, *10*, 46-48.
9. Chatelain, G.; Ripert, M.; Farre, C.; Ansanay-Alex, S.; Chaix, C., *Electrochimica Acta* **2012**, *59* (0), 57-63.
10. Prakash, T. P., *Chemistry & Biodiversity* **2011**, *8* (9), 1616-1641.
11. (a) Cobb, A. J. A., *Org. Biomol. Chem.* **2007**, *5*, 3260-3275;(b) Hyrosova, E.; Fisera, L.; Medvecký, M.; Reissig, H.-U.; Al-Harrasi, A.; Koos, M., *ARKIVOC* **2009**, *ix* (5), 122-142.
12. Sirivolu, V. R.; Chittepū, P.; Seela, F., *ChemBioChem* **2008**, *9* (14), 2305-2316.
13. (a) Shida, T.; Iwaori, H.; Arakawa, M.; Sekiguchi, J., *Chem. Pharm. Bull.* **1993**, *41* (5), 961-4;(b) Sau, S. P.; Hrdlicka, P. J., *J. Org. Chem.* **2011**, *77* (1), 5-16.
14. Fujino, T.; Yamazaki, N.; Hasome, A.; Endo, K.; Isobe, H., *Tetrahedron Lett.* **2012**, *53* (7), 868-870.
15. (a) Briones, C.; Moreno, M., *Anal. Bioanal. Chem.*, 1-19;(b) Crumpton, J. B.; Santos, W. L., *Chem. Commun.* **2012**, *48*, 2018-2020.
16. Wang, Y.; Tkachenko, B. A.; Schreiner, P. R.; Marx, A., *Org. Biomol. Chem.* **2011**, *9*, 7482-7490.
17. Seo, T. S.; Li, Z.; Ruparel, H.; Ju, J., *J. Org. Chem.* **2002**, *68* (2), 609-612.
18. Kolb, H. C.; Finn, M. G.; Sharpless, K. B., *Angew. Chem. Int. Ed.* **2001**, *40* (11), 2004-2021.
19. Liang, L.; Astruc, D., *Coord. Chem. Rev.* **2011**, *255* (23-24), 2933-2945.
20. Boren, B. C.; Narayan, S.; Rasmussen, L. K.; Zhang, L.; Zhao, H.; Lin, Z.; Jia, G.; Fokin, V. V., *J. Am. Chem. Soc.* **2008**, *130* (28), 8923-8930.
21. Rostovtsev, V. V.; Green, L. G.; Fokin, V. V.; Sharpless, K. B., *Angew. Chem. Int. Ed.* **2002**, *41* (14), 2596-2599.
22. Himo, F.; Lovell, T.; Hilgraf, R.; Rostovtsev, V. V.; Noodleman, L.; Sharpless, K. B.; Fokin, V. V., *J. Am. Chem. Soc.* **2005**, *127* (1), 210-216.
23. Rodionov, V. O.; Presolski, S. I.; Díaz Díaz, D.; Fokin, V. V.; Finn, M. G., *J. Am. Chem. Soc.* **2007**, *129* (42), 12705-12712.
24. Monson, C. F.; Woolley, A. T., *Nano Letters* **2003**, *3* (3), 359-363.
25. Gierlich, J.; Burley, G. A.; Gramlich, P. M. E.; Hammond, D. M.; Carell, T., *Org. Lett.* **2006**, *8* (17), 3639-3642.

26. (a) Chan, T. R.; Hilgraf, R.; Sharpless, K. B.; Fokin, V. V., *Org. Lett.* **2004**, *6* (17), 2853-2855;(b) Rondelez, Y.; Bertho, G.; Reinaud, O., *Angew. Chem. Int. Ed.* **2002**, *41* (6), 1044-1046.
27. Pradere, U.; Roy, V.; McBrayer, T. R.; Schinazi, R. F.; Agrofoglio, L. A., *Tetrahedron* **2008**, *64* (38), 9044-9051.
28. Valeur, E.; Bradley, M., *Chem. Soc. Rev.* **2009**, *38* (2), 606-631.
29. Nakano, S.-i.; Uotani, Y.; Uenishi, K.; Fujii, M.; Sugimoto, N., *Nucleic Acids Research* **2005**, *33* (22), 7111-7119.
30. (a) Caprioara, M.; Fiammengo, R.; Engeser, M.; Jäschke, A., *Chem.-Eur. J.* **2007**, *13* (7), 2089-2095;(b) Sakurai, K.; Snyder, T. M.; Liu, D. R., *J. Am. Chem. Soc.* **2005**, *127* (6), 1660-1661.
31. Detz, R. J.; Heras, S. A.; de Gelder, R.; van Leeuwen, P. W. N. M.; Hiemstra, H.; Reek, J. N. H.; van Maarseveen, J. H., *Org. Lett.* **2006**, *8* (15), 3227-3230.
32. McGuigan, C.; Univ Cardiff (GB) Chemical compounds. WO 2005012327 20040720, 2005.
33. de Koning, M. C.; Ghisaidoobe, A. B. T.; Duynstee, H. I.; Ten Kortenaar, P. B. W.; Filippov, D. V.; van der Marel, G. A., *Org. Process Res. Dev.* **2006**, *10* (6), 1238-1245.
34. Byun, Y.; Yan, J.; Al-Madhoun, A. S.; Johnsamuel, J.; Yang, W.; Barth, R. F.; Eriksson, S.; Tjarks, W., *J. Med. Chem.* **2005**, *48* (4), 1188-1198.
35. Bowler, F. *Final report*; University of St Andrews: St Andrews, 2005.
36. Nakane, M.; Ichikawa, S.; Matsuda, A., *J. Org. Chem.* **2008**, *73* (5), 1842-1851.



One turn in B-DNA takes approximately 10 base pairs. Although DNA consists of just 4 building blocks 1,048,576 combinations are achievable for one turn.<sup>5</sup> It is therefore understandable that a lot of work has been put into finding MGBs that target a specific sequence.<sup>6</sup>

Natural MGBs distamycin A and netropsin bind to sequences within the DNA double helix that contain 4 or 5 successive A,T base pairs. Through NMR and crystal structure studies it was discovered how the specific binding occurs. The minor groove is completely filled with the pyrrole rings and a bifurcated hydrogen bond is formed between the amide hydrogen of the N-methyl pyrrolecarboxamide and the N3 of adenine and the O2 of thymine (Figure 2). The N-methylpyrrole amide does not form hydrogen bonds with G,C base pairs, presumably because the hydrogen on the pyrrole is located too deep within the minor groove to allow room for binding to the NH<sub>2</sub> of guanine.<sup>7</sup>

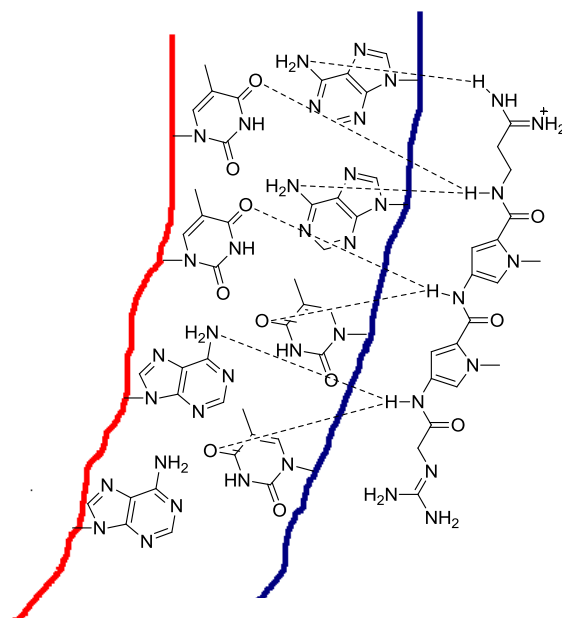


Figure 2: Distamycin A binding to AATT

Therefore polyamide chains containing pyrroles (Py), as in distamycin A, can specifically target A,T base pairs in DNA. When a 2:1 ratio of distamycin A to DNA is used the distamycin A aligns itself side-by-side in an antiparallel fashion within the minor groove of DNA.<sup>4</sup>

By adding imidazoles (Im) to the polyamide sequence G-C base pairs can be targeted. The imidazole facilitates base-specific recognition *via* the formation of hydrogen bonds between the nitrogens in the ring and the amino groups of guanosine.<sup>8</sup> The MGBs align themselves side-by-side across the minor groove in an antiparallel fashion within the double helix of

DNA.<sup>8</sup> PyPy pairs show a preference for A,T base pairs but cannot distinguish between A,T or T,A whereas a pairing of ImPy targets G,C while PyIm targets C,G.<sup>6</sup> ImIm base pairs favour the mismatched pair T,G.<sup>9</sup> 3-Hydroxy-1H-pyrrole (Hp) is a minor groove binder which favours A-T base pairs over T-A, however, introducing Hp into the sequence lowers the binding affinity, the capability of the polyamide to hold the helical DNA together.<sup>4</sup> These specific recognition characteristics have led to a single-letter code for each MGB pair. This code denotes the specific sequence which will be targeted so that PyPy is written as W (indicating either A or T), PyIm as C, ImPy as G. The polyamides are often depicted with symbols; for example a filled circle represents Im and an open circle Py (Figure 3). The tail is generally formed by a  $\beta$ -alanine group, represented in Figure 3 by a diamond, and dimethylaminopropyl, represented as a half circle with a plus.

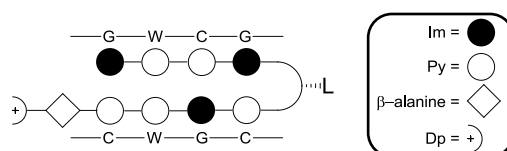


Figure 3: Representation of a polyamide binding to a DNA strand

This specific recognition does not indicate how strong the affinity is of individual polyamide sequences to their cognate DNA sequence. For example ImHpPyPy-turn-ImHpPyPy binds 160-fold better to GATC than ImPyPyPy-turn-ImHpHpPy binds to its cognate target even though they both contain 1 Im, 2 Py and 1 Hp.<sup>4</sup>

To allow the polyamide chain to fold back onto its self a turn is often incorporated in the scaffold creating a hairpin structure. Studies have shown that the ideal length of the turn unit is three methylene blocks. This led to the use of  $\gamma$ -aminobutyric acid as the turn.<sup>10</sup> The optimum number of pyrrole or imidazole rings in the sequence (before the turn) is five; shorter or longer sequences show a decrease in both affinity and specificity. This decrease is caused by mismatching between the curvature of the polyamide and the groove of DNA.<sup>8</sup>

By adding substituents to the butyric acid moiety, the turn functionality, the affinity to a DNA sequence could be enhanced. By adding an extra amino group as in the case of (R)-2,4-diaminobutyric acid a 15-fold increase in binding affinity was observed. On the other hand (S)-2,4-diaminobutyric acid showed a decrease in binding affinity which is rationalised by the steric clash of the amine with the wall of the minor groove. The turn in the hairpin also exhibits a specific recognition preference. It was found that the turn favours T and A containing base pairs over those that contain C and G. There have been reports that state the

turn can show improved selectivity when an  $\alpha$ -hydroxy is present on the  $\gamma$ -aminobutyric acid or when  $\alpha$ -diaminobutyric acid is used. Utilising these substances can increase the ability to target specific sequences however the overall binding strength, the capability to hold the two strands of the helical DNA together, is lowered.<sup>10</sup>

Table 1: Melting temperatures of DNA/polyamide complexes<sup>10</sup>

Polyamide	$T_m$	$\Delta T_m$
-	45.1 ( $\pm 0.1$ )	-
	54.3 ( $\pm 0.3$ )	9.2
	59.8 ( $\pm 0.3$ )	14.7
	60.0 ( $\pm 0.2$ )	14.9
	59.8 ( $\pm 0.2$ )	14.7
	54.9 ( $\pm 0.1$ )	10.1
	55.1 ( $\pm 0.2$ )	10.0
	53.4 ( $\pm 0.2$ )	8.3
	50.9 ( $\pm 0.2$ )	5.8
	53.0 ( $\pm 7.9$ )	7.9

DNA = 50-CTATGGTA GAC-30

By exchanging 2,4-diaminobutyric acid for 3,4-diaminobutyric acid an improved binding affinity was observed for A,T-rich sequences. It was also found that the tolerance for synthetic modification of the amine was enhanced. It was postulated that this stability was caused by the more central location of the 3,4-diaminobutyric moiety of the turn, on the floor of the minor groove.

In Table 1 the relative melting temperatures of DNA duplexes in the presence of polyamides containing a variety of turns are depicted. It was assumed that relative melting temperatures correlate to the binding affinities, the larger the relative melting temperature the higher the binding affinities. This was confirmed by analysing several DNA/polyamide complexes *via* footprinting.<sup>10</sup>

From a synthetic point of view and for comparison with the natural MGBs the C-terminus, also known as the tail, is charged. This tail typically consists of a  $\beta$ -alanine connected *via* an amide to a dimethylaminopropyl (Dp) group. The tail also shows some specificity to A,T base pairs.<sup>8</sup> In early studies of the binding of distamycin A it was discovered that the tail was always directed to the 5' end of the adenosine sequence and is thus referred to as 5' directional binding. The binding of ImPyPy-Dp to both WCWGW and to WGWCW was also tested. Surprisingly it was discovered that the polyamide would bind to WGWCW but not to WCWGW which would only require a rotation of the polyamide. This suggests that there is a strong energetic preference for orientation.<sup>8</sup>

In this chapter we will discuss the synthesis of the polyamides as minor groove binders (Figure 4) along with the synthesis of the ligands that will bind to the transition metal. Complex studies of the ligand metal complexes and catalysis results will be discussed in Chapter 4.

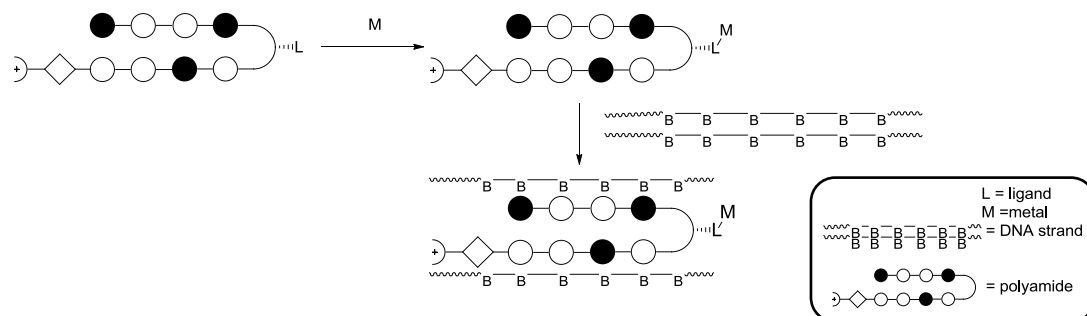


Figure 4: Schematic representation of our non-covalent approach

## 3.2 Results and discussion

### 3.2.1 Synthesis of minor groove binders

The choice of the polyamide sequence is very important as it dictates how strong the binding affinity is. Dervan *et al.*<sup>11</sup> published an article which contained a list of binding affinities for several polyamides and this list was used to choose a suitable polyamide. Polyamide ImPyPyIm-turn-PyImPyPy- $\beta$ -Dp, has an association constant with the double strand oligonucleotide 5'-ATGACGT-3' of  $1 \times 10^{10} \text{ M}^{-1}$ . This polyamide contains a 2,4-diaminobutyric acid derivate whereas in our case we used a 3,4-derivative (Figure 5). As explained in the introduction this should have a beneficial effect on the binding affinity.

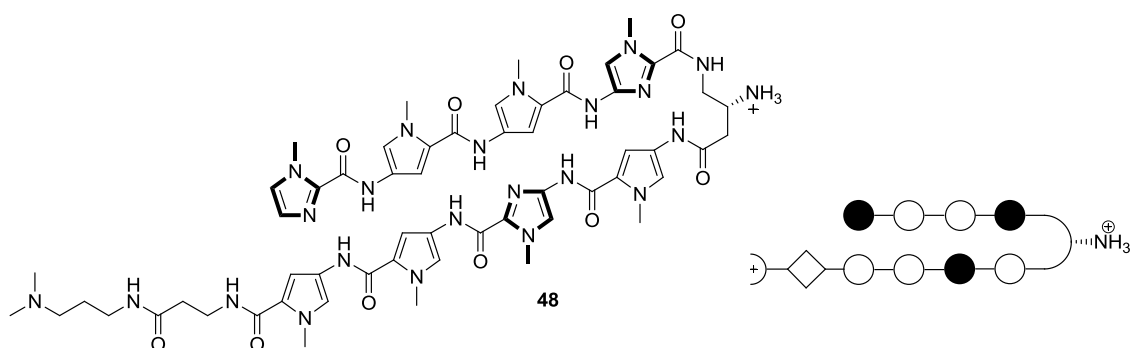


Figure 5: Structure of polyamide ImPyPyIm-(R)NH<sub>2</sub>-PyImPyPy- $\beta$ -Dp (48)

The polyamide was synthesised on solid support using a PAM resin containing a  $\beta$ -alanine moiety (Figure 6) and a number of building blocks (Scheme 1). PAM-resin is a PEG based resin which has become popular in solid-phase peptide synthesis because of its tolerance to trifluoroacetic acid (TFA).

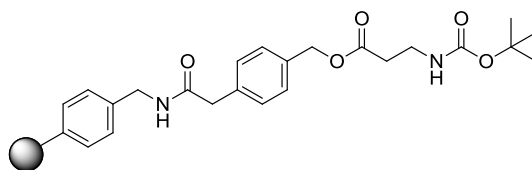
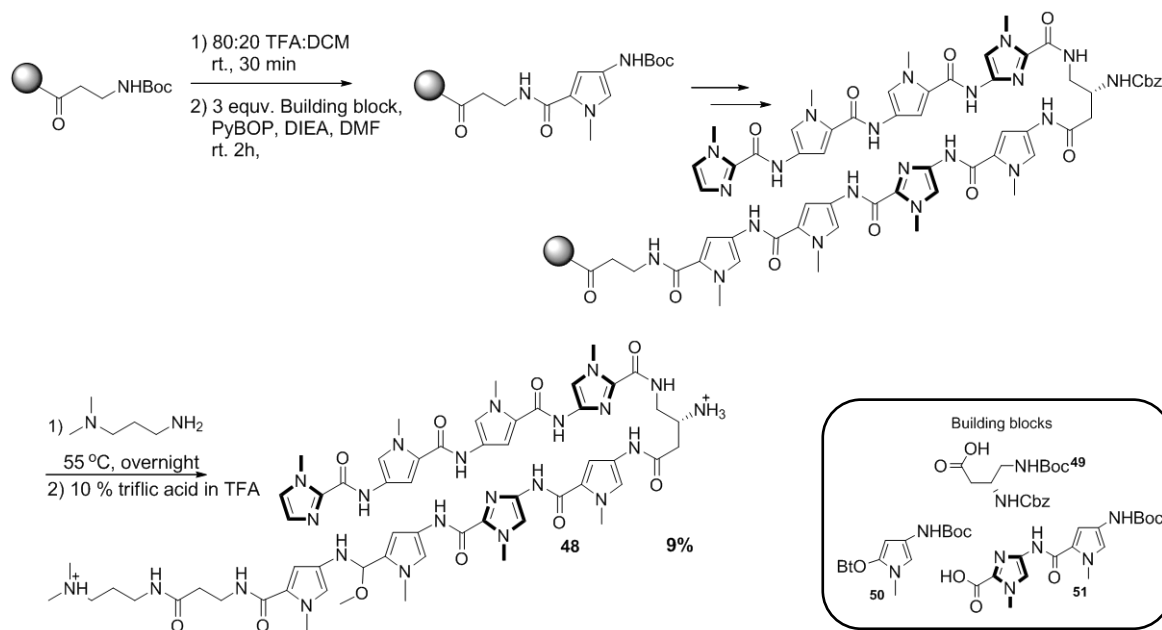


Figure 6: PAM-resin containing a Boc- $\beta$ -alanine moiety

Dervan *et al.*<sup>12</sup> noticed that the coupling of an activated imidazole amine with Boc-Py-OBt ester did not proceed with a high yield. In order to obtain a higher yield of the polyamide they prepared Boc-PyIm dimer unit **51** (Scheme 1). This dimer unit can be prepared on a large scale and subsequently be used as a building block during the synthesis of polyamides.

The butyric acid derivate contains two amines that have different protecting groups thus requiring different conditions for deprotection. The different deprotection conditions ensure

that the amines can be deprotected individually and prevent the formation of side chains. The carboxylic acid on the pyrrole building blocks had been activated *via* 1-hydroxybenzotriazole hydrate (HOBt). The Im-Py-dimer was activated just before use with (benzotriazol-1-yloxy)tripyrrolidin phosphonium hexafluorophosphate (PyBOP) and diisopropylethyl amine (DIEA). After the final coupling the carboxybenzyl (Cbz) group on the turn is removed using a strong acid, a mixture of TFA and triflic acid, and purified *via* HPLC, providing an overall yield of 9 %. After lyophilisation the polyamide was ready to couple to a ligand.

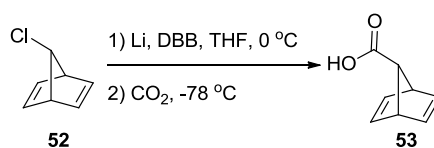


Scheme 1: Synthesis of polyamide GWCG

### 3.2.2 Ligand synthesis

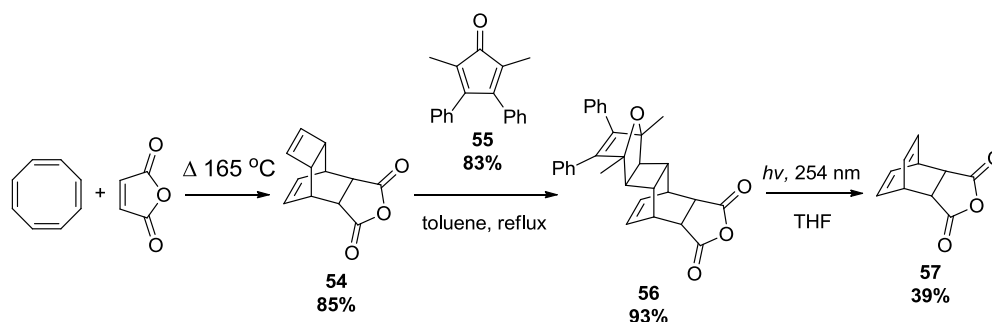
To circumvent the problem of oxidation associated with phosphine ligands, we also aimed to modify the polyamide with diene-ligands.

We decided to use a 7-norbornadiene (nbd) derivative containing a carboxylic acid functionality which was first reported by Klumpp *et al.*<sup>13</sup> Bicyclo[2.2.1]hepta-2,5-diene-7-carboxylic acid (**53**) (Scheme 2) is formed by converting chloro-nbd **52** into a radical using lithium *p,p'*-di-*t*-butylbiphenyl (LiDBB) and subsequently quenching it with carbon dioxide.



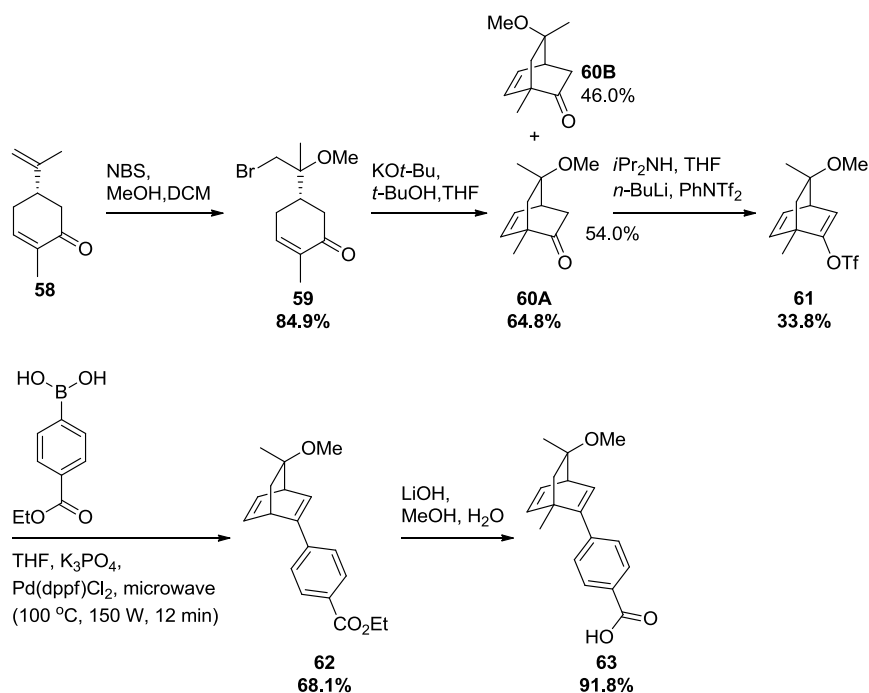
Scheme 2: Synthesis of NBD diene 53

In 1976 Zimmerman *et al.*<sup>14</sup> reported the synthesis of diene **57** (Scheme 3). The synthesis encompasses two successive Diels-Alder reactions followed by a photoinduced aromatisation. Diene **57** was obtained as a solid which was difficult to purify. An added difficulty was that the compound was unstable. As a solid it was relatively stable especially when kept cool however when placed in solution it had the tendency to undergo a retro Diels-Alder generating benzene and maleic anhydride.



Scheme 3: Synthesis of diene **57**

The chiral diene which Jäschke *et al.*<sup>15</sup> used was also synthesised. This diene (**63**, Scheme 4) had a [2.2.2] structure and could be obtained in five steps starting from the cheap and commercially available carvone (**58**). In the first step a good leaving group was introduced into the carvone frame work by reacting carvone with N-bromosuccinimide (NBS). The leaving group was needed to facilitate the intramolecular alkylation reaction to form **60**. After the alkylation, the formed diastereomers could easily be separated *via* flash chromatograph on silica gel. In step 3 *N*-Phenyl-bis(trifluoromethanesulfonimide) (PhNTf<sub>2</sub>) was used as triflating agent. It was imperative that it was dried before use as the water content present in the compound when purchased was high enough to quench the lithium diisopropylamide (LDA). Once the triflated product **61** was obtained a Suzuki coupling was performed with the assistance of a microwave. The final step of this synthesis was a simple hydrolysis using a strong base.



Scheme 4: Synthesis of chiral diene 63

### 3.2.3 Combining minor groove binders with ligands

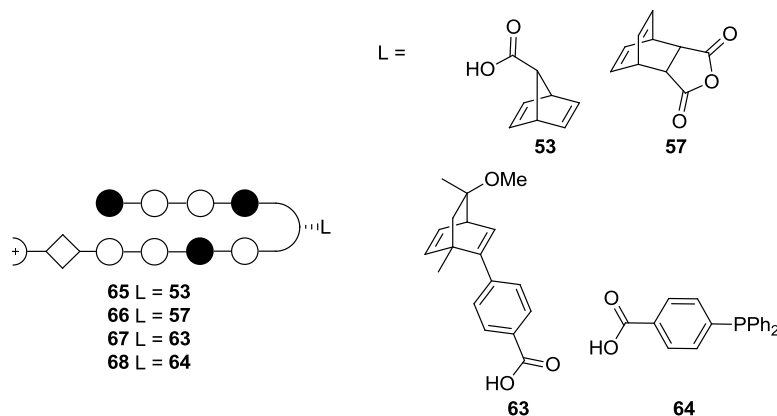


Figure 7: Polyamides that were attempted to synthesise

Once the polyamide and ligand had been synthesised they were ready to be coupled to each other. The carboxylic acid groups of **53**, **63**, and **64** (Figure 7) were activated using a mixture of PyBOP and DIEA before coupling to the polyamide. During the activation of compound **53** the solution turned a deep purple colour.

The reaction mixtures of the turn modified polyamides were analysed with analytical HPLC to check if the reactions had gone to completion. These turn modified polyamides were subsequently purified *via* HPLC. The isolated yields of the dienes were low; a mere 20 %. This can probably be improved by adjusting the HPLC conditions. The analytical HPLC

traces of the unmodified polyamide and purified compound **65** are shown in Figure 8. The shift in retention time is clearly evident (7.5 min. shifts to 9 min).

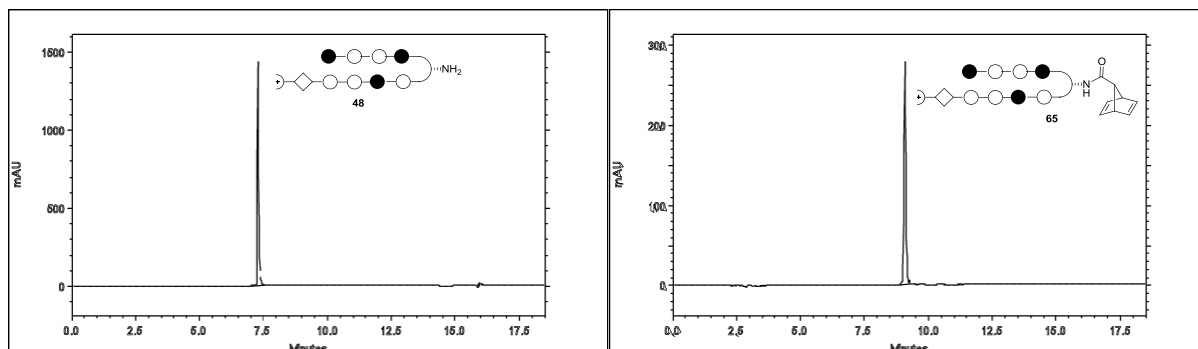


Figure 8: Left: the HPLC trace of unmodified polyamide **48** Right: the HPLC trace of purified compound **65**

The synthesis of compound **68** was followed by analytical HPLC (Figure 9). By comparing the two HPLC traces it was concluded that the starting polyamide was completely converted (no peak at 7.3 min. in the right trace). The peak at 5.6 min (right trace) was the OBt group from the PyBOP. The other two peaks correspond to the oxidised (10.3 min.) and unoxidised (12.5 min.) phosphine polyamide **68**.  $^{13}\text{P}$ -NMR of this crude reaction mixture showed no evidence of the phosphine oxide indicating that the oxidation occurred during the running of the HPLC sample. To avoid oxidation during purification other methods need to be explored. One option is precipitating the polyamide out of solution by adding diethyl ether to a concentrated volume of the reaction mixture.

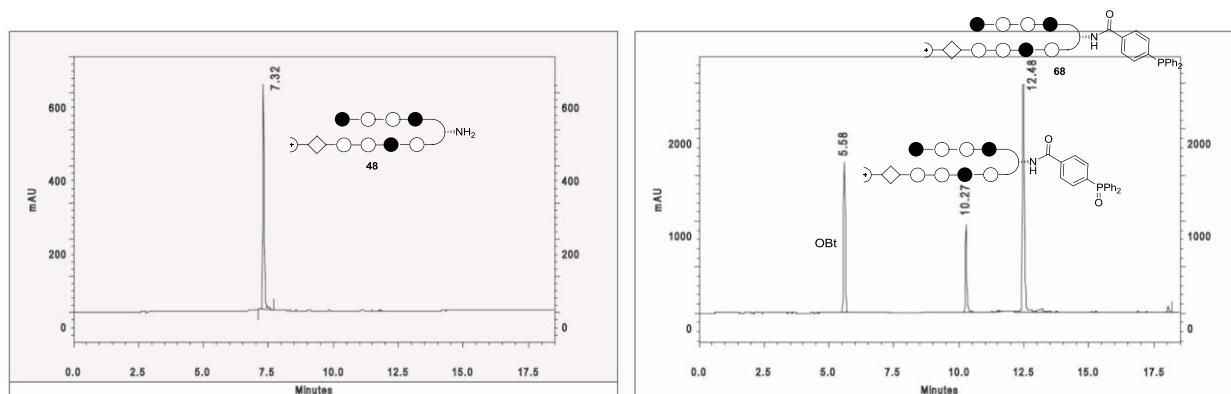
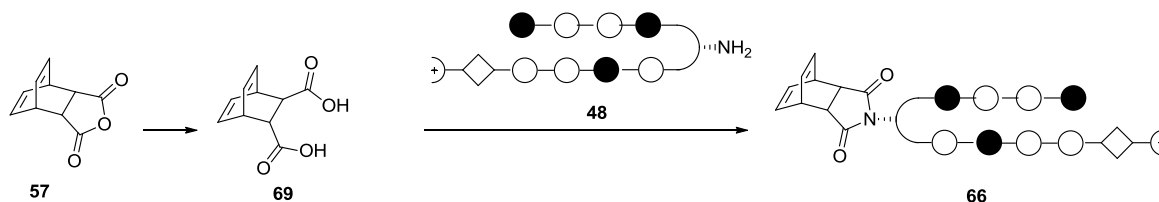


Figure 9: Left: HPLC trace of the unmodified polyamide Right: HPLC trace of the reaction mixture at the end of the synthesis of compound **45**

Problems arose with coupling diene **57** to the polyamide. Initially it was attempted to convert the anhydride into diacid **69** (Scheme 5). There are various methods known for the formation of a diacid from an anhydride, probably the most common being heating. This was not attempted as it would likely facilitate the retro Diels-Alder. Acid and base assisted<sup>16</sup> ring opening reactions are also known. Sodium hydroxide was dissolved in water and added to a

solution of diene **57** in THF. This gave a biphasic system. After separating the layers the aqueous layer was acidified and lyophilised. Degradation of the product occurred somewhere between the acidification and lyophilisation. This method should work but due to the small amount of **57** that was acquired and its instability no further attempts were made and no effort was put into looking into what went wrong.



Scheme 5: Schematic representation of the coupling of diene **6** with the unmodified polyamide

It is important that the introduced ligands do not have a detrimental effect on the binding between the polyamide and the DNA double helix. To assess the influence these modifications have on the binding affinity the melting temperature ( $T_m$ ) of polyamide **65** (Figure 10) complexed with its DNA target sequence was measured. As a standard polyamide **71** was also synthesised and its  $T_m$  measured. The results are shown in Table 2. The introduction of the diene did not have a negative impact on the binding constant, in fact it appears to have a stabilising effect on the helical DNA.

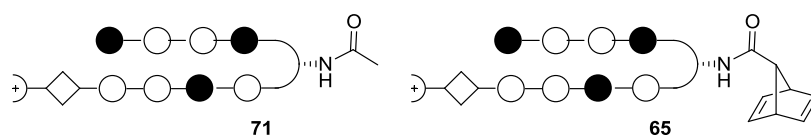


Figure 10: Polyamides where the melting temperature was required

Table 2: Melting temperature

	$T_m$ ( $^{\circ}\text{C}$ )	$\Delta T_M$
DNA	$55.39 \pm 0.46$	--
DNA + 71	$67.13 \pm 0.31$	$11.74 \pm 0.56$
DNA + 65	$68.63 \pm 0.22$	$13.24 \pm 0.51$

$T_m$ -buffer: 10mM sodium cacodylate, 10mM KCl, 10mM  $\text{MgCl}_2$ , 5mM  $\text{CaCl}_2$  pH 7  
DNA = 5'-CGATGGTCAAGC-3'

Because the  $T_m$ 's are not determined under anaerobic conditions the  $T_m$  of polyamide **68** could not be measured.

### 3.3 Conclusion

The synthesis and subsequent coupling of diene **57** to a polyamide was cumbersome so this approach was quickly discarded.

Dienes **53** and **63** were coupled to the polyamide using standard amide coupling procedures resulting in polyamides **65** and **67**. The melting temperatures of these polyamides were also measured and the results indicated that the dienes have a positive effect on the binding affinity of the polyamide DNA complex.

The  $T_m$  of the DNA complex of **68** was not measured as oxidation of the phosphine would occur which could potentially result in an enhancing the  $\Delta T_m$ . NMR indicated that oxidation had occurred during HPLC. This means other purification methods should be tried.

## 3.4 Experimental

### General Procedures

All air- and water-sensitive reactions were carried out under argon utilising standard schlenk techniques. Chemicals were purchased from Sigma Aldrich, Acros, Link Technologies, Fisher Scientific, Strem and used as is unless otherwise stated. Diisopropylethylamine was distilled from  $\text{CaH}_2$ ,  $\text{CDCl}_3$  was distilled from  $\text{CaCl}_2$  and stored under argon over  $\text{K}_2\text{CO}_3$ . THF and diethyl ether were distilled from sodium/benzophenone. All the distilled solvents were stored under argon or nitrogen. Dry DMF was purchased and transferred into a youngs ampule. Organic solvents were degassed by three freeze/thaw cycles. Aqueous solutions were degassed by bubbling argon or nitrogen through for several hours.

Thin Layer Chromatography (TLC) was performed using silica plates (polygram 0.3 mm silica gel with fluorescent indicator UV254 on aluminium plates) purchased from Merck. Compounds on TLC were visualised by UV-detection unless otherwise stated. Flash chromatography or purification on a chromatotron<sup>TM</sup> were performed using the indicated eluent. The silica used for flash chromatography was silica gel 60 mesh 70-230 and was purchased from Fluka.

NMR spectra were recorded at room temperature on a Bruker Avance NMR spectrometer (300,400 or 500 MHz) or a Varian NMR Spectrometer (300, 400 or 600 MHz). NMR spectra recorded at 37 °C were measured on a Varian NMR Spectrometer (400 MHz). Chemical shifts ( $\delta$ ) are given in ppm. Shifts are relative to a TMS reference ( $^1\text{H}$  or  $^{13}\text{C}$ ) or an 85%  $\text{H}_3\text{PO}_4$  reference ( $^{31}\text{P}$ ).  $^{13}\text{C}$  and  $^{31}\text{P}$  spectra were measured with  $^1\text{H}$  decoupling unless otherwise stated.

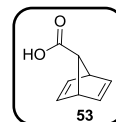
MALDI-TOF mass spectra were recorded on a 4800 Plus MALDI TOF/TOF<sup>TM</sup> Analyzer using  $\alpha$ -cyano-4-hydroxycinnamic acid as a matrix.

$T_m$  measurements were recorded on a Cary 100 spectrophotometer equipped with a thermo-controlled cell holder. The cell path length was 1 cm.

**Bicyclo[2.2.1]hepta-2,5-diene-7-carboxylic acid (53)**

Compound **53** was synthesised in accordance with the literature procedure.<sup>13</sup>

A white solid was obtained in yield 40 % (40 mg, 0.3 mmol).



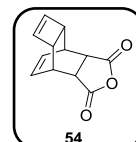
<sup>1</sup>H NMR (CDCl<sub>3</sub>, 300 MHz)  $\delta_{\text{H}} = 3.14$  (1H, t,  $J = 1.7$  Hz), 3.85 (2H, sextet,  $J = 1.9$  Hz), 6.75 (4H, dt  $J = 5.9$  and 4.0 Hz)

<sup>13</sup>C NMR (DMSO-*d*<sub>6</sub>, 75 MHz)  $\delta_{\text{C}} = 51.5, 85.4, 141.4, 143.3, 171.5$

**(4R,4aR,6aS,7S)-4,4a,7,7a-tetrahydro-4,7-ethenocyclobuta[f]isobenzofuran-1,3(3aH,6aH)-dione (54)**

Compound **54** was synthesised in accordance with the literature procedure.<sup>13</sup>

A yellowish solid was obtained in 85 % yield (1.7 g, 8.4 mmol).



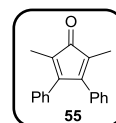
<sup>1</sup>H NMR (CDCl<sub>3</sub>, 400 MHz)  $\delta_{\text{H}} = 2.74$  (2H, s), 3.00 (2H, s), 3.17 (2H, bs), 5.84 (2H, s), 5.96-5.98 (2H, m)

<sup>13</sup>C NMR (CDCl<sub>3</sub>, 100 MHz)  $\delta_{\text{C}} = 36.8, 43.3, 43.9, 129.0, 138.1, 172.5$

**2,5-dimethyl-3,4-diphenylcyclopenta-2,4-dienone (55)**

Compound **55** was synthesised in accordance with the literature procedure.<sup>13</sup>

A yellowish solid was obtained in 83 % yield (5.1 g, 10.0 mmol).



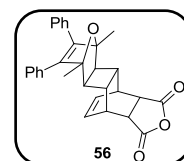
<sup>1</sup>H NMR (CDCl<sub>3</sub>, 400 MHz)  $\delta_{\text{H}} = 0.49$  (3H, s), 1.17 (3H, s), 1.57 (3H, s), 2.23 (3H, s), 6.56-7.2 (20H, m)

<sup>13</sup>C NMR (CDCl<sub>3</sub>, 100 MHz)  $\delta_{\text{C}} = 25.9, 28.6, 30.0, 149.3, 150.6, 153.8$

**exo-4,7-Dimethyl-1,5,6-diphenylpentacyclo[8.2.2.1.4,7.0'.y.0''.L]-entadeca-5,13-dien-15-enedicarboxylic Anhydride (56)**

Compound **56** was synthesised in accordance with the literature procedure.<sup>14</sup>

A brownish solid was obtained in 93 % yield (818mg, 1.8 mmol).

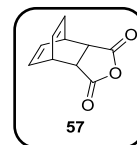


<sup>1</sup>H NMR (CDCl<sub>3</sub>, 400 MHz)  $\delta_{\text{H}} = 1.13$  (6H, s), 1.94-2.00 (4H, m), 2.97 (2H, s), 3.27 (2H, bs), 6.42 (2H, t,  $J = \text{Hz}$ ), 6.85-6.89 (4H, m), 7.07-7.16 (6H, m)

**Bicyclo[2.2.2]octa-2,5-diene-7,8-dicarboxylic Anhydride (57)**

Compound **57** was synthesised in accordance with the literature procedure.<sup>13</sup>

The compound was not obtained in pure form.

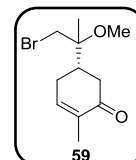


<sup>1</sup>H NMR (CDCl<sub>3</sub>, 400 MHz)  $\delta_{\text{H}} = 3.12$  (2H, s), 4.17 (2H, s), 6.44-6.46 (4H, m)

**(5R)-5- [(2.9-1 -Bromo-2-methoxypropan-2-yl) -2-methylcy clohex-2-enone (59)**

Compound **59** was synthesised in accordance with the literature procedure.<sup>17</sup>

Compound **59** was obtained as an oil in 85 % yield (7.4 g, 28 mmol).

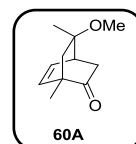


<sup>1</sup>H NMR (CDCl<sub>3</sub>, 300 MHz)  $\delta_{\text{H}} = 1.26$  (3 H, s, tert-CH<sub>3</sub>), 1.78(3 H, s, CH<sub>3</sub>), 2.1-2.65 (5 H, m), 3.24 (3 H, s, OCH<sub>3</sub>), 3.45 (2 H, CH<sub>2</sub>Br), 6.7 (1 H, br s, olefin)

**(1S,4S,SR)-Methoxy-1 ,8-dimethylbicyclo-[2.2.2]oct-5-en-2-one (60A)**

Compound **60A** was synthesised in accordance with the literature procedure.<sup>17</sup>

Compound **60A** was obtained as an oil in 64 % yield (1.2 g, 6.6 mmol).

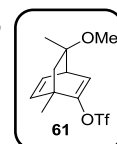


Characterisation agreed with the literature.<sup>17</sup>

**Trifluoro-methanesulfonic acid 8-methoxy-1,8-dimethyl-bicyclo[2.2.2]octa-2,5-dien-2-yl ester (61)**

Compound **61** was synthesised in accordance with the literature procedure.<sup>18</sup>

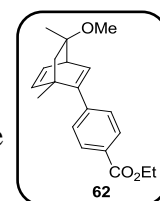
Compound **61** was obtained as an oil in 33 % yield (110 mg, 0.35 mmol).



<sup>1</sup>H NMR (CDCl<sub>3</sub>, 300 MHz)  $\delta_{\text{H}} = 1.26$  (3H, s, Me), 1.28 (1H, d,  $J = 12.1$  Hz, CH<sub>2</sub>), 1.46 (3H, s, Me), 1.78 (1H, d,  $J = 12.1$  Hz, CH<sub>2</sub>), 3.16 (3H, s, OMe), 3.59 (1H, dt,  $J = 6.5, 6.5$ Hz), 6.14-6.08 (2H, m), 6.31 (1H, t,  $J = 13.2$  Hz)

**(1S,4R,8R)-ethyl4-(8-methoxy-1,8-dimethylbicyclo[2.2.2]octa-2,5-dien-2-yl)benzoate (62)**

Compound **62** was synthesised according to the literature procedure.<sup>15</sup> The product was obtained as yellow oil. Yield 68 % (154 mg, 0.49 mmol).



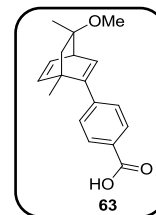
<sup>1</sup>H NMR (300 MHz, CDCl<sub>3</sub>):  $\delta_{\text{H}} = 1.33-1.38$  (7H, m), 1.39 (3H, t,  $J = 7.1$  Hz), 1.63 (1H, d,  $J = 12.3$  Hz), 3.25 (3H, s), 3.70 (1H, dt,  $J = 1.2$  Hz, 6.1 Hz), 4.41 (2H, q,  $J = 67.1$  Hz), 6.19 (1H, dd,  $J = 1.3$  Hz, 7.2 Hz), 6.26 (1H, d,  $J = 5.9$  Hz), 6.42 (1H, t,  $J = 6.7$  Hz), 7.22-7.26 (2H, m), 7.98-8.02 (2H, m)

$^{13}\text{C}$  NMR (75 MHz,  $\text{CDCl}_3$ ):  $\delta_{\text{C}} = 14.4, 21.97, 24.8, 45.4, 47.8, 50.0, 50.6, 60.9, 84.2, 128.4, 128.6, 129.0, 132.8, 134.1, 141.5, 144.5, 149.2, 166.7$

**(1S,4R,8R)-4-(8-methoxy-1,8-dimethylbicyclo[2.2.2]octa-2,5-dien-2-yl)benzoic acid (63)**

Compound **63** was synthesised according to the literature procedure.<sup>15</sup>

The product was obtained as a white solid. Yield 92 % (39.1mg, 0.14 mmol).

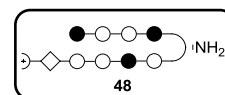


$^1\text{H}$  NMR (300 MHz,  $\text{DMSO-d}_6$ ):  $\delta_{\text{H}} = 1.22$  (3H, s), 1.27 (1H, d,  $J = 11.9$  Hz), 1.29 (3H, s), 1.57 (1H, d,  $J = 11.9$  Hz), 3.10 (3H, s), 3.68 (1H, td,  $J = 6.2$  Hz, 1.3 Hz), 6.15 (1H, dd,  $J = 7.3$  Hz, 1.4 Hz), 6.17 (1H, d,  $J = 6.0$  Hz), 6.39 (1H, t,  $J = 6.9$  Hz), 7.21 (2H, m), 7.88 (2H, m), 12.84 (1H, s)

$^{13}\text{C}$  NMR (75 MHz,  $\text{DMSO-d}_6$ ):  $\delta_{\text{C}} = 21.3, 24.5, 44.6, 46.8, 49.3, 50.4, 83.3, 128.0, 128.7, 128.8, 132.9, 133.9, 141.0, 143.8, 148.1, 167.1$

**Polyamide 48**

Polyamide was synthesised in accordance with literature protocols.<sup>10</sup> The



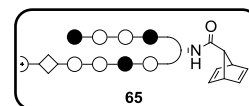
resin which was used for the synthesis was a pre-loaded Boc- $\beta$ -Ala PAM resin (0.81 mequiv/g). Neat 3-dimethylamino-1-propylamine at 60 °C for 16 h was used to cleave the polyamide from the resin. Products were purified by preparative reverse-phase HPLC and characterised by analytical HPLC, UV-visible spectroscopy, and MALDI-TOF mass spectrometry.

UV ( $\text{H}_2\text{O}$ ) max at 318 nm

MALDI-TOF-ms: 1239 m/z

**Polyamide 65**

The coupling of diene **53** with the polyamide proceeded *via* the coupling protocols used for polyamide synthesis. Purified *via* preparative reverse-phase HPLC.

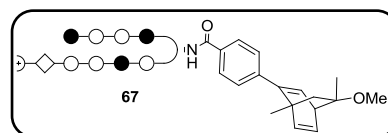


UV( $\text{H}_2\text{O}$ ) max at 318 nm

MALDI TOF-ms: 1358 (expected mass 1356)

**Polyamide 67**

The coupling of diene 53 with the polyamide proceeded via the coupling protocols used for polyamide synthesis. Purified via preparative reverse-phase HPLC.

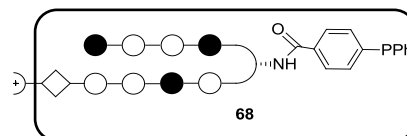


UV(H<sub>2</sub>O) max at 318 nm

MALDI TOF-ms: 1504 (expected mass 1504)

**Polyamide 68**

The coupling of diphenyl phosphine benzoic acid with the polyamide proceeded *via* the coupling protocols used for polyamide synthesis. Attempts were made to purify *via* precipitating the polyamide out of solution and by washing. Neither method had the desired out come as only the oxidised compound was obtained.



UV max at 318 nm

MALDI TOF-ms: 1542 (expected mass 1526, expected mass if oxidised 1542)

<sup>31</sup>P-NMR (162 MHz, unlock): -5.78

**Melting temperature**

2 nmol of each single strand oligonucleotide was placed in quartz cuvette (1 ml) before adding 690  $\mu$ l degassed T<sub>m</sub> buffer (T<sub>m</sub>-buffer: 10 mM sodium cacodylate, 10 mM KCl, 10 mM MgCl<sub>2</sub>, 5 mM, CaCl<sub>2</sub> pH 7) and 310  $\mu$ l of the desired degassed dioxane/water mixture. The cuvette was placed in the spectrophotometer. Before commencing with the measurement the samples were heated to 90 °C and cooled to a starting temperature of 25 °C. The measurement was carried out by heating the samples from 25 to 90 °C at a rate of 5 °C/min while the UV absorption was recorded at  $\lambda = 260$  nm. The measurement was repeated before 2.2 nmol of polyamide was added and the samples were remeasured twice.

### 3.5 References

1. (a) Boersma, A. J.; Feringa, B. L.; Roelfes, G., *Angew. Chem. Int. Ed.* **2009**, *48* (18), 3346-3348;(b) Roelfes, G.; Boersma, A. J.; Feringa, B. L., *Chem. Commun.* **2006**, (6), 635-637;(c) Roelfes, G.; Feringa, B. L., *Angew. Chem. Int. Ed.* **2005**, *44* (21), 3230-3232.
2. Baraldi, P. G.; Tabrizi, M. A.; Preti, D.; Fruttarolo, F.; Avitabile, B.; Bovero, A.; Pavani, G.; Nunez, C. M. d. C.; Romagnoli, R., *Pure Appl. Chem.* **2003**, *75* (2-3), 187-194.
3. Fuchs, J. E.; Spitzer, G. M.; Javed, A.; Biela, A.; Kreutz, C.; Wellenzohn, B.; Liedl, K. R., *J. Chem. Inf. Model.* **2011**, *51* (9), 2223-2232.
4. Buchmueller, K. L.; Bailey, S. L.; Matthews, D. A.; Taherbhai, Z. T.; Register, J. K.; Davis, Z. S.; Bruce, C. D.; O'Hare, C.; Hartley, J. A.; Lee, M., *Biochemistry* **2006**, *45* (45), 13551-13565.
5. Dervan, P. B., *Bioorg. Med. Chem.* **2001**, *9* (9), 2215-2235.
6. Gottesfeld, J. M.; Neely, L.; Trauger, J. W.; Baird, E. E.; Dervan, P. B., *Nature* **1997**, *387* (6629), 202-205.
7. Wade, W. S.; Mrksich, M.; Dervan, P. B., *J. Am. Chem. Soc.* **1992**, *114*, 8783-94.
8. Hawkins, C. A.; de Clairac, R. P.; Dominey, R. N.; Baird, E. E.; White, S.; Dervan, P. B.; Wemmer, D. E., *J. Am. Chem. Soc.* **2000**, *122* (22), 5235-5243.
9. Chavda, S.; Liu, Y.; Babu, B.; Davis, R.; Sielaff, A.; Ruprich, J.; Westrate, L.; Tronrud, C.; Ferguson, A.; Franks, A.; Tzou, S.; Adkins, C.; Rice, T.; Mackay, H.; Kluza, J.; Tahir, S. A.; Lin, S.; Kiakos, K.; Bruce, C. D.; Wilson, W. D.; Hartley, J. A.; Lee, M., *Biochemistry* **2011**, *50* (15), 3127-3136.
10. Farkas, M. E.; Li, B. C.; Dose, C.; Dervan, P. B., *Bioorg. Med. Chem. Lett.* **2009**, *19* (14), 3919-3923.
11. Hsu, C. F.; Phillips, J. W.; Trauger, J. W.; Farkas, M. E.; Belitsky, J. M.; Heckel, A.; Olenyuk, B. Z.; Puckett, J. W.; Wang, C. C. C.; Dervan, P. B., *Tetrahedron* **2007**, *63* (27), 6146-6151.
12. Baird, E. E.; Dervan, P. B., *J. Am. Chem. Soc.* **1996**, *118* (26), 6141-6146.
13. Stapersma, J.; Klumpp, G. W., *Tetrahedron* **1981**, *37* (1), 187-189.
14. Dauben, W. G.; Rivers, G. T.; Twieg, R. J.; Zimmerman, W. T., *J. Org. Chem.* **1976**, *41* (5), 887-9.
15. Fournier, P.; Fiammengo, R.; Jäschke, A., *Angew. Chem. Int. Ed.* **2009**, *48* (24), 4426-4429.
16. Rajsfus, D. E.; Alter-Zilberfarb, S.; Sharon, P.; Meador, M. A. B.; Frimer, A. A., *J. Fluorine Chem.* **2011**, *132* (5), 339-347.
17. Srikrishna, A.; Sharma, G. V. R.; Daniello, S.; Hemamalini, P., *J. Chem. Soc., Perkin Trans. 1* **1996**, (11), 1305-1311.
18. Fischer, C.; Defieber, C.; Suzuki, T.; Carreira, E. M., *J. Am. Chem. Soc.* **2004**, *126* (6), 1628-1629.

## Chapter 4: Catalysis

### 4.1 Introduction

Chapter 1 highlighted the need for catalysis. In the past water was often neglected as a suitable solvent because of the low water-solubility of organic substrates and the water-sensitivity of some reagents and reactive species.<sup>1</sup> However there are some clear benefits of using water as the solvent. Water is an abundant naturally occurring solvent which makes it inexpensive. Furthermore water is a non-flammable and environmentally safe solvent with no toxicity. In addition water has some unique properties. For example compared to most organic solvents it has a high dielectric constant, a high heat capacity and high cohesive energy density (550 cal/ml (2302740 kJ/m<sup>3</sup>)). These characteristics give rise to the so called hydrophobic effects, clustering of compounds with nonpolar regions in water to reduce the hydrocarbon-water interfacial area, which plays an essential role in the formation of micelles and the folding of biological molecules such as proteins and assists with molecular recognition.<sup>1-2</sup> By utilising these properties enzymes have been able to conduct highly efficient and selective reactions under mild conditions.<sup>3</sup>

In 1980 Rideout and Breslow<sup>2</sup> reported that the hydrophobic interactions also play a role in catalytic reactions with small hydrophobic molecules in water. They reported that the Diels Alder reaction of cyclopentadiene and butenone (Figure 1) was 100 fold faster when carried out in water than in 2,2,4-trimethylpentane. In methanol the speed of the reaction was found to be in between these two extremes. Ions present in the water will also have an effect on the hydrophobic effect because they change the way that water interacts with nonpolar molecules.<sup>4</sup> Since Rideout and Breslow's discovery a range of other reactions have been carried out in water,<sup>5</sup> these include Friedel-Crafts rearrangements,<sup>6</sup> Aldol reactions,<sup>7</sup> Michael additions<sup>7</sup> and [3,3]-Sigmatropic Rearrangement.<sup>8</sup>

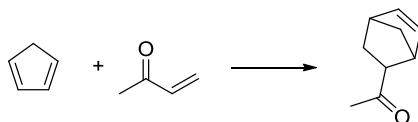


Figure 1: The Diels-Alder reaction of cyclopentadiene and butenone

The bases present in helical DNA form a hydrophobic cleft (Figure 2) which we plan to exploit. By introducing a catalyst into this cleft and by performing the catalytic reactions in an aqueous system we plan to make full use of the hydrophobic effects.

The rest of this chapter will focus on three types of water-compatible asymmetric catalytic reactions, these are:

- 1) Allylic amination
- 2) 1,4 Cycloaddition
- 3) Hydroformylation

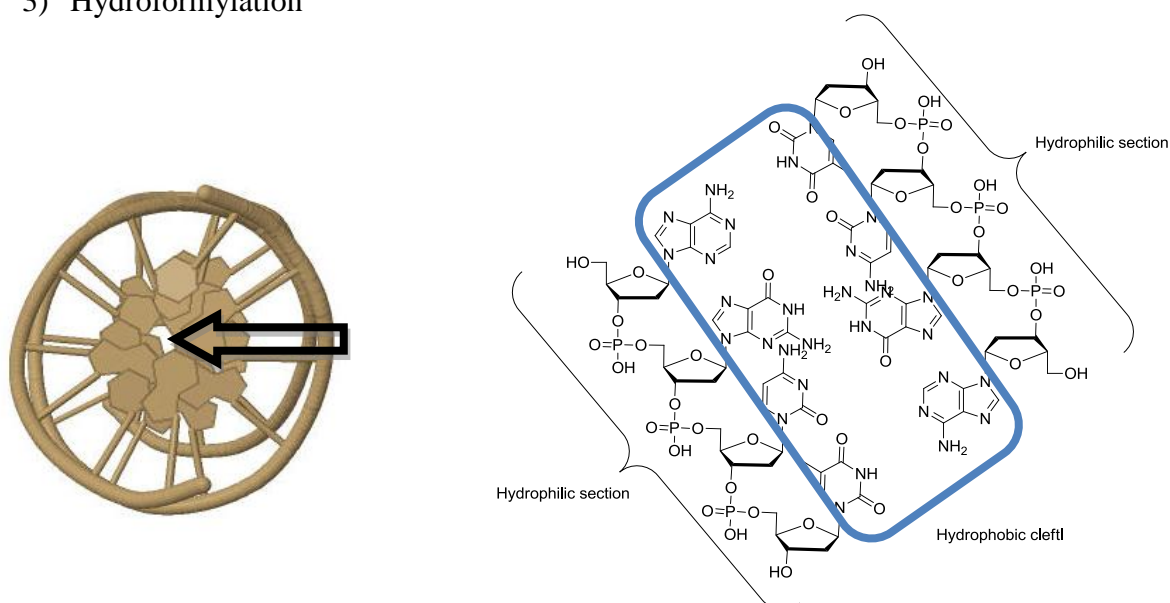


Figure 2: Left: Crystal structure of B-DNA (CGC GAA TTC GCG)<sup>9</sup> represented as a cartoon and seen from above. The arrow indicates the hydrophobic cleft. Right: Schematic side view with the square highlighting the location of the hydrophobic cleft.

#### 4.1.1: Allylic substitution

Transition metal catalysis has proved a useful method for the formation of C-C, C-N and C-O bonds, especially allylic substitution reactions facilitate these formations. In allylic substitution a leaving group on the allylic position is displaced by a nucleophile so that the resulting product still contains a double bond allowing further functionalisation (Scheme 1). Although various metals have been employed in these reactions, Pd complexes have received the most attention.<sup>10</sup> An allyl can coordinate to a metal centre in three different ways (Figure 3); the manner in which it does this and its dynamic behaviour, influence the stereogenic outcome of reactions which proceed through these allyl intermediates.<sup>11</sup>

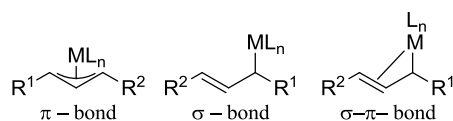


Figure 3: Different ways an allyl can coordinate to a transition metal

Assigning names to these complexes follow the standard Cahn-Ingold-Prelog rules which means that *R* and *S* terminology can be used to describe the stereochemistry.<sup>11</sup> The syn and anti-positions in a planar allyl complex are depicted in Figure 4.

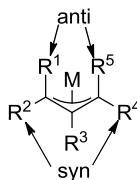


Figure 4: Syn and anti definition in a planar allyl complex

In the  $\pi$ -allyl intermediate there are three possible geometries which can be adopted: syn-syn, syn-anti or anti-anti (Figure 5). Linear olefins in the *E*-configuration form complexes which prefer the syn-syn geometry while cyclic substrates are required to adopt the anti-anti geometry.<sup>12</sup>

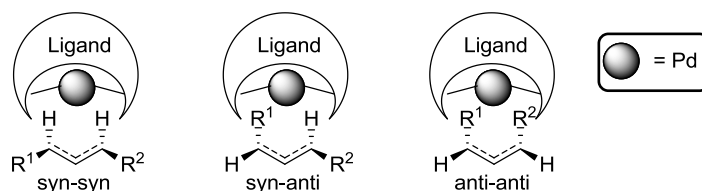
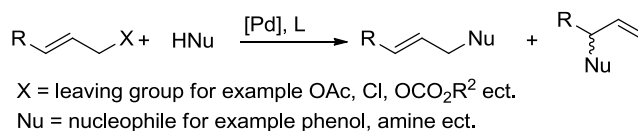


Figure 5: The possible geometries of the  $\pi$ -allyl palladium complex

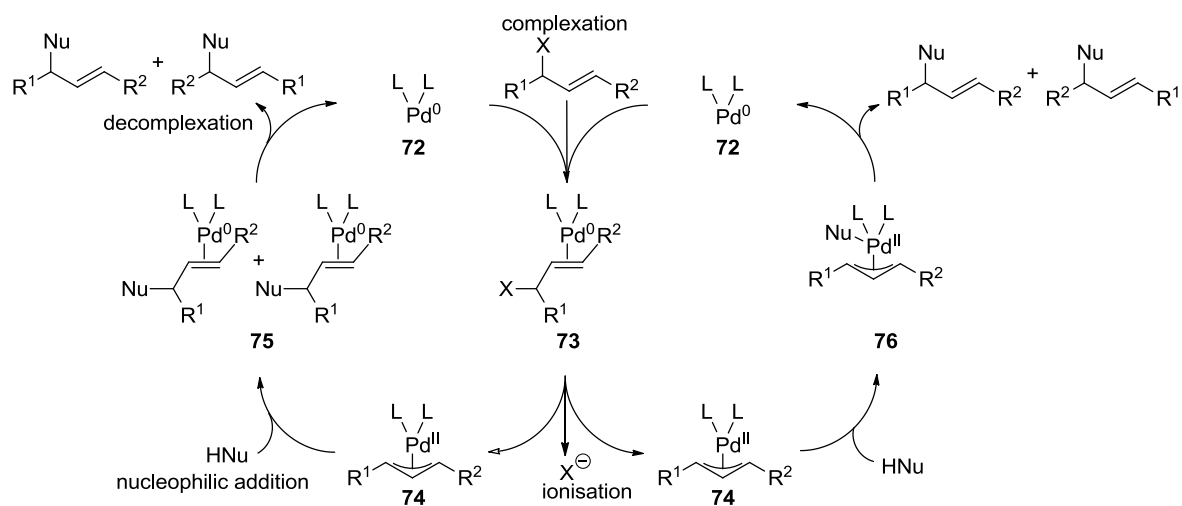
#### 4.1.1.1 Palladium catalysed allylic substitution

In 1965 Tsuji *et al.*<sup>13</sup> were the first to report a palladium assisted allylic substitution reaction using a stoichiometric amount of palladium. About a decade later Trost *et al.*<sup>14</sup> reported the first catalytic version of this reaction using palladium complexes with phosphines as ligands which they patented as the first catalytic allylic alkylation.<sup>15</sup> This palladium catalysed allylation of a nucleophile (Scheme 1) has since been named after its discoverers and is known as the Tsuji-Trost reaction.<sup>16</sup> The reaction has increased in scope covering not only alkylation (C-C bond formation) but also amination (C-N bond formation) and C-O bond formation and has become a benchmark reaction for testing the efficiency of new chiral ligands.<sup>17</sup> It is generally accepted that the catalytic cycle proceeds as depicted in Scheme 2.



Scheme 1: The Tsuji-Trost reaction

The substitution occurs *via* a  $S_N2$  type reaction. This does not mean that it is similar to the uncatalysed  $S_N2$  reactions. In the catalysed version of a  $S_N2$  reaction the metal moiety displaces the leaving group to form an  $\eta^3$ -allyl complex.<sup>18</sup>



**Scheme 2: Catalytic cycle of palladium catalysed nucleophilic allylic substitution of soft (left) and hard (right) nucleophiles**

The catalytic cycle begins with Pd<sup>0</sup> complex **72** which often is generated *in situ* from a Pd<sup>II</sup> source such as [Pd(( $\eta^3$ -allyl)Cl)<sub>2</sub>]. Complex **72** activates the allylic compound containing a leaving group such as an acetate group forming stable cationic ( $\eta^3$ -allyl) Pd<sup>II</sup> intermediate **74** by oxidative addition.<sup>19</sup> After this step the catalytic cycle can follow one of two routes depending on the nucleophile used. In the case of a soft nucleophile (left cycle in Scheme 2) the attack on the allyl fragment occurs outside the coordination sphere of the metal. In this complex the allyl group is formally an anion but can undergo nucleophilic attack owing to the high electrophilicity of palladium to form the allyl product. The product is bound to the Pd<sup>0</sup> complex *via* a  $\eta^2$ -Pd-alkene bond before it is released liberating complex **72** to partake in the cycle once again.<sup>12a, 19</sup>

Hard nucleophiles, whose conjugate acids have a  $pK_a > 25$ , have a slightly different catalytic cycle (right cycle in Scheme 2).<sup>12</sup> Instead of attacking the allyl group directly they attack the metal centre and the product is formed by reductive elimination.<sup>20</sup> Soft nucleophiles are more commonly used in allylic substitution reactions.

For a reaction to give 100 % enantiomeric excess (*ee*) and conversion, one step must be able to differentiate between the enantiotopic groups or faces. Each step in the cycle provides an opportunity for enantioselection to take place, with the exception of the decomplexation step.<sup>12</sup> There are five potential sources where enantioselection can occur (Figure 6): a) metal-

olefin complexation, b) departure of the leaving group c) enantiofacial discrimination of the  $\pi$ -allyl complex d) nucleophilic attack at the enantiotopic termini and e) enantiofacial discrimination in the nucleophile.<sup>12</sup>

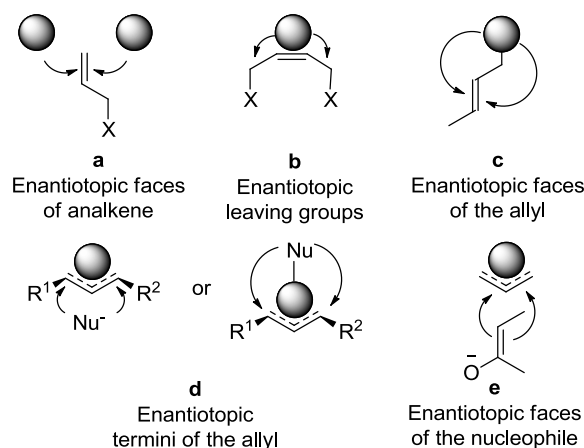


**Figure 6 : Potential sources of enantiomeric-discrimination in allylic substitution**

As with other asymmetric reactions the ability to differentiate between the enantiotopic faces of the olefin is a possible mechanism of enantio selection. The ligand-metal complex must distinguish between the two prochiral faces of an unsymmetrically substituted olefin. Although it is generally considered that the complexation of an olefin with palladium is rapid and reversible the stability of the  $d^{10}$  metal-olefin complex varies widely. Examples where enantioselective olefin complexation is the enantiodetermining step are limited. A combination of factors are required for this to be the enantiodetermining step,<sup>12a</sup> these include faster ionisation of one enantiomer of the olefin over the other and a slow  $\pi$ - $\sigma$ - $\pi$  equilibration relative to the nucleophilic capture of the diastereomer (Figure 6, **a**).<sup>12a, 19</sup>

If there are two potential leaving groups on a *meso* or achiral disubstituted system then enantiotopic ionisation (Figure 6, **b**) is the enantiodetermining step. When ionisation of a racemic chiral allylic system leads to a *meso*- $\pi$ -allyl intermediate then the enantiodetermining step is determined by differentiation of the enantiotopic allyl termini (Figure 6, **c**). Two diastereomeric palladium complexes can form when the initial olefin coordination is fast and reversible (equilibration through a  $\pi$ - $\sigma$ - $\pi$  rotation). In this case the product is formed from either the most abundant or more reactive diastereomer (Figure 6, **d**). Lastly a prochiral nucleophile can determine the enantioselectivity by enantiofacial discrimination of an achiral allyl complex (Figure 6, **e**).<sup>12</sup>

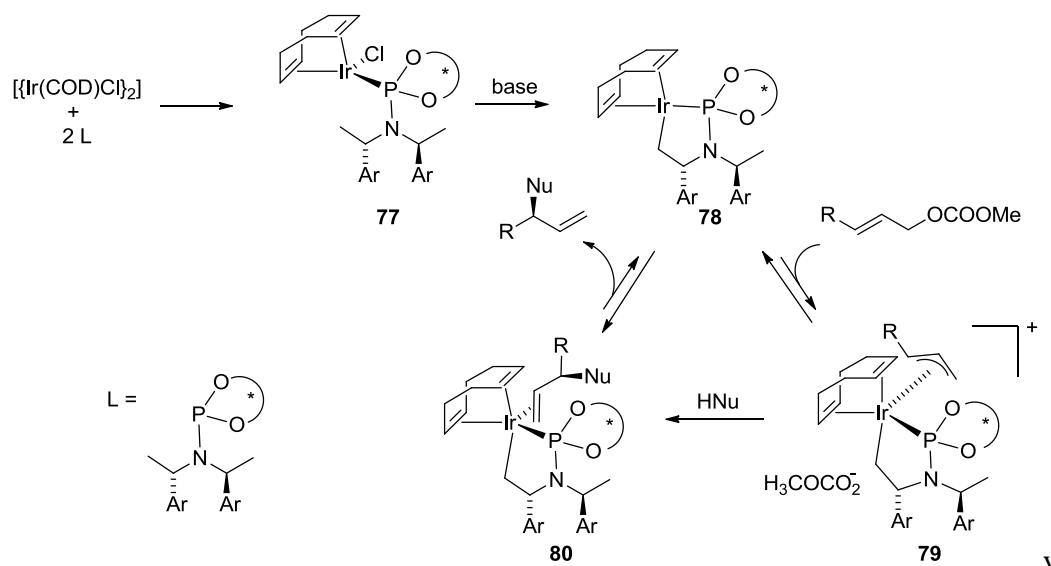
Allylic amination, the Tsuji-Trost reaction with an amine as nucleophile, generates allyl amines which are fundamental building blocks in organic chemistry and therefore synthetic methods to prepare them are very important.<sup>21</sup> Because the amines are usually sufficiently basic themselves, no additive needs to be added, which is required with alkylation, to facilitate the reaction. The reaction is compatible with aqueous environments<sup>22</sup> which makes it an interesting reaction for our nucleotide based catalysis.

Other metals than palladium have been shown to catalyse allylic substitution reactions often showing different regioselectivities than palladium. Generally but not always, palladium forms linear products out of terminal allylic electrophiles whereas complexes composed of other metals tend to favour the branched products.<sup>23</sup> Iridium is one such metal.

#### 4.1.1.2 Iridium diene catalysts in allylic substitution

It has been well established that phosphorous donor compounds are efficient ligands in asymmetric catalysis. However they have the potential to oxidise making them inactive. There are other compounds available that are effective ligands in catalysis which do not have this drawback.<sup>24</sup> Since 1827 when Zeise's salt ( $K[PtCl_3(C_2H_4)]$ ), one of the first organometallic compounds, was discovered, numerous metal-alkene complexes have been synthesised. Olefins are labile ligands which can easily be replaced with ligands which exhibit a stronger binding affinity such as phosphines and nitrogen and this makes them useful as precatalysts. It is therefore understandable that using chiral dienes as ligands in catalysis has received little attention. Hayashi *et al.*<sup>25</sup> and Carreira *et al.*<sup>26</sup> changed this by independently demonstrating that chiral dienes can be used in asymmetric catalysis.<sup>27</sup>

It is fair to say that the majority of the attention that iridium catalysed allylic substitution has received in recent years has focused on the use of  $[Ir(COD)Cl]_2$  complexes with phosphoramidites as ligands.<sup>18</sup> Since it was first developed in 1997 by Takeuchi<sup>28</sup> iridium catalysed allylic substitution has rapidly developed and slowly our understanding of the mechanism has developed (Scheme 3).<sup>18</sup>



Scheme 3: Mechanism for phosphoramidite-iridium catalyzed catalysis<sup>23a</sup>

In the absence of a phosphorus ligand, iridium complexes are still active. By employing chiral dienes high *ee*'s (over 98 %) can even be obtained.<sup>18, 26</sup> It should be noted however that the enantiodetermining step differs from that of reactions utilising complexes containing a phosphorous moiety. When a racemic starting compound is used and the reaction is allowed to run until complete conversion is obtained then the product is racemic. However impressive enantiomeric excesses are obtained when the reaction is stopped after 50 % conversion. When the remaining starting material is analysed enantiomeric enrichment is observed in the same ratio as the product.<sup>26</sup> It is assumed that steric hindrance plays a crucial role in the observed selectivity (Figure 7).

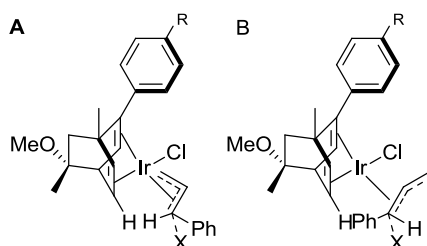
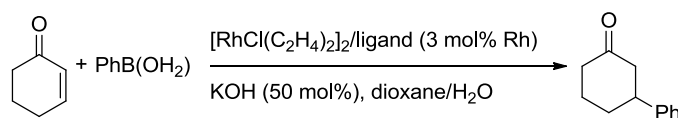


Figure 7: Proposed explanation for the selectivity of the diene-iridium catalyzed allylic substitution<sup>26</sup>

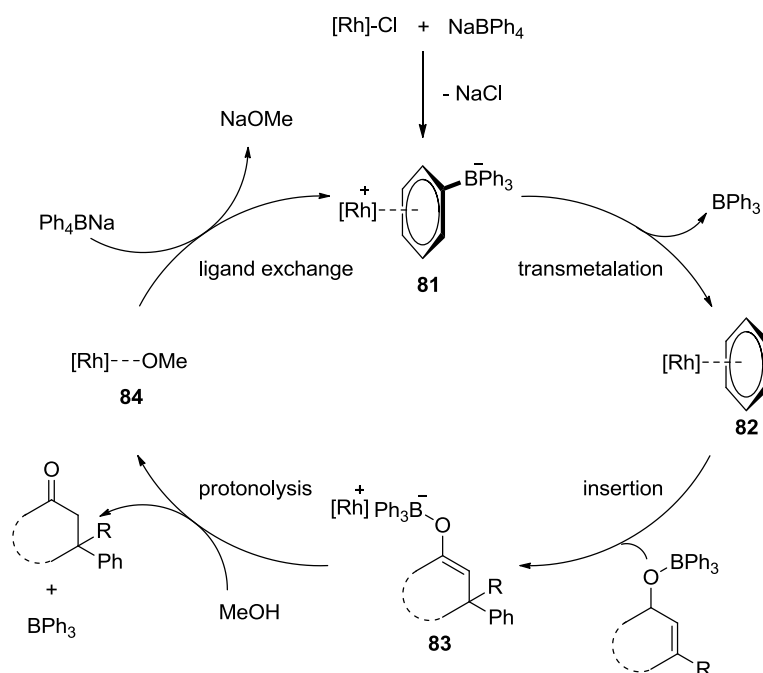
#### 4.1.2: 1,4 Cycloaddition

Hayashi *et al.*<sup>25</sup> developed a catalytic 1,4-cycloaddition (Scheme 4) employing dienes as ligands around the same time as Carreira was using dienes with iridium.



Scheme 4: 1,4 cycloaddition using boronic acids

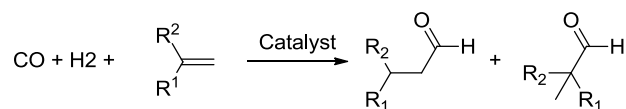
The mechanism that Hayashi proposed<sup>25</sup> is depicted in Scheme 5. Active catalyst **81** is formed by reacting the rhodium precatalyst with sodium tetraphenylborate after which the complex undergoes transmetalation to give rise to triphenylborane and species **82**. With the aid of the Lewis acidic triphenylborane the enone can subsequently insert itself into the phenyl-rhodium bond generating species **83**. This is followed by protonolysis which produces the product along with an alkoxyrhodium intermediate (**84**). Finally the active species is regenerated by ligand exchange with sodium tetraphenylborate.



Scheme 5: Proposed mechanism for the rhodium catalysed 1,4 cycloaddition with sodium tetraphenylborate

#### 4.1.3 Hydroformylation

Hydroformylation also known as oxo synthesis (Scheme 6), is one of the most important reactions in industry that uses homogeneous catalysts<sup>29</sup> and has an annual production of 6 million metric tons.<sup>30</sup> During the reaction an alkene is converted into an aldehyde using syngas (synthesis gas: a 1 to 1 mixture of hydrogen and carbon oxide) making the atom economy of the reaction 100%.



Scheme 6: General hydroformylation reaction

The reaction was first discovered in 1938 by Roelen<sup>29</sup> and is a versatile method to functionalise alkenes and create enantiomerically pure aldehydes.<sup>31</sup> The original catalyst was

a cobalt species,  $\text{HCo}(\text{CO})_4$ , but nowadays the most commonly used catalyst motif for these reactions is based on diphosphines chelating to a rhodium species.<sup>31b</sup>

In 1993 Takaya *et al.*<sup>31a</sup> played a significant role in the breakthrough in the field of asymmetric hydroformylation (AHF) with their chiral phosphinephosphite ligand, (*R,S*)-BINAPHOS ((*R*)-(2-(diphenylphosphino)-1,1'-binaphtalen-2'-yl)-((*S*)-1,1'-binaphtalen-2,2'-yl)phosphite) (Figure 8). Since then other chiral ligands have been developed containing two different phosphorus moieties.

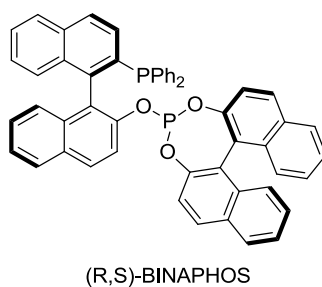
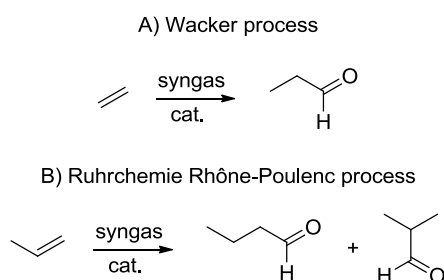


Figure 8: (*R,S*)-BINAPHOS

#### 4.1.3.1 Hydroformylation in water

In order to minimise the environmental impact water based reactions have been receiving much attention. Besides the fact that water is cheap, non-flammable and non-toxic it allows for easier recycling of the catalyst.<sup>32</sup> Two important industrial applications which employ this concept are the Wacker process (since the late 50's early 60's) and the Ruhrchemie Rhône-Poulenc process (since 1984).<sup>30</sup>

The Wacker process was used for the manufacturing of acetaldehyde from ethylene (Scheme 7). At the time acetaldehyde was an important industrial intermediate and with a production exceeding 2 million tons per year it sparked a lot of attention. Today this acetaldehyde is less important as the intermediates used in industry can be manufactured using different methods.<sup>33</sup>



Scheme 7: Hydroformylation of A) ethylene (wacker process) B) propene (Ruhrchemie Rhône-Poulenc process)

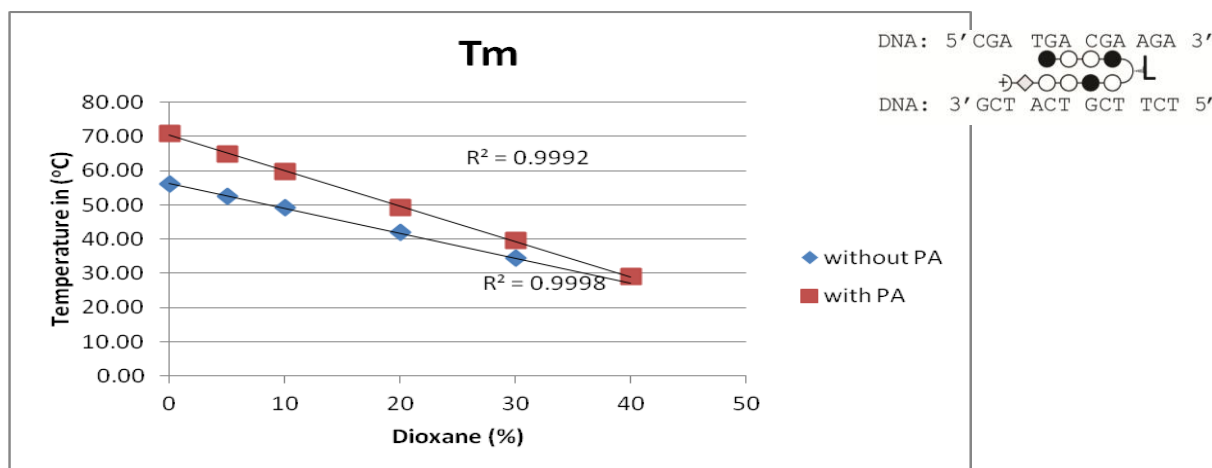


## 4.2 Results and discussion

In organic solvents the double helix form, which nucleic acids can adopt, have a tendency to dissociate giving two single strands. To take full advantage of using nucleotides the chiral environment of the double helix needs to remain intact. The extent of dissociation in organic solvent is dependent on several factors. These factors include the organic solvent which was utilised as well as on the sequence of the nucleic acid. Dioxane is a solvent which is often used as a co-solvent in the aqueous reactions we are looking into.

Melting temperature graphs can be used to find out at what temperature more than half the double helix of oligonucleotides has dissociated. That is why the melting temperature of double helix 5'-CCA TGACGA AGA-3' was determined in different concentrations of dioxane (Graph 1). The pyrrole/imidazole minor groove binders tend to increase the temperature of dissociation, because extra hydrogen bonds can be formed to hold the helix together. Polyamide **71** (Chapter 3, Figure 10) was added to the oligonucleotide solutions containing different concentrations of dioxane in order to determine at what temperature and concentration most of the oligonucleotides are found as single stands.

Graph 1: The melting temperature of DNA in different concentrations of dioxane.



Each reaction was carried out in 690  $\mu$ l T<sub>m</sub> buffer (T<sub>m</sub>-buffer: 10 mM sodium cacodylate, 10 mM KCl, 10 mM MgCl<sub>2</sub>, 5 mM CaCl<sub>2</sub> pH 7), 310  $\mu$ l dioxane/water mixture and 2 nmol DNA. After running the T<sub>m</sub>'s with the DNA only 2.2 nmol polyamide was added.

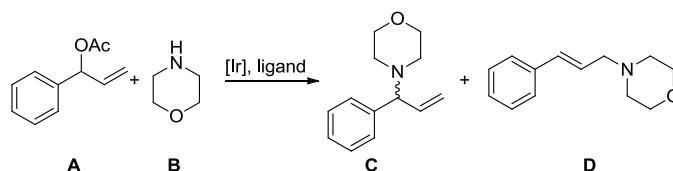
The decrease in integrity of the double helix in elevated concentrations of dioxane is clearly visible (the downward slope in Graph 1). The integrity decreases more quickly, although it remains higher, when polyamides are used. That is why at 30 °C and 40 % dioxane the two virtually merge. Because the graph indicates when more than half the nucleotides have dissociated it is advisable to remain above the line when choosing reaction conditions. That is

why it was decided not to go above 30 % dioxane when reactions are to be done at room temperature.

#### 4.2.1 Allylic substitution

##### 4.2.1.1 Diene-Ir catalysis

The purpose of synthesising the dienes described in Chapter 3, was to use them as ligands in allylic substitution reactions with Ir. 3-Acetoxy-3-phenylprop-1-en-1-ylum (**A**) was chosen as substrate with morpholine (**B**) as nucleophile (Scheme 9). Unlike palladium, which favours nucleophilic attack at the least hindered position resulting in linear product **D**, iridium favours the more hindered option to form the chiral branched product **C**.



Scheme 9: allylic substitution reaction for iridium catalysis

Several dienes containing a suitable linker for coupling to polyamide **48** (Chapter 3, Figure 5) were prepared. Ligands **53** and **57** in Figure 9, were chosen because they are achiral which would increase the likelihood that the chirality seen in the product was caused by the oligonucleotides. Diene **53** was put on hold when it was discovered that it was unlikely to form a stable complex with iridium (see later in this chapter). Diene **57** turned out to be very unstable and coupling to the polyamide was unsuccessful. Therefore dienes **62/63** were also studied.

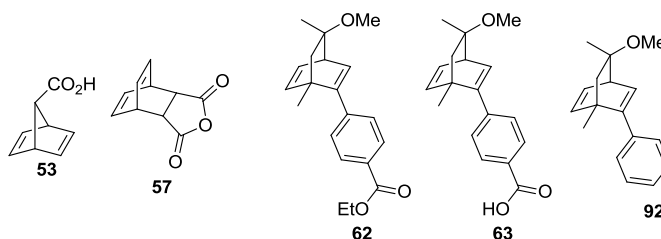


Figure 9: Dienes with a [2.2.2] motif that have been investigated

Carreira *et al.*<sup>26</sup> observed that after mixing norbornadiene (nbd) with [IrCl(COE)<sub>2</sub>]<sub>2</sub> (COE = cyclooctene) for 4 days only by-products were formed. However Osborn *et al.*<sup>37</sup> reported that nbd displaces the COE in [IrCl(COE)<sub>2</sub>]<sub>2</sub> to form a microcrystalline compound with an unconfirmed structure. They claim that the structure is unlikely to be monomeric. This compound is not readily soluble nevertheless it can be converted into other iridium

complexes (Figure 11). To avoid the formation of a microcrystalline compound we theorised that this compound was a polymer and that having a bulky substituent on the bridge would prevent the formation of this species. Therefore, we studied complex formation between chloro-nbd **93** (Figure 10) and iridium(I).

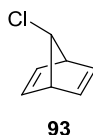


Figure 10: Chloro-nbd **93**

After stirring chloro-nbd **93** and  $[\text{IrCl}(\text{COE})_2]_2$  for 24 hours at room temperature no complex formation was visible in the  $^1\text{H-NMR}$  spectrum. Therefore it was decided to heat the mixture overnight at  $37\text{ }^\circ\text{C}$ .  $^1\text{H-NMR}$  showed the formation of a new species (Figure 12). When the reaction mixture was concentrated and subsequently redissolved the iridium complex decomposed. On the other hand when the complex remained in solution it was stable for several weeks.

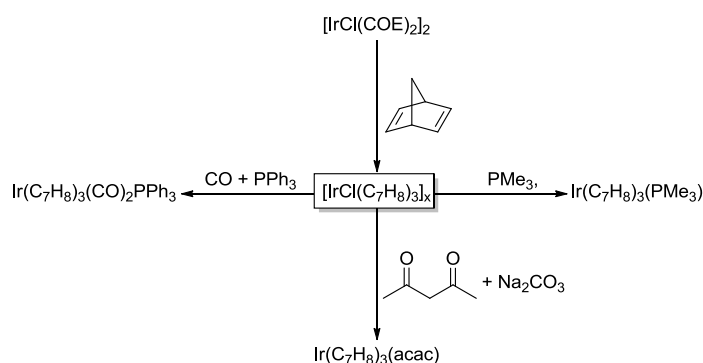


Figure 11: Possible iridium complexes formed from the iridium-nbd microcrystalline complex

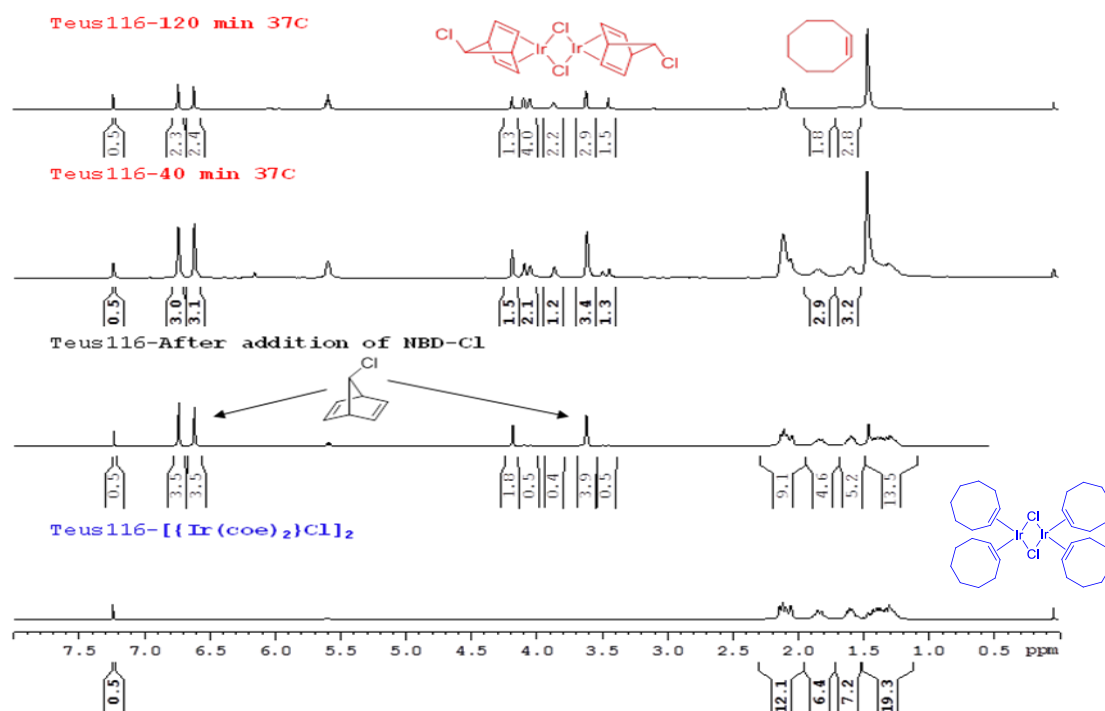
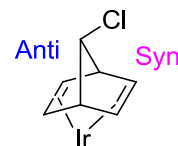


Figure 12: NMR of the formation of chloro-nbd Ir complex

To establish if the NMR data corresponded to the desired complex the chemical shifts of the olefin were compared to the calculated chemical shifts using computational methods (Table 1). The validity of this method was tested by comparing the measured chemical shifts of  $[\text{IrCl}(\text{COD})]_2$  (COD = cyclooctadiene) to those computationally predicted using the B3LYP function as specified in GAUSSIAN 09 (Table 2).

Table 1: Measured and calculated chemical shifts of COD and Ir-(nbd-Cl) complex

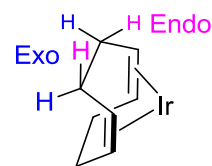
Proton	nbd-Cl		Ir-(nbd-Cl) complex	
	Experimental	Calculated	Experimental	Calculated
<b>Diene</b>	6.7, 6.6	7.2 (Cl, anti)	4.1, 4.0	3.4 (Cl, anti)
		7.0 (Cl, syn)		3.8 (Cl, syn)
<b>CH</b>	3.6	3.6	3.8	3.6
<b>CH-Cl</b>	4.1	4.3	3.4	3.8



<sup>1</sup><http://www.sigmaaldrich.com/spectra/fnmr/FNMR004153.PDF> <sup>2</sup>Grobelaar, E. *et al. Inorganica Chimica Acta* 2006 359 3800 \* Calculated by Dr. Jevgenij A. Raskatov. All computations were performed using the B3LYP function as specified in GAUSSIAN 09. Optimisations were performed using the combined basis set BS1 (SDD+ECP augmented by an f polarisation function ( $z = 0.938$ ) on Ir, 6-311G(d) otherwise), NMR chemical shifts were calculated with the larger basis set BS2 (SDD+ECP augmented by an f polarisation function ( $z = 0.938$ ) on Ir, 6-311+G(d,p) otherwise). TMS (0.0 relative ppm) was used for reference.

Table 2: Measured and calculated chemical shifts of COD and [IrCl(COD)]<sub>2</sub>

Proton	COD <sup>1</sup>		[IrCl(COD)] <sub>2</sub> <sup>2</sup>	
	Experimental	Calculated	Experimental	Calculated
Diene	5.6	6.0	4.2	3.4
CH <sub>2</sub>	2.3	2.5	2.2, 1.6	2.4 (endo) 1.9 (exo)



<sup>1</sup><http://www.sigmaaldrich.com/spectra/fnmr/FNMR004153.PDF> <sup>2</sup>Grobbelaar, E. *et al. Inorganica Chimica Acta* 2006 359 3800. Calculated by Dr. Jevgenij A. Raskatov. All computations were performed using the B3LYP function as specified in GAUSSIAN 09. Optimisations were performed using the combined basis set BS1 (SDD+ECP augmented by an f polarisation function ( $z = 0.938$ ) on Ir, 6-311G(d) otherwise), NMR chemical shifts were calculated with the larger basis set BS2 (SDD+ECP augmented by an f polarisation function ( $z = 0.938$ ) on Ir, 6-311+G(d,p) otherwise). TMS (0.0 relative ppm) was used for reference.

It is clear that the chemical shifts correspond closely to those predicted by the calculations (Table 2). This is also true for the free ligand **93**. For the complexation of iridium with COD the calculated value is slightly off for the olefin protons but the trend is clear. The same trend is visible with the nbd complex and therefore, it can be assumed that the desired complex has been formed.

The complex was formed in an aprotic solvent (CDCl<sub>3</sub>) but the catalytic reaction will take place in a protic solvent. To test the stability of the complex deuterated methanol was added to the solution containing the metal complex. After 1 hour degradation products were clearly visible and after two days there were only trace amounts of complex left (Figure 13). Because the complex proved to be unstable under protic conditions dienes with a [2.2.2] structure were also investigated.

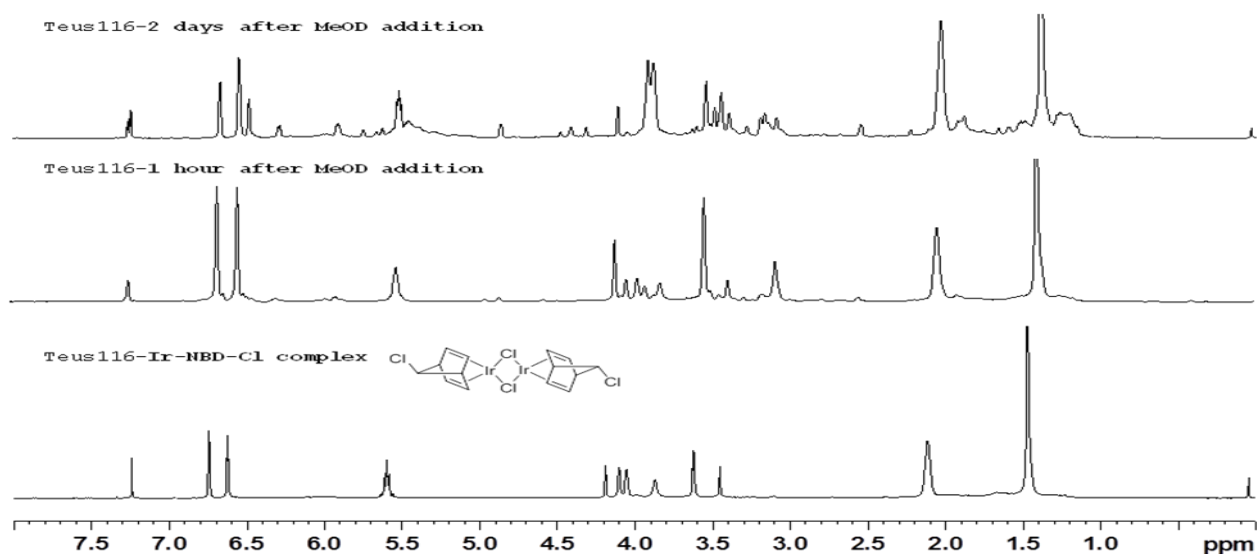


Figure 13: NMR spectra of chloro-nbd Ir complex after addition of a protic solvent

The [2.2.2] structure of dienes **62/63** has been tried and tested in the allylic amination reactions<sup>22</sup> so no problems were expected. The scale on which the catalytic reactions were to be carried out on was very small, 50  $\mu\text{l}$ , and therefore, test reactions were carried out to compare the outcome with the experiments done on a larger scale (1 ml). The following complexes were used to do this:

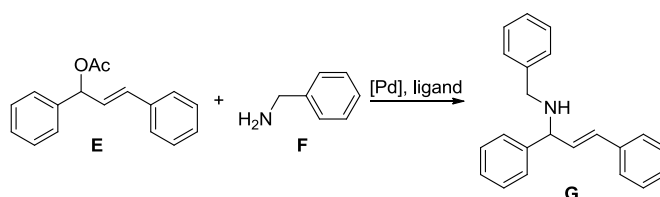
- 1)  $[\text{Ir}(\text{COD})\text{Cl}]_2$  (formed from  $[\text{Ir}(\text{COE})_2\text{Cl}]_2$  and COD))
- 2)  $[\text{Ir}(\text{COE})_2\text{Cl}]_2$
- 3)  $[\text{Ir}(\text{COE})_2\text{Cl}]_2$  with diene **62**

The test reactions were carried out in dichloromethane (DCM). When the reaction was carried out on the 1 ml scale only the  $[\text{Ir}(\text{COD})\text{Cl}]_2$  reactions showed conversion. This was surprising as Jäschke *et al.*<sup>22</sup> reported the  $[\text{Ir}(\text{COE})_2\text{Cl}]_2$  complex was active as well as diene **92** as ligand. On the small scale the DCM evaporated overnight. The reaction was repeated in an aqueous medium with dioxane as a co-solvent.  $[\text{Ir}(\text{COD})\text{Cl}]_2$  was used as the catalyst because it was the only active complex. The reactions were left for 4 days and in the case of the small scale reaction the internal standard, substrate and product had evaporated to varying degrees. On the large scale this was not detected therefore it is advisable that the reactions are carried out on a larger scale than 50  $\mu\text{l}$ .

To find out why the catalytic reaction with diene **62** showed no conversion NMR experiments were conducted. Upon mixing diene **62** with  $[\text{Ir}(\text{COE})_2\text{Cl}]_2$  in  $\text{CDCl}_3$  no complexation could be detected even when the complex was heated for 48 hours at 37  $^\circ\text{C}$ . It is known that  $[\text{Ir}(\text{COE})_2\text{Cl}]_2$  forms complexes with dienes slowly,<sup>22, 26</sup> which is why a more reactive Ir precatalyst was tried:  $[\text{Ir}(\text{C}_2\text{H}_4)_2\text{Cl}]_2$ . Unfortunately no complexation was seen using this precatalyst either, not even upon heating to 40  $^\circ\text{C}$  for 48 h. It is possible that higher temperatures are needed.

#### 4.2.1.2 Phosphine-Pd catalysis

Because palladium favours the least hindered position in allylic substitution a different substrate, 1,3-diphenylallylacetate (**E**), was chosen (Scheme 10).



Scheme 10: Allylic substitution with palladium

Nucleosides modified with a phosphorous have been tested in catalysis in the past.<sup>38</sup> In all likelihood if the monomer is not catalytically active, then a longer strand will also be inactive. Therefore monomer **46a** (Figure 14) was deprotected using methanol and after the removal of  $\text{BH}_3$  protecting group and evaporation of the solvent ligand **46b** was used in allylic amination (Scheme 10). Both diastereomers of **25a** were also tested in this reaction because it is known that phosphoramidite also perform well in substitution reactions.

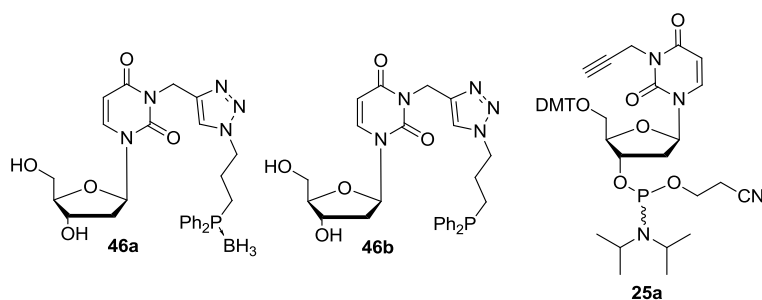


Figure 14: Ligands tested in palladium catalysed allylic substitution

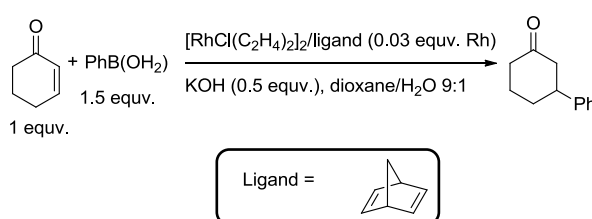
The results are shown in Table 3. The reactions were carried out in DCM. It was also tested to see if adding  $\text{K}_2\text{CO}_3$  as a base would have any effect on the reaction, this turned out not to be the case. Ligand **46b** was the only ligand that gave any conversion. The *ee* could not be determined by HPLC because there was an impurity present in the reaction mixture after filtration which was UV active and overlapped with the peak of one of the enantiomers.

Table 3: Conversions of the allylic substitution reactions with palladium

Ligand	$\text{K}_2\text{CO}_3$	Conversion (100 %)
--	--	0 %
--	--	0 %
<b>46a</b>	--	100 %
<b>46a</b>	--	100 %
<b>25a diastereomer 1</b>	--	0 %
<b>25a diastereomer 1</b>	--	0 %
<b>25a diastereomer 2</b>	--	0 %
<b>25a diastereomer 2</b>	--	0 %

### 4.2.2 1,4-Cycloaddition

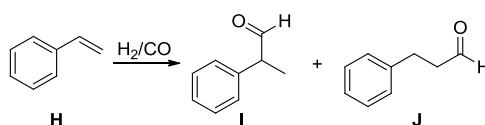
The 1,4-cycloaddition which Hayashi reported was done in only 10 % water and 90 % dioxane (Scheme 11). From the melting temperature graph (Graph 1) it is clear that when the co-solvent is dioxane a minimum of 70 % water is required to avoid dissociation. For this reason the cycloaddition was tested with different water concentrations. Above 60 % water no conversion was measurable. This does not mean that the reaction does not proceed with higher concentrations of water as a precipitate was observed which could indicate that the complex was precipitating out of solution. Therefore a water soluble diene should be synthesised to further test the limitations of this reaction.



**Scheme 11: The 1,4-cycloaddition**

### 4.2.3 Hydroformylation

Aqueous biphasic systems for rhodium catalysed hydroformylation are of interest in industry as they allow for quantitative recycling of the catalyst. As of yet the industrial viability has only been proven in the case of lower olefins (under four carbon atoms). In the case of higher olefins problems occur due to their low solubility in the aqueous phase.<sup>39</sup> Because of this lower solubility we opted to use a single phase system using a co-solvent to transfer the substrate into the aqueous layer. Styrene is often used as a bench mark substrate for hydroformylation so it was decided to use this substrate (Scheme 12).



**Scheme 12: Hydroformylation of styrene**

To determine the best co-solvent test reactions were carried out with tppts as ligand. The results are shown in Table 4

**Table 4: Conversion of styrene in an aqueous co-solvent system**

Entry	co-solvent	5%	10 %	20 %
		Conversion (b:1)	Conversion (b:1)	Conversion (b:1)
1	DMF	26 % (9:1)	43 % (11:1)	90 % (16:1)
2 <sup>a)</sup>	DMF	90 % (18:1)	Full conversion (20:1)	--
3	MeOH	32 % (10:1)	35 % (8:1)	53 % (12:1)
4	Dioxane	21 % (10:1)	39 % (9:1)	77 % (9:1)
5 <sup>a)</sup>	Dioxane	Full conversion (20:1)	Full conversion (21:1)	--

Reaction conditions: Rh(acac)CO = 0.33  $\mu$ mol, tppts = 3.05  $\mu$ mol, styrene = 0.1 mmol, temperature = 30°C, 24 hours, buffer B (20 mM MOPS, 48 mM NaCl) in water), total V = 1.0 ml pressure = 50 bar <sup>a)</sup>pressure = 80 bar

Out of the three solvents which were investigated, methanol (Table 4, entry 3), gave the lowest overall conversions. The better performing co-solvents (DMF (dimethylformamide) and dioxane) were also tested at a higher pressure (entry 2 and 5). By increasing the pressure full conversion could be obtained. The ratio between the branched and linear products also increased. In the future reactions will be carried out with the higher pressure (80 bars) with dioxane as co-solvent. The three ligands tested in allylic amination reaction were also used as ligands in the hydroformylation of styrene. Compound **46b** was used in this test reaction to determine if it would be worthwhile to carry the reaction out using longer strands of oligonucleotides containing this triazole motif. Phosphoramidites **25a** were also tried because the use of phosphoramidites in catalytic reactions has been growing in popularity.<sup>40</sup> Their potential hydrolysis sensitivity prevents the reactions being performed in aqueous media therefore chloroform was chosen as the solvent. The results are shown in Table 5.

**Table 5: Conversion and enantioselectivity in hydroformylation of styrene**

Entry	Ligand	Conversion (%)	ee (%)
1	--	100	0
2	<b>46b</b>	0	-
3	<b>25a diastereomer 1</b>	15	8 % enantiomer 2
4	<b>25a diastereomer 2</b>	27	18 % enantiomer 1

Reaction conditions: Rh(acac)CO = 1.0  $\mu$ mol, ligand = 5.1  $\mu$ mol, styrene = 1.2 mmol, diphenyl ether = 0.5 mmol, 1.0 ml chloroform, pressure 40 bars, 18 hours, 40 °C

When ligand **46b** was added to the rhodium pre-catalyst the solution instantly turned yellow which was taken as an indication that the ligand had coordinated to the rhodium. This was also evident from the lack of conversion (Table 5, entry 2). If no or partial complexation had

occurred then the results would have mimicked that of Rh(acac)CO (Table 5, entry 1), in other words there would have been product formation. Because no product formation had occurred it indicated that an inactive rhodium species was formed. Until more data are obtained explaining the reason why no conversion was observed it is not recommended attempt is reaction using the more costly (both financially and time consuming) longer nucleotides.

No colour change was noticed when the phosphoramidites were added to the rhodium complex however the phosphoramidites did form an active complex with rhodium as conversions were detected, and more importantly, enantiomeric excess was observed. Ojima *et al.*<sup>40</sup> also used monodentate phosphoramidites in the hydroformylation. As substrate they opted for the more volatile and thus for us incompatible, substrate allyl cyanide. Several members of our group noticed that on the scale we do our reactions volatile substrates/products are lost when purging the autoclave. The catalyst system of Ojima *et al.* gave high conversions (often 100 %) and enhanced enantioselectivities. They found that ligand/metal ratio had little effect on the reaction. Therefore it is unlikely that changing the ligand metal ratio in our system will improve the conversion but using a different substrate or solvent might prove to be more promising.

### 4.3 Conclusion

There are only a few examples known where iridium complexes have a nbd derivative as a ligand<sup>37, 41</sup> and these complexes generally have a phosphine as a co-ligand. We wished to synthesise an iridium nbd complex without adding a phosphine. To achieve this a nbd-derivative with a bulky group on the bridge was coordinated to an iridium COE complex. The formation proceeded smoothly but the complex had stability issues, although it remained stable in solution in an aprotic solvent for up to two weeks decomposition occurred when the sample was concentrated or when a protic solvent was added. It was therefore decided that ligand **53** was not very suitable for iridium DNA assisted catalysis. Stable nbd complexes with rhodium are known so changing the transition metal to rhodium and the reaction to, for example, the 1,4-cycloaddition, could be a possibility. Initial steps were undertaken to determine if the 1,4-cycloaddition was an option by increasing the water content compared to the reported reaction conditions. When the water content reached above 60 % no product formation was observed and a precipitate was formed, possibly indicating that the metal

complex had precipitated from solution. A more water soluble metal complex is needed to further test the limits of this reaction.

Dienes with a [2.2.2] structure are known to coordinate to  $[\text{Ir}(\text{COE})_2\text{Cl}]_2$  but unfortunately attempts to coordinate diene **62** were unsuccessful, even when the more reactive precatalyst  $[\text{Ir}(\text{C}_2\text{H}_4)\text{Cl}]_2$  was used and the complex was subjected to an elevated temperature of 40 °C. This result is surprising as ligands very similar to diene **92** which has been used with both precatalysts in allylic substitution.

Double stranded oligonucleotides have the tendency to lose their double helix three dimensional structure and become two single strands in the presence of organic solvents. Dioxane has been used as a co-solvent in water containing reactions which we were interested in. Therefore it was a good co-solvent to start with. To determine at which concentration dioxane significantly alters the composition of the oligonucleotides  $T_m$  experiments were done. Using this method it was discovered that the concentration of dioxane should not exceed 30 % otherwise the majority of the oligonucleotides will be present in their single strand form. This means that the chiral environment created by the double helix will be lost.

Because oligonucleotides are expensive and synthetic oligonucleotides are obtained on  $\mu\text{mol}$  scale test reactions were carried out to determine the effect of the reaction volume on the reaction rate for allylic substitution. The initial reactions were carried out in DCM using  $[\text{Ir}(\text{COD})\text{Cl}]_2$  as catalyst, on two different scales 1.0 ml and 50  $\mu\text{l}$ . Reproducible results were only obtained with the large volumes. On the small scale, even in closed eppendorfs, the solvent evaporated. To reduce the amount of evaporation the solvent was changed to water containing  $\text{MgClO}_4$  and  $\text{Na}(\text{ClO}_4)_2$  with dioxane as a co-solvent. After the desired length of time the results were analysed by GC. Unfortunately the amount of substrate and therefore product was too small to be extracted and measured reliably. Larger volumes are thus needed although 1.0 ml might be too large.

High pressures are required for hydroformylation when water is used as a solvent and improved the ratio between linear and branched product. Of the three co-solvents that were investigated methanol gave the worst results. The difference between dioxane and DMF was small and because  $T_m$  measurements of oligonucleotide-polyamide complexes in different concentrations of dioxane had been measured it was decided to proceed with dioxane.

Ligands **46b**, **25a diastereomer 1** and **25a diastereomer 2** were tested in the allylic amination of 1,3-diphenylallyl acetate with benzylamine and the hydroformylation of styrene with some interesting results. Both of these reactions were carried out in organic solvents. In allylic amination only ligand **46b** showed full conversion after 12 hours while the other two showed no conversion. The addition of the  $K_2CO_3$  had no effect on the conversion giving the same results as the reactions carried out without the addition of this extra base. The fact that **46b** gave full conversion within a mere 12 hours is promising as the same ligand motif will be present when strands of oligonucleotides are tried.

In hydroformylation the opposite was observed, **46b** gave no conversion while **25a diastereomer 1** and **25a diastereomer 2** showed some reactivity.  $Rh(acac)CO$  showed the highest reactivity giving full conversion within the 18 hour timeframe; naturally the product was racemic. Although the enantiomeric excesses obtained with **25a diastereomer 1** and **25a diastereomer 2** were low, 8 % and 18 % respectively, they did show that the chirality of the nucleotide has an effect on the enantiodetermining step giving opposite selectivities. It is also interesting to note that the reaction speed of these enantiomers also differs. Although these results are fascinating, this type of ligand should not be introduced into a oligonucleotide because phosphoramidites are water sensitive and hydrolysis of the ligand will occur. Oligonucleotides with a triazole motif like ligand **46b** are not recommended to be used in hydroformylation because the smaller more accessible ligand showed no conversion and the longer oligonucleotides are not expected to improve reaction rates but enhance the enantiomeric excess.

## 4.4 Experimental

### General Procedures

All air and water sensitive reactions were carried out under argon utilising standard Schlenk techniques. Chemicals were purchased from Sigma Aldrich, Acros, Link Technologies, Fisher Scientific, Strem and used as is unless otherwise stated.  $\text{CHCl}_3$  and  $\text{CDCl}_3$  were distilled from  $\text{CaCl}_2$  and stored over  $\text{K}_2\text{CO}_3$  under argon. Dioxane and hexanes were distilled over sodium. MeOH was distilled from  $\text{I}_2/\text{CaH}_2$ . All the distilled solvents were stored under argon or nitrogen. Dry DMF was purchased and transferred into a young's ampoule. Degassing of organic solvents was done by three freeze/thaw cycles. Aqueous solutions were degassed by bubbling argon or nitrogen through for several hours.

Thin Layer Chromatography (TLC) was performed using silica plates (polygram 0.3 mm silica gel with fluorescent indicator  $\text{UV}_{254}$  on aluminium plates) purchased from Merck. Compounds on TLC were visualised by UV-detection unless otherwise stated. Flash chromatography or purification on a chromatotron<sup>TM</sup> were performed using the indicated eluent. The silica used for flash chromatography was silica gel 60 mesh 70-230 and was purchased from Fluka.

NMR spectra were recorded at room temperature on a Bruker Advance NMR spectrometer (300, 400 or 500 MHz) or a Varian NMR Spectrometer (300, 400 or 600 MHz). NMR spectra recorded at 37 °C were measured on a Varian NMR Spectrometer (400 MHz). Chemical shifts ( $\delta$ ) are given in ppm. Shifts are relative to a TMS reference ( $^1\text{H}$  or  $^{13}\text{C}$ ) or an 85%  $\text{H}_3\text{PO}_4$  reference ( $^{31}\text{P}$ ).  $^{13}\text{C}$  and  $^{31}\text{P}$  spectra were measured with  $^1\text{H}$  decoupling unless otherwise stated.

$T_m$  measurements were recorded on a Cary 100 spectrophotometer equipped with a thermo-controlled cell holder. The cell path length was 1 cm.

**Melting temperature**

2 nmol of each single oligonucleotide strand was placed in a quartz cuvette (1 ml) before adding 690  $\mu$ l degassed  $T_m$  buffer ( $T_m$ -buffer: 10 mM sodium cacodylate, 10 mM KCl, 10 mM  $MgCl_2$ , 5 mM,  $CaCl_2$  pH 7) and 310  $\mu$ l of the desired degassed dioxane/water mixture. The cuvette was placed in the spectrophotometer. Before commencing with the measurement the samples were heated to 90 °C and cooled to a starting temperature of 25 °C. After which the samples were heated from 25 to 90 °C at a rate of 5 °C/min while the UV absorption was recorded at  $\lambda = 260$  nm. The measurement was repeated before 2.2 nmol of polyamide was added and the samples were remeasured twice.

**Chlorobis(ethylene)iridium dimer  $[Ir(CH_2=CH_2)_2Cl]_2$** 

500 mg of chlorobis(cyclooctene)iridium dimer was dissolved in 5 ml hexane. The reaction mixture was cooled to -40 °C before vigorously stirring while bubbling ethylene gas through the reaction mixture for 1 hour. The yellow brownish colour changed to grey. The suspension was allowed to settle before cooling to -70 °C and washing 3x with 5 ml of hexane under ethylene pressure. The residue was placed under vacuum to dry. Upon placing under argon the solid turned dark red.

The complex is stable up to three months if kept at -20 °C under argon.

**Iridium complex with dienes**

Chlorobis(cyclooctene)iridium dimer or chlorobis(ethylene)iridium dimer was dissolved in deuterated chloroform. A  $^1H$  NMR spectrum was taken before adding an excess of diene. The reaction mixture was warmed to 37 °C and an NMR was taken at set intervals

The complex with 7-chlorobicyclo [2.2.1] hepta-2,5-diene was stable in solution for up to two weeks but degrades when concentrated.

$^1H$  NMR ( $CDCl_3$ )  $\delta_H = 4.0$  (4H, m possible dd 29 Hz, 25 Hz), 3.8 (2H, s), 3.4 (1H, s)

The complex with diene **62** would not form.

**Degradation of the 7-chlorobicyclo[2.2.1]hepta-2,5-diene iridium complex**

To a solution of the 7-chlorobicyclo[2.2.1]hepta-2,5-diene iridium complex in  $CDCl_3$  a couple of drops of deuterated methanol were added. After which a  $^1H$ -NMR was taken at set intervals registering the decomposition of the original complex.

**General procedure for the 1,4-cycloaddition**

[Rh (COE)Cl]<sub>2</sub> (1 equiv.) and norbornadiene (1.1 equiv.) were dissolved in degassed dioxane. To this solution cyclohexenone (30 equiv.) was added followed by sodium tetraarylborate (45 equiv.) and the desired amount of water. The reaction was stirred for 24 hours at room temperature after which the reaction mixture was passed over a silica gel plug and washed through with EtOAc. Conversion was determined by TLC.

**General procedure for allylic amination of 1,3-diphenylallyl acetate with benzylamine**

The reactions were carried out in GC vials. In some of the vials 0.03 mmol K<sub>2</sub>CO<sub>3</sub> was added. Separate stock-solutions were made of the metal complex [Ir(COE)<sub>2</sub>Cl]<sub>2</sub>, [Ir(CH<sub>2</sub>=CH<sub>2</sub>) or Pd(η<sup>3</sup>-C<sub>3</sub>H<sub>5</sub>)Cl]<sub>2</sub> in either dioxane or dichloromethane and the desired amount was placed in a GC vial or eppendorf. To this the appropriate amount and ligand (in dioxane or DCM) was added. The reaction mixture was further diluted with distilled water (containing Mg(OCl<sub>4</sub>)<sub>2</sub> M, Na<sub>2</sub>(OCl<sub>4</sub>) M), or DCM before adding the substrate and internal standard (in DCM or dioxane). Finally the nucleophile (in dioxane or DCM) was added. Once the reaction had been stirred for the desired length of time a sample was removed to determine the conversion by GC before passing the reaction mixture over silica gel to remove the metal to determine the *ee*.

A RTX column was used and helium was used a carrier gas. The pressure was isocratic at 100 bar. The temperature was held at 50 °C for 2 minutes before heating to 300 °C at a rate of 20 °C/min. This was held for 10 minutes. Retention times: benzylamine: 6.87 min, diphenyl ether (internal standard): 8.06 min, 1,3-diphenylallyl acetate (starting material): 11.79 min, 1,3-diphenylallyl benzylamine (product): 14.49 min.

The *ee* was determined with HPLC using a CHIRACEL OD-H column. An isocratic mixture of 99.5:0.5 hexane:iso-propanol with a flow rate of 0.5 ml/min was used. An impurity overlapped one of the peaks of the enantiomers so *ee* was not determined.

**General procedure for hydroformylation of styrene**

The hydroformylation experiments were carried out in an autoclave with magnetic stirring. The reactions were carried out in 6 ml vials with caps containing septa. Stock solutions were made of the Rh(acac)(CO)<sub>2</sub> and styrene. After adding the appropriate amounts the vials were capped and a needle was placed through the septa of each cap. The autoclave was purged with argon before the vials were added. The autoclave was purged 3 times with 10 bars of syngas. Before it was charged with 40 bars and the temperature was brought to 40 °C. The reaction

mixture was stirred for 24 hour after which the autoclave was cooled by placing in an ice bath before releasing the pressure.

Conversion was determined by GC. A RTX column was used and helium was used a carrier gas. The pressure was isocratic at 100 bar. The temperature was held at 50 °C for 2 minutes before heating to 300 °C at a rate of 20 °C/min. This was held for 10 minutes. Retention times were: styrene: 3.60 min, branched product: 5.57 min, linear product: 6.10 min. and diphenyl ether (internal standard): 8.07 min.

The *ee* was determined by GC. A supelco beta-dex column was used. He was the carrier gas. An isocratic temperature was used of 80 °C and 100 bar. Retention times were: enantiomer 1: 10.16 min, enantiomer 2: 10.39 min, linear product 14.12, internal standard diphenyl ether: 19.32, styrene and solvent peak overlap.

## 4.5 References

1. Cornils, B.; Herrmann, W. A.; Editors, *Aqueous-Phase Organometallic Catalysis, 2nd Ed: Aqueous Phase Organometallic Catalysis*. Wiley-VCH Verlag GmbH & Co. KGaA: 2004; p 750 pp.
2. Rideout, D. C.; Breslow, R., *J. Am. Chem. Soc.* **1980**, *102* (26), 7816-7817.
3. Kobayashi, S., *Pure Appl. Chem.* **2007**, *79* (2), 235-245.
4. Von Hippel, P. H.; Schleich, T., *Acc. Chem. Res.* **1969**, *2* (9), 257-265.
5. Lindström, U. M., *Chem. Rev.* **2002**, *102* (8), 2751-2772.
6. Boersma, A. J.; Feringa, B. L.; Roelfes, G., *Angew. Chem. Int. Ed.* **2009**, *48* (18), 3346-3348.
7. Boersma, A. J.; Megens, R. P.; Feringa, B. L.; Roelfes, G., *Chem. Soc. Rev.* **2010**, *39*, 2083-2092.
8. Jeon, J.-H.; Kim, M. R.; Jun, J.-G., *Synthesis* **2011**, (3), 370-376.
9. Drew, H. R.; Wing, R. M.; Takano, T.; Broka, C.; Tanaka, S.; Itakura, K.; Dickerson, R. E., *Proc. Natl. Acad. Sci. U. S. A.* **1981**, *78* (PDB ID: 1BNA), 2179-83.
10. Sirivolu, V. R.; Chittepu, P.; Seela, F., *ChemBioChem* **2008**, *9* (14), 2305-2316.
11. Consiglio, G.; Waymouth, R. M., *Chem. Rev.* **1989**, *89* (1), 257-276.
12. (a) Trost, B. M.; Crawley, M. L., *Chem. Rev.* **2003**, *103* (8), 2921-2944;(b) Trost, B. M.; Van Vranken, D. L., *Chem. Rev.* **1996**, *96* (1), 395-422.
13. Tsuji, J.; Takahashi, H.; Morikawa, M., *Tetrahedron Lett.* **1965**, *6* (49), 4387-4388.
14. Trost, B. M.; Strege, P. E., *J. Am. Chem. Soc.* **1977**, *99* (5), 1649-1651.
15. Trost, B. M.; Verhoeven, T. R. Catalytic allylic alkylation. US4051157A, 1977.
16. Li, J. J.; Gribble, G. W., *Palladium in heterocyclic chemistry: a guide for the synthetic chemist*. Elsevier: 2007.
17. Kazmaier, U., *Transition Metal Catalyzed Enantioselective Allylic Substitution in Organic Synthesis*. Springer: 2011.
18. Hartwig, J.; Pouy, M., Iridium-Catalyzed Allylic Substitution Iridium Catalysis. Andersson, P. G., Ed. Springer Berlin / Heidelberg: 2011; Vol. 34, pp 169-208.
19. Ramdeehul, S.; Dierkes, P.; Aguado, R.; Kamer, P. C. J.; van Leeuwen, P. W. N. M.; Osborn, J. A., *Angew. Chem. Int. Ed.* **1998**, *37* (22), 3118-3121.
20. Shue, Y.-J.; Yang, S.-C., *Appl. Organomet. Chem.* **2011**, *25* (12), 883-890.
21. Ricci, A., *Modern Amination Methods*. John Wiley & Sons: 2008.
22. Fournier, P.; Fiammengo, R.; Jäschke, A., *Angew. Chem. Int. Ed.* **2009**, *48* (24), 4426-4429.
23. (a) Hartwig, J. F.; Stanley, L. M., *Acc. Chem. Res.* **2010**, *43* (12), 1461-1475;(b) Prétôt, R.; Pfaltz, A., *Angew. Chem. Int. Ed.* **1998**, *37* (3), 323-325.
24. Edwards, C. W.; Shipton, M. R.; Alcock, N. W.; Clase, H.; Wills, M., *Tetrahedron* **2003**, *59*, 6473-6480.
25. Shintani, R.; Tsutsumi, Y.; Nagaosa, M.; Nishimura, T.; Hayashi, T., *J. Am. Chem. Soc.* **2009**, *131* (38), 13588-13589.
26. Fischer, C.; Defieber, C.; Suzuki, T.; Carreira, E. M., *J. Am. Chem. Soc.* **2004**, *126* (6), 1628-1629.
27. Wei, W.-T.; Yeh, J.-Y.; Kuo, T.-S.; Wu, H.-L., *Chem.-Eur. J.* **2011**, *17* (41), 11405-11409.
28. Takeuchi, R.; Kashio, M., *Angew. Chem. Int. Ed.* **1997**, *36* (3), 263-265.
29. Cornils, B.; Herrmann, W. A.; Rasch, M., *Angew. Chem. Int. Ed.* **1994**, *33* (21), 2144-2163.

- 
30. Kohlpaintner, C. W.; Fischer, R. W.; Cornils, B., *Appl. Catal., A* **2001**, *221* (1–2), 219-225.
  31. (a) Sakai, N.; Mano, S.; Nozaki, K.; Takaya, H., *J. Am. Chem. Soc.* **1993**, *115* (15), 7033-7034;(b) Aguado-Ullate, S.; Saureu, S.; Guasch, L.; Carbó, J. J., *Chem.-Eur. J.* **2011**, n/a-n/a.
  32. Gonsalvi, L.; Peruzzini, M., Aqueous Phase Reactions Catalysed by Transition Metal Complexes of 7-Phospha-1,3,5-triazaadamantane (PTA) and Derivatives Phosphorus Compounds. Peruzzini, M.; Gonsalvi, L., Eds. Springer Netherlands: 2011; Vol. 37, pp 183-212.
  33. Jira, R., *Angew. Chem. Int. Ed.* **2009**, *48* (48), 9034-9037.
  34. Paganelli, S.; Zanchet, M.; Marchetti, M.; Mangano, G., *J. Mol. Catal. A: Chem.* **2000**, *157* (1–2), 1-8.
  35. Evans, D.; Osborn, J. A.; Wilkinson, G., *Journal of the Chemical Society A: Inorganic, Physical, Theoretical* **1968**, 3133-3142.
  36. (a) Gillespie, J. A.; Dodds, D. L.; Kamer, P. C. J., *Dalton Trans.* **2010**, *39*, 2751-2764;(b) Leeuwen, P. W. N. M., *Homogeneous Catalysis understanding the Art*. Kluwer Academic Publishers: Dordrecht, 2004.
  37. Bezman, S. A.; Bird, P. H.; Fraser, A. R.; Osborn, J. A., *Inorg. Chem.* **1980**, *19* (12), 3755-3763.
  38. Ropartz, L.; Meeuwenoord, N. J.; van der Marel, G. A.; van Leeuwen, P. W. N. M.; Slawin, A. M. Z.; Kamer, P. C. J., *Chem. Commun.* **2007**, (15).
  39. Tilloy, S.; Genin, E.; Hapiot, F.; Landy, D.; Fourmentin, S.; Genêt, J.-P.; Michelet, V.; Monflier, E., *Adv. Synth. Catal.* **2006**, *348* (12-13), 1547-1552.
  40. Hua, Z.; Vassar, V. C.; Choi, H.; Ojima, I., *Proc. Natl. Acad. Sci. U. S. A.* **2004**, *101* (15), 5411-5416.
  41. Chaplin, A. B.; Green, J. C.; Weller, A. S., *J. Am. Chem. Soc.* **2011**, *133* (33), 13162-13168.

# List of Abbreviations

Abbreviation	Name in full
A	adenine
AAC	azide alkyne cycloaddition
Ac	acetyl
acac	acetylacetone
Ada	adamantylacetyl
AHF	asymmetric hydroformylation
aq.	aqueous
( <i>R,S</i> )-BINAPHOS	( <i>R</i> )-(2-(diphenylphosphino)-1,1'-binaphtalen-2'-yl)-(( <i>S</i> )-1,1'-binaphtalen-2,2'-yl)phosphite
BINAP	2,2'-bis(diphenylphosphino)-1,1'-binaphthyl
BINOL	1,1'-Binaphthalene-2,2'-diol
Biot	biotin
BOC	Di- <i>tert</i> -butyl dicarbonate
BOP	(Benzotriazol-1-yloxy) <i>tris</i> (dimethylamino)phosphonium hexafluorophate
<i>t</i> -Bu	<i>tertiary</i> -butyl
C	cytosine
cald	calculated
CAMP	cyclohexyl (2-methoxyphenyl)(methyl)phosphine
cat.	catalyst
Cbz	carboxybenzyl
CDI	1,1'-carbonyldiimidazole
COD	cyclooctadiene
COE	cyclooctene
Cp <sup>*</sup>	pentamethylcyclopentadienyl
CPG	controlled pore glass
CuAAC	copper catalysed azide alkyne cycloaddition
Cy	cyclohexyl
d	deoxy
D	Dalton
DABCO	1,4-diazabicyclo[2.2.2]octane)
DBB	4,4'-di- <i>tert</i> -butylbiphenyl
DCI	4,5-dicyanoimidazole
DCC	dicyclohexylcarbodiimide
DCM	dichloromethane
DIC	1,3-diisopropylcarbodiimide
DIEA	<i>N,N</i> -diisopropylethylamine
DMAP	4-(Dimethylamino) pyridine
DMF	dimethylformamide
DMT	4,4'-dimethoxytrity

---

DNA	deoxyribonucleic acid
<i>L</i> -Dopa	<i>L</i> -3,4-dihydroxyphenylalanine
Dp	dimethylaminopropyl
dpp	diphenylphosphine
dppf	1,1'-Bis(diphenylphosphino)ferrocene
Duphos	(+)-1,2-Bis[(2 <i>R</i> ,5 <i>R</i> )-2,5-diisopropylphospholano]benzene
EDC	ethyl-( <i>N</i> ', <i>N</i> '-dimethylamino)propylcarbodiimide hydrochloride
ee	enantiomeric excess
E-factor	environmental factor
equiv.	equivalent
ES	enzyme substrate complex
Et	ethyl
FPLC	fast protein liquid chromatography
G	guanine
GC	gas chromatography
h.	hour
HATU	<i>O</i> -(7-Azabenzotriazol-1-yl)- <i>N,N,N',N'</i> -tetramethyluronium hexafluorophosphate
HOBt	1-hydroxy-1 <i>H</i> -benzotriazole
Hp	3-Hydroxy-1 <i>H</i> -pyrrole
HPLC	high pressure liquid chromatography
Im	imidazole
L	ligand
LDA	Lithium diisopropylamide
lyrs	light years
M	metal
MALDI -TOF	Matrix-Assisted Laser Desorption Ionisation Time of Flight
Me	methyl
MGB	minor groove binder
min.	minute
MOPS	4-morpholinepropanesulfonic acid
MS	mass spectrometry
Mw	molecular weight
nbd	norbornadiene
NBS	<i>N</i> -bromosuccinimide
NMR	nuclear magnetic resonance
PA	polyamide
PAM	4-hydroxymethyl-phenylacetamidomethyl
PCR	polymerase chain reactions
PEG	polyethylene glycol
Ph	phenyl
pI	isoelectric point
POM	chloromethylpivalate
ppm	parts per million

---

---

Pr	propyl
PTFE	polytetrafluoroethylene
Py	pyrrole
PyBOP	benzotriazol-1-yloxy)tripyrrolidin phosphonium hexafluorophosphate
Q	environmental quotation
RhAAC	rhodium catalysed azide alkyne cycloaddition
R <sub>f</sub>	retention factor
RNA	ribonucleic acid
RP	reverse phase
rRNA	ribosomal ribonucleic acid
rt.	room temperature
SELEX	Systematic Evolution of Ligands by eXponential Enrichment
syngas	synthesis gas
T	thymine
TBTA	<i>tris</i> -(benzyltriazolylmethyl)amine
TBTU	<i>O</i> -(Benzotriazol-1-yl)- <i>N,N',N'</i> -tetramethyluronium tetrafluoroborate
TCA	trichloroacetic acid
TCEP	tris(2-carboxylethyl)phosphine
Tf	triflic
TFA	trifluoroacetic acid
THF	tetrahydrofuran
TLC	thin layer chromatography
T <sub>m</sub>	melting temperature
TMGA	<i>N,N,N',N'</i> -tetramethylguanidinium azide
TMS	Tetramethylsilane
TNT	trinitrotoluene
TOF	turn over frequency
TPP	triphenylphosphine
tppts	3,3',3''-Phosphinidynetris(benzenesulfonic acid)
U	uracil
UV	ultra violet
v/v	volume/volume
w/w	weight/weight

## Acknowledgments

As is the case in most things in life failure is the sole responsibility of one person, in this case it would have been me. Success on the other hand is a team achievement and that is why I need to give thanks a great many people. Firstly I would like to thank my supervisor Professor Paul Kamer for the opportunity to take part in this challenging and inspirational project. Professor Paul Kamer's second in command Dr. Wouter Laan also receives my thanks for proof reading a number of chapters and for making me laugh by pointing his finger at me. Wouter take good care of the finger!!!!. Marzia Nuzzelo, now a Dr., worked on a similar project within our group and gave me a lot of support during my first year and for that I will forever be in her debt. I apologise to Christine Czauderna and Jason Gillespie, who recently passed his viva, for mentioning them both in one sentence but I want to thank them both for their support in difficult times, their advice in chemistry matters and making my time in the lab enjoyable. I would also like to thank Dr. Debbie Dobbs for helping me to conquering my fear of opening ampoules. Thanks is also due to Peter Deuss (Dr.) for the interesting articles he brought to my attention even after he move away. Thanks to Michiel Samuels for the entertaining game nights. Michiel and Jason thank you both for keeping the GC's in good working order. Gracias Dr. Arnold Grabulosa for your early morning Spanish lessons. To all the past and present members of the PCJK group I would like to say thank you/dank je wel for keeping me motivated and making my journey a pleasant one.

I also need to thank people outside of my group. I am grateful to Dr. Catherine Botting, Dr. Sally Shirran, Mr. Alex Houston and Ms Caroline Horsburgh for their expertise of mass spectroscopy. Mrs Melanja Smith and Dr. Tomas Lebl thank you for keeping the NMR machines running smoothly and helping with the analysis of the spectra. For helping keep our machines (GCs and DNA synthesiser) running my thanks has to go to Mr. Bobby Cathcart, Mr George Anthony and Mr Brian Walker. Mr Colin Smith I thank for the glassware he made for us. For the morning chats and motivational speeches I thank the cleaners Ann, Darren, Stan, Ray and Alan. My thanks is also extended to members of other groups. I would like to thank the following people for the use of their groups machines Thibault Smidt for the analytical HPLC Nouchali and the other members of her group for the FPLC and Qingzhi Zhang for the HPLC. Thank you Qingzhi for keeping the HPLC running for as long as it was and I know it wasn't easy.

My thanks now goes across the pond to thank Professor Peter Dervan for giving me the chance to go to the United States of America and for his graceful hospitality. His group also requires a heartfelt thank you for accepting me into their group and making my stay there very enjoyable with a special thank you to Dr. Jevgenij Raskatov for his help with the iridium complexes and computational study.

For keeping me sane, as far as that was possible, I would like to thank my friends Helen Slootweg and Renske Lemmens and my family especially my parents.

I would like to thank Dr. Colin Allison (postgraduate pro-dean) for approving my extensions, Dr Joe Crayston and Prof. Dr. Rob Liskamp for accepting the task of being my assessors and the Marie Curie and ESPRC for their financial funding.

Lastly I would like to thank anyone I may have forgotten to mention, please forgive me for that.

Thank you all so much I couldn't do it without you.